Constraints on the Dense Matter Equation of State from Neutron Stars

David Blaschke[a,b,c]

Thanks to: M. Cierniak[a], O. Ivanytskyi[a], T. Fischer[a], M. Shahrbaf[a], A. Ayriyan[b], A. Bauswein[d] & S. Typel[d]

a – University Wroclaw, b - JINR Dubna, c – NRNU (MEPhI) Moscow, d – GSI Darmstadt

1. Introduction: Recent relevant multi-messenger observations

2. New paradigm: Only hybrid stars fulfil new M-R constraints

3. Outlook: Supernovae & Mergers in the QCD phase diagram
→ Constraints for the Onset of Deconfinement?

STRONG-2020 Workshop of NA7-Hf-QGP, Hersonissos, 8.10.2021

Grant No. UMO 2019 / 33 / B / ST9 / 03059

Grant No. 18-02-40137

Discovery: neutron star merger !

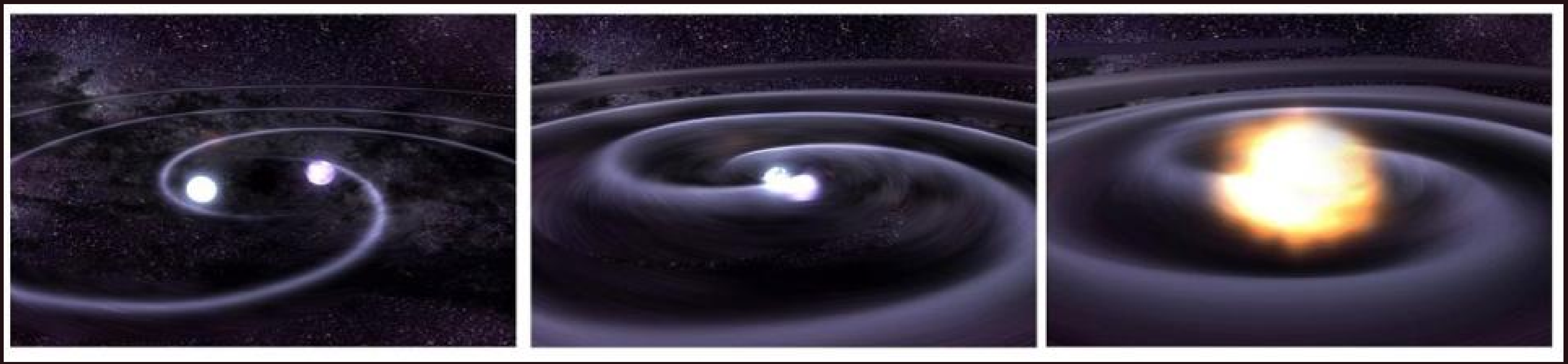

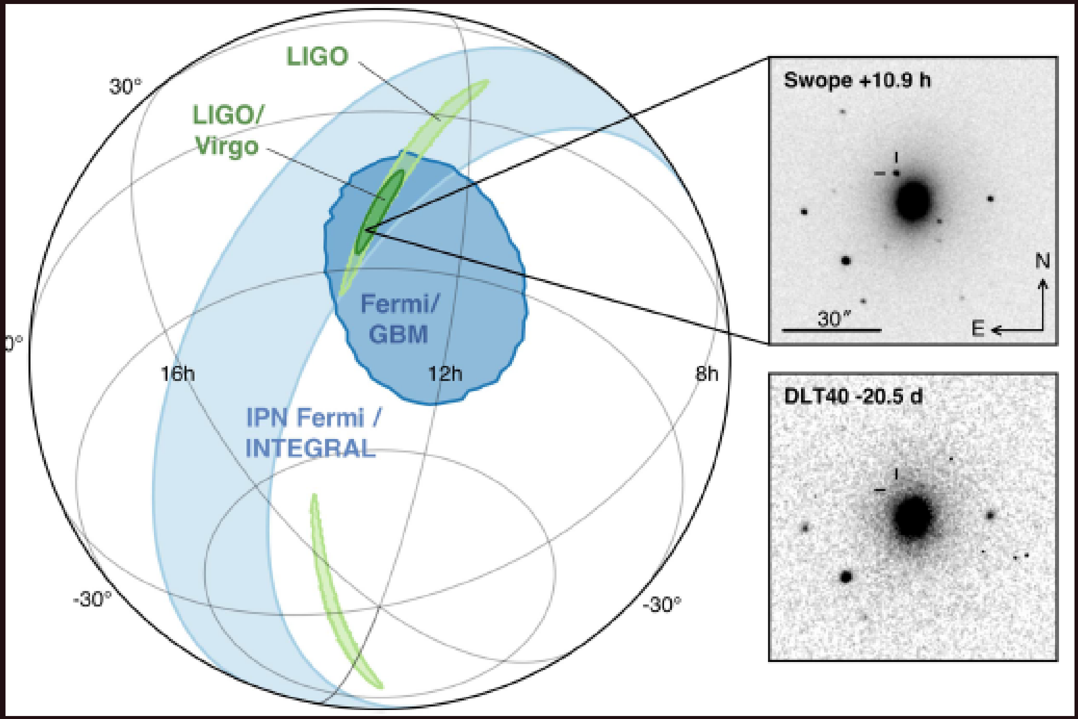

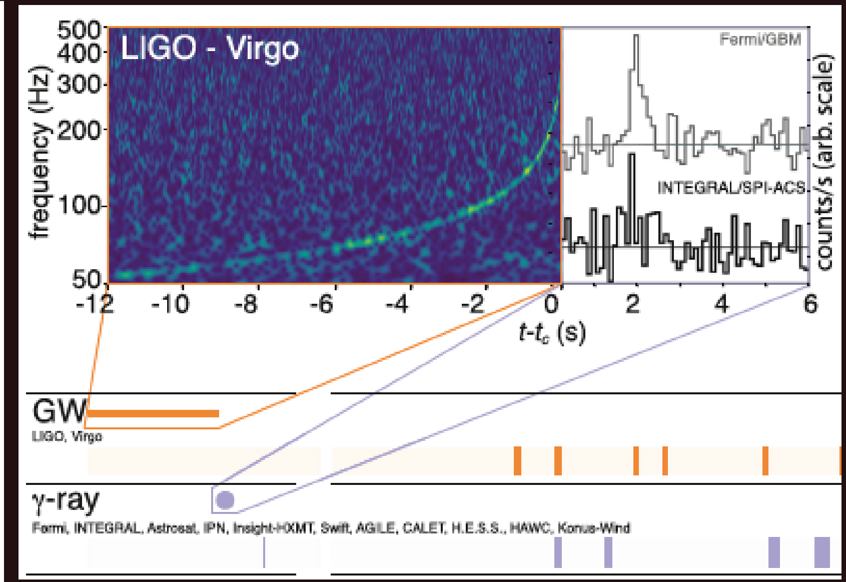

GW170817A , announced 16.10.2017 *)

*) B.P. Abbott et al. [LIGO/Virgo Collab.], PRL 119, 161101 (2017); ApJLett 848, L12 (2017)

NS-NS merger !

GW170817A , announced 16.10.2017 *)

Multi-Messenger Astrophysics !!

	Low-spin priors ($|\chi| \leq 0.05$)
Primary mass m_1	$1.36–1.60\ M_\odot$
Secondary mass m_2	$1.17–1.36\ M_\odot$
Chirp mass $\mathcal{M}$	$1.188^{+0.004}_{-0.002} M_\odot$
Mass ratio m_2/m_1	$0.7–1.0$
Total mass m_{tot}	$2.74^{+0.04}_{-0.01} M_\odot$
Radiated energy E_{rad}	$> 0.025 M_\odot c^2$
Luminosity distance D_L	40^{+8}_{-14} Mpc

Constraint on neutron star maximum mass

M_{TOV} < 2.17 M_sun

(Margalit & Metzger, arxiv:1710.05938)

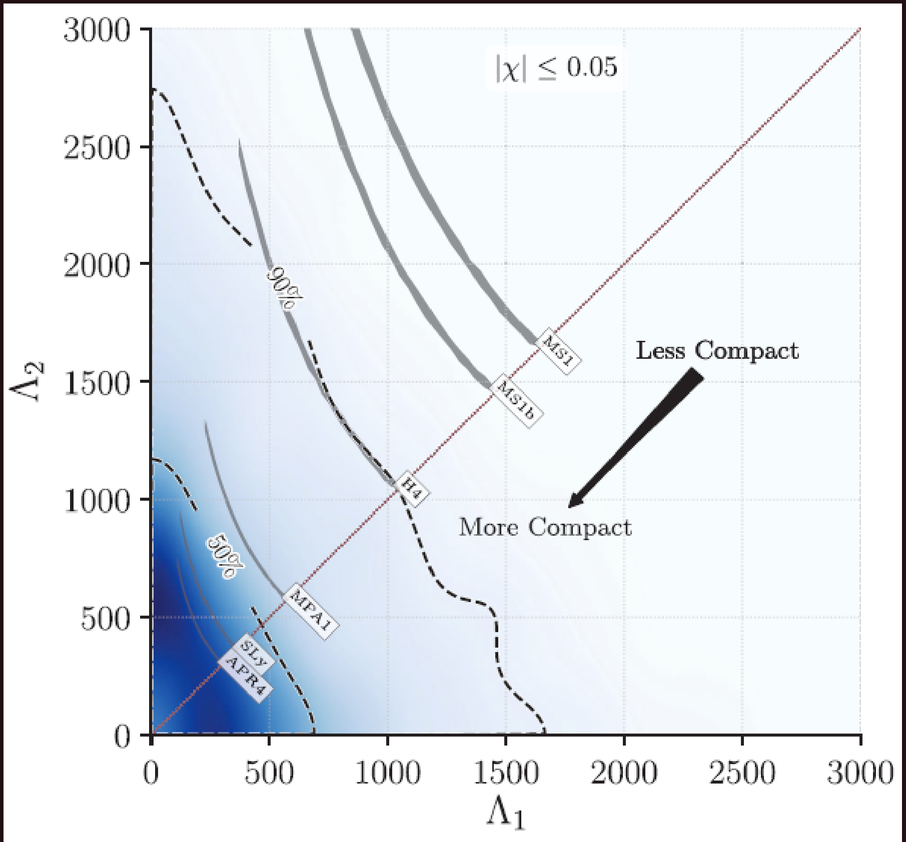

Constraint on parameter (Λ<800)

$$\tilde{\Lambda} = \frac{16}{13}\frac{(m_1 + 12m_2)m_1^4\Lambda_1 + (m_2 + 12m_1)m_2^4\Lambda_2}{(m_1 + m_2)^5}$$

Dimensionless tidal deformability

$$\Lambda = (2/3)k_2[(c^2/G)(R/m)]^5$$

*) B.P. Abbott et al. [LIGO/Virgo Collab.], PRL 119, 161101 (2017); ApJLett 848, L12 (2017)

Compact stars and black holes in Einstein's General Relativity theory

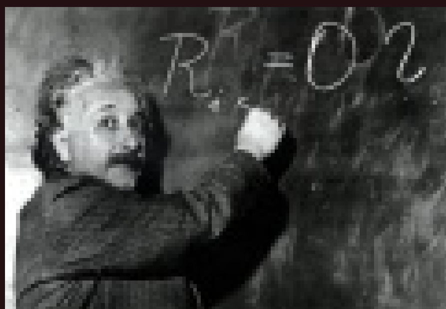

Space-Time $G_{\mu\nu} = 8\pi G\, T_{\mu\nu}$ Matter

Massive objects curve the Space-Time

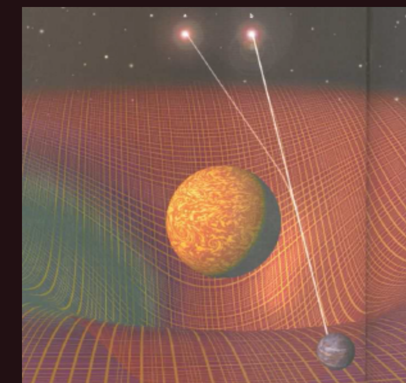

Non-rotating, spherical masses → Schwarzschild Metrics

$$ds^2 = -(1 - \frac{2M}{r})dt^2 + (1 - \frac{2M}{r})^{-1}dr^2 + r^2 d\Omega^2$$

Einstein eqs. → Tolman-Oppenheimer-Volkoff eqs.*)
For structure and stability of compact stars

$$\frac{dP(r)}{dr} = -G\frac{m(r)\varepsilon(r)}{r^2}\left(1 + \frac{P(r)}{\varepsilon(r)}\right)\left(1 + \frac{4\pi r^3 P(r)}{m(r)}\right)\left(1 - \frac{2Gm(r)}{r}\right)^{-1}$$

Newtonian case x GR corrections from EoS and metrics

*) R. C. Tolman, Phys. Rev. 55 (1939) 364 ; J. R. Oppenheimer, G. M. Volkoff, ibid., 374

The 1:1 relation P(ε) ↔ M(R) via TOV

Simple examples*)

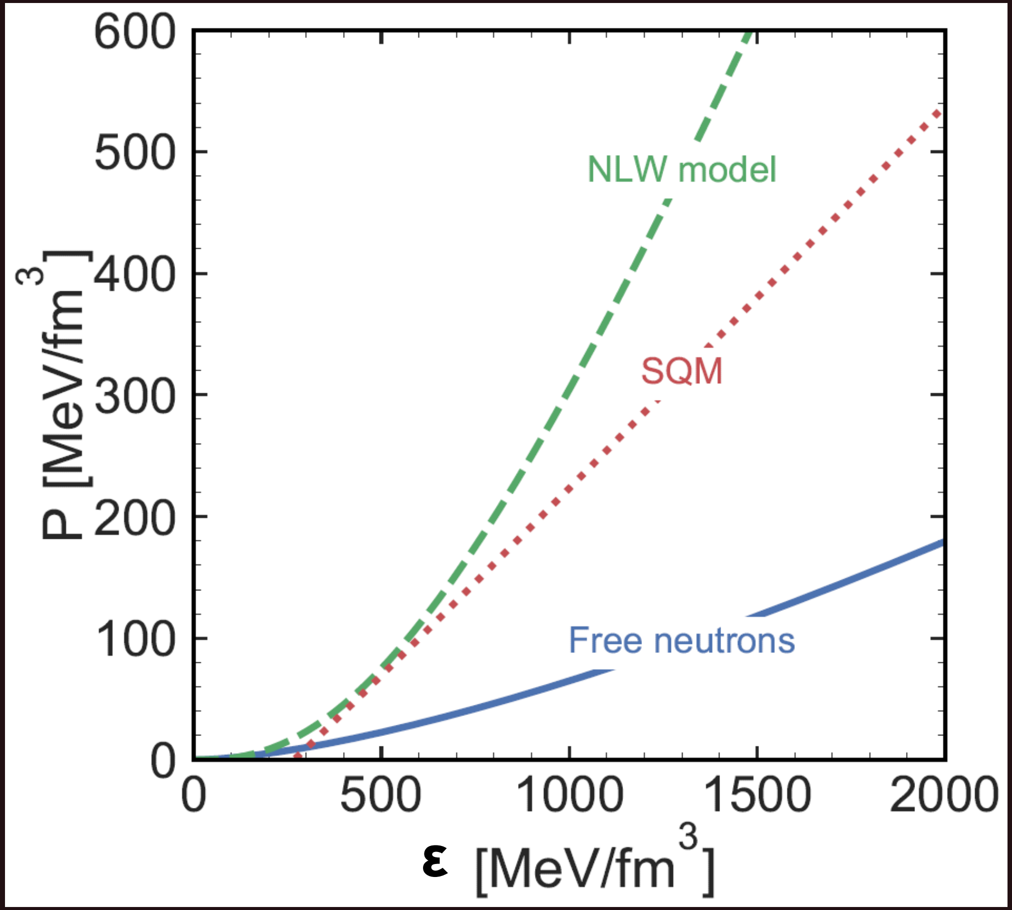

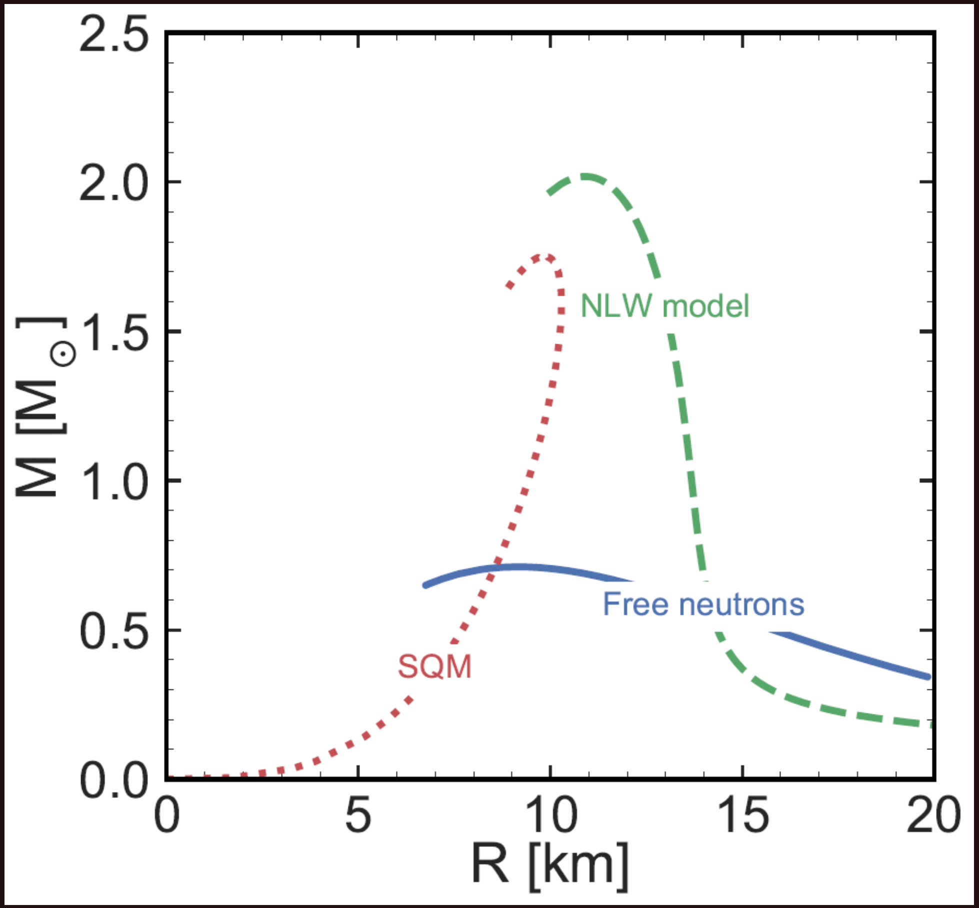

Free neutrons: Oppenheimer & Volkoff, Phys. Rev. 55 (1939) 374
NLW (nonlinear Walecka) model: N. K. Glendenning, Compact Stars (Springer, 2000)
SQM (strange quark matter): P. Haensel, J. L. Zdunik, R. Schaeffer, A&A 160 (1986) 121

*) courtesy: Konstantin Maslov

The 1:1 relation P(ε) ↔ M(R) via TOV

Simple examples*)

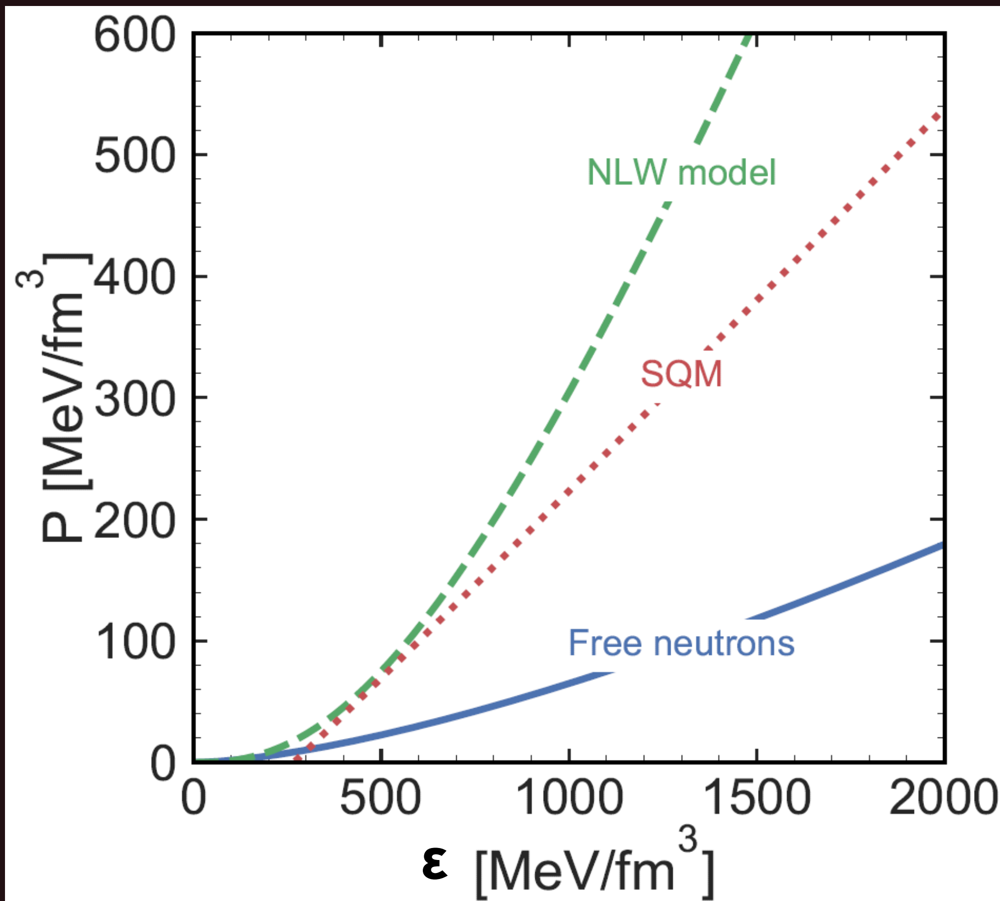

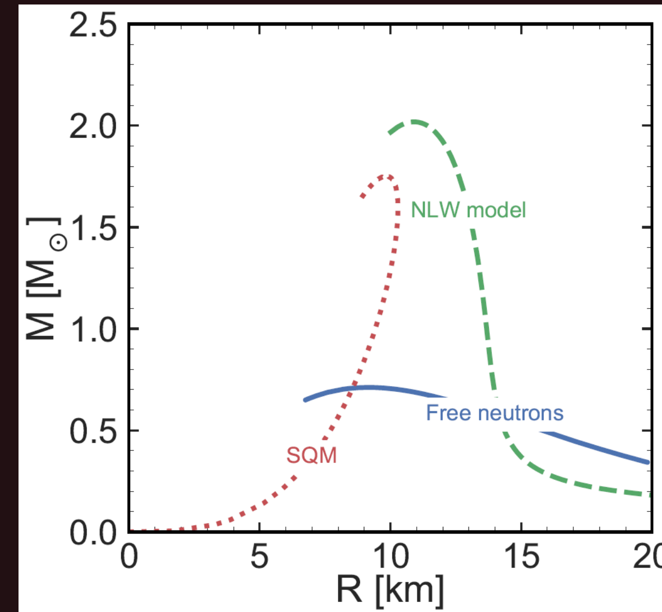

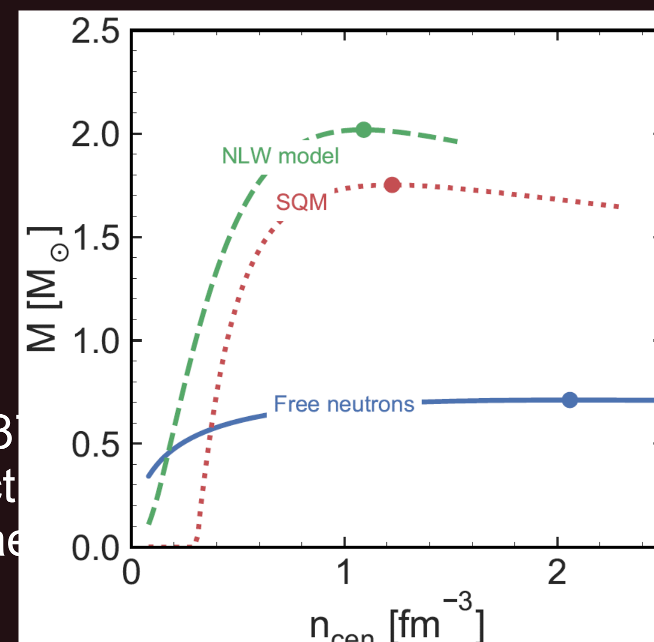

Free neutrons: Oppenheimer & Volkoff, Phys. Rev. 55 (1939) 37
NLW (nonlinear Walecka) model: N. K. Glendenning, Compact
SQM (strange quark matter): P. Haensel, J. L. Zdunik, R. Schae

*) courtesy: Konstantin Maslov

Constraints on NS mass and radii !

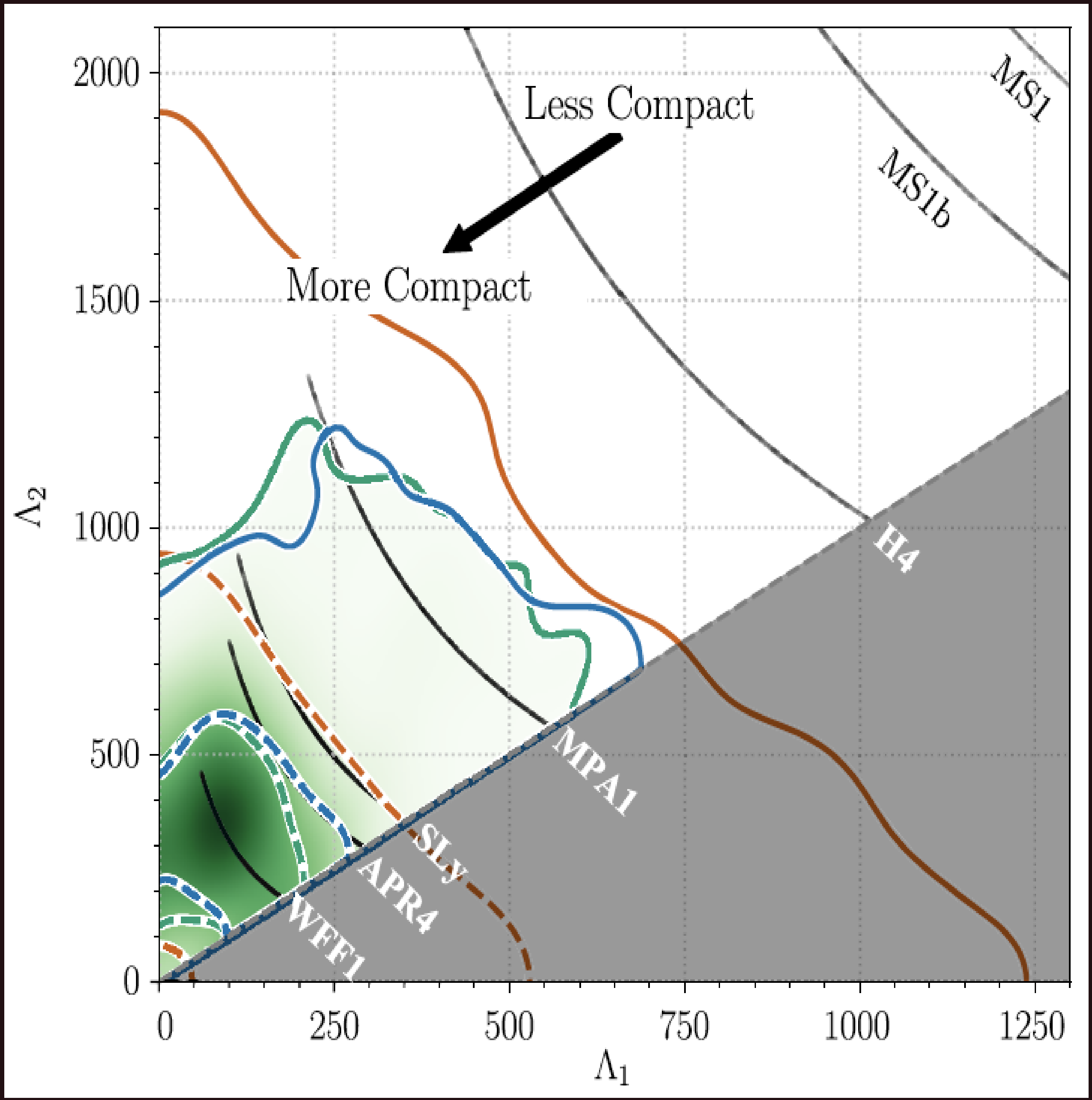

Constraint on maximum mass

2.01 < M_{TOV}/M_O < 2.16

(Rezzolla et al., arxiv:1710.05938)

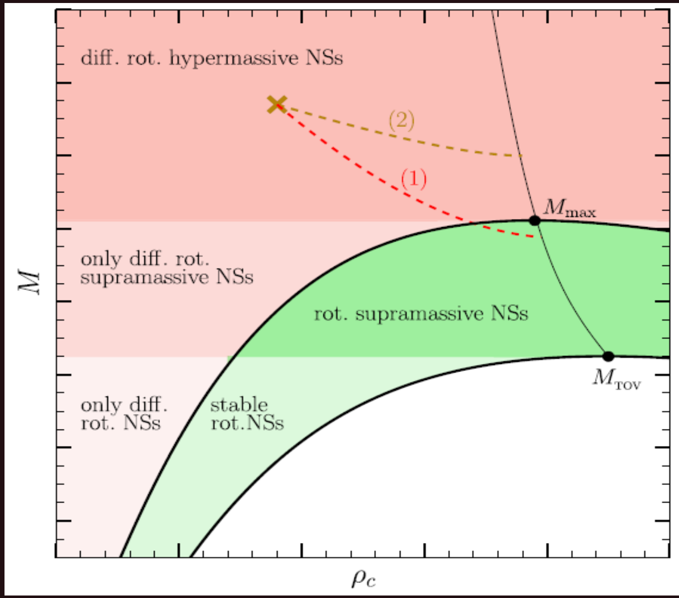

LVC radius constraint

GW170817

(Abbott et al., PRL (2018))

GW190425

(Abbott et al., arxiv:2001.01761)

NICER mass -radius constraint

PSR J0030+0451

(Miller et al., ApJLett. (2019))

Measure NS Radii ...

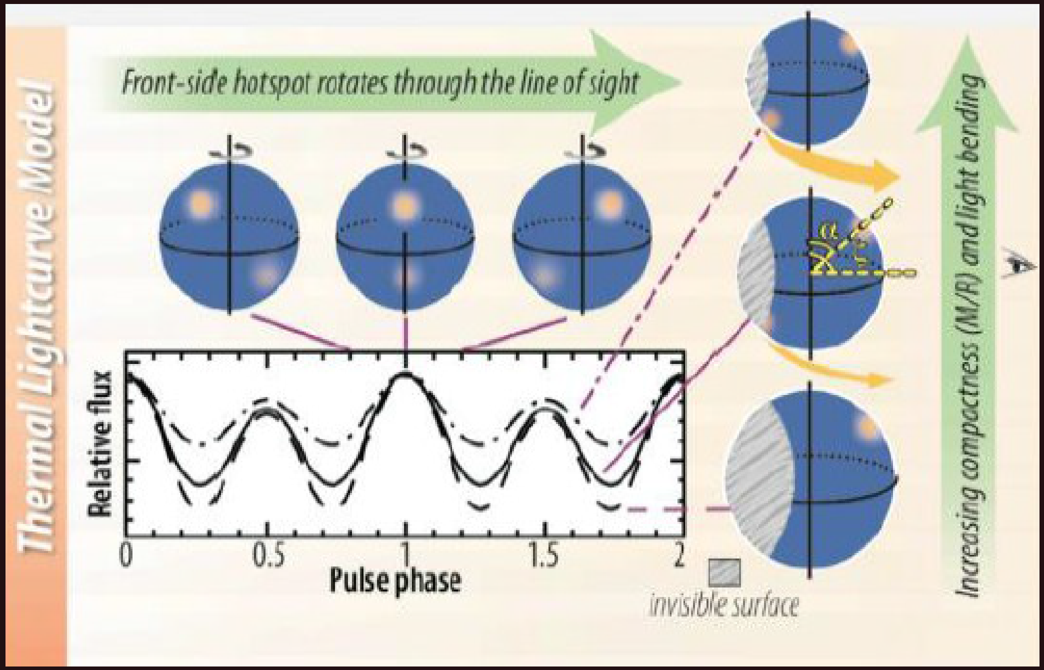

Thermal lightcurves: NS with "hot spots"

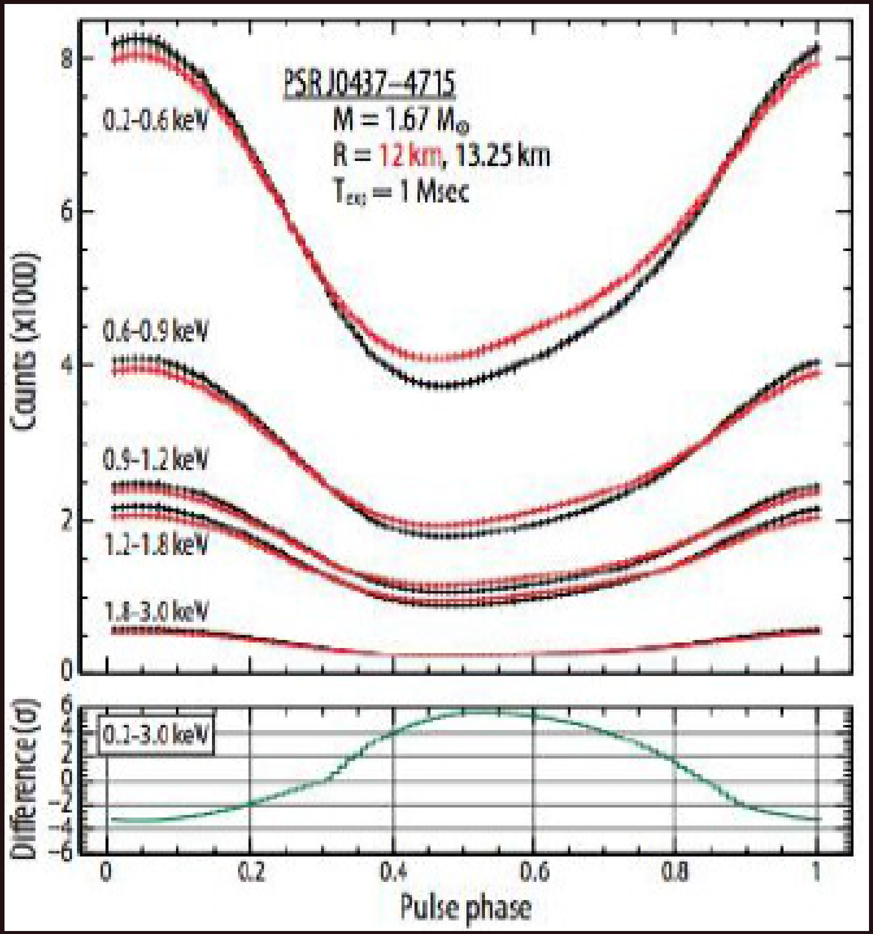

K.C. Gendreau et al., Proc. SPIE 8443 (2012) 844313 – first results end of 2019 !!

Constraints on NS mass and radii !

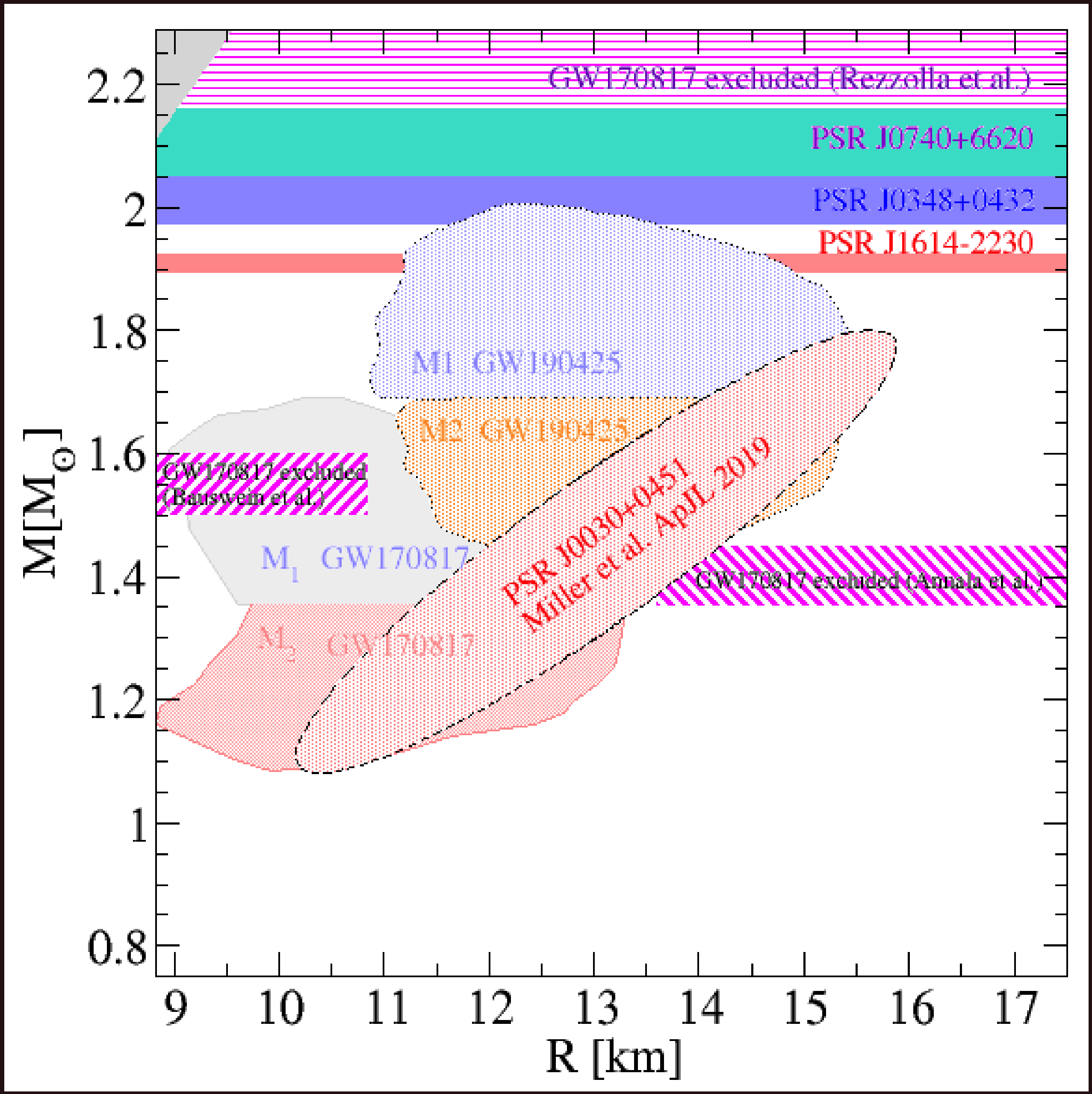

Constraint on maximum mass

$2.01 < M_{TOV}/M_{O} < 2.16$

(Rezzolla et al., arxiv:1710.05938)

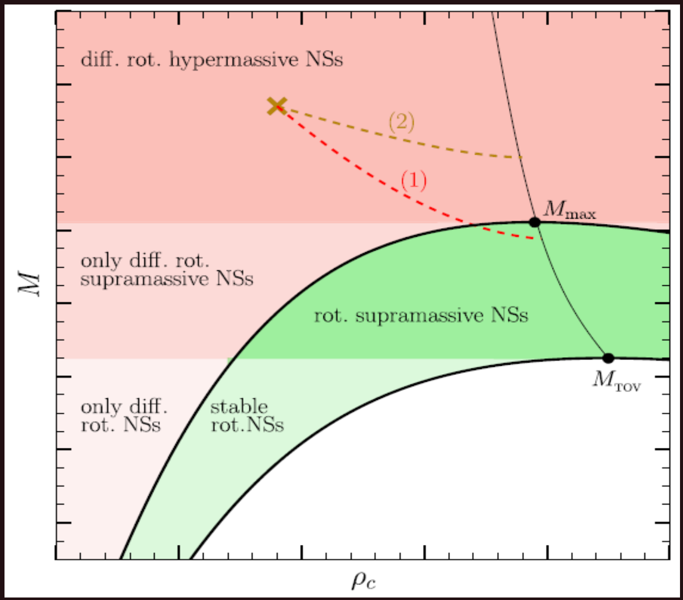

LVC radius constraint

GW170817

(Abbott et al., PRL (2018))

GW190425

(Abbott et al., arxiv:2001.01761)

NICER mass -radius constraint

PSR J0030+0451

(Miller et al., ApJLett. (2019))

Constraints on NS mass and radii !

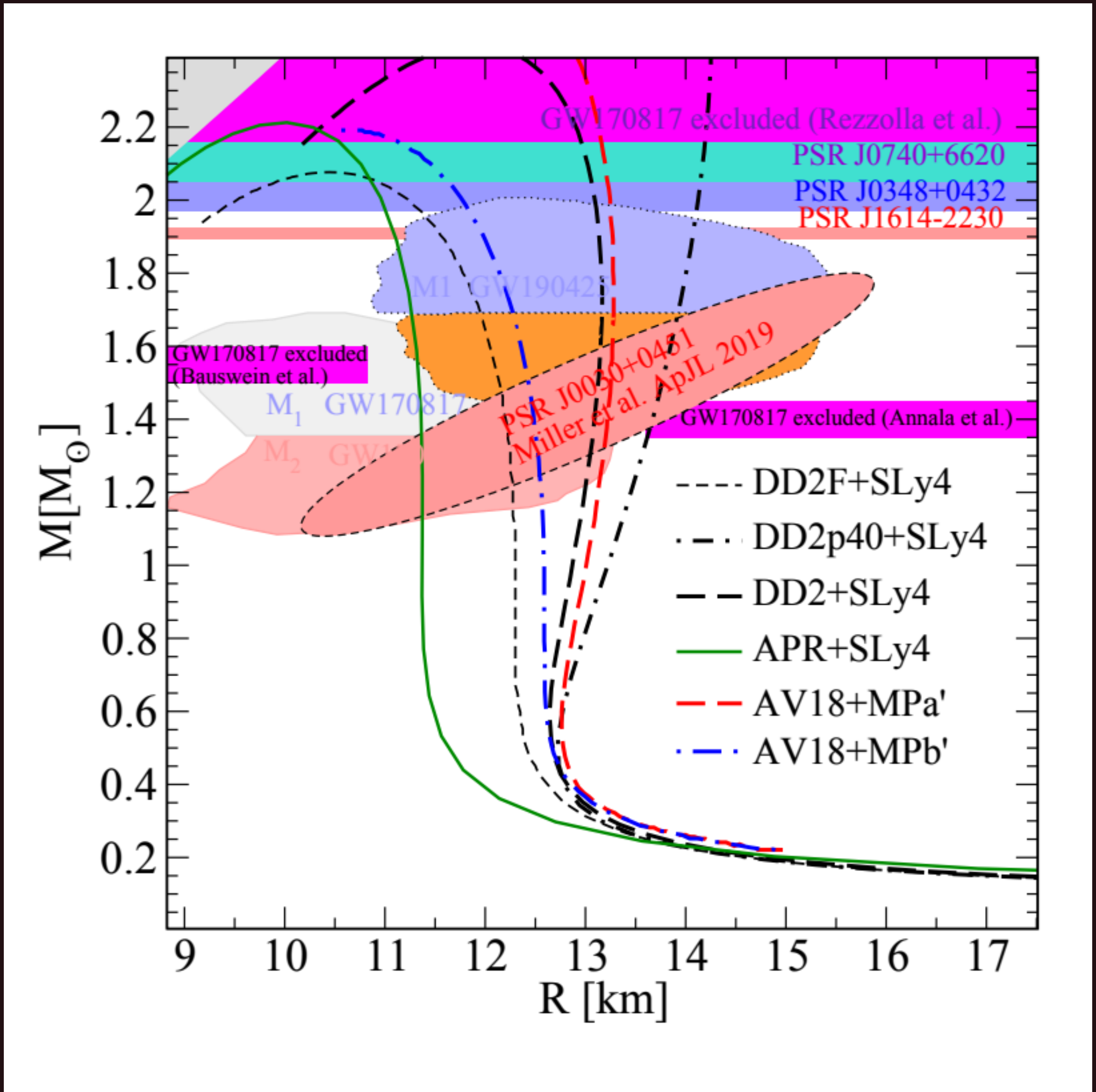

Examples of hadronic EoS
all do fulfill the constraints
but none of them is applicable for
Massive stars (M > 1.5 M_sun),
Because of missing hyperons etc.

AV18*: Yamamoto, Togashi et al., Phys. Rev C 96 (2017) 065804
DD2*: Typel, Röpke, Klähn, et al., Phys. Rev. C 81 (2010) 015803

LVC radius constraint
GW170817
(Abbott et al., PRL (2018))
GW190425
(Abbott et al., arxiv:2001.01761)
NICER mass -radius constraint
PSR J0030+0451
(Miller et al., ApJLett. (2019))

Constraints on NS mass and radii !

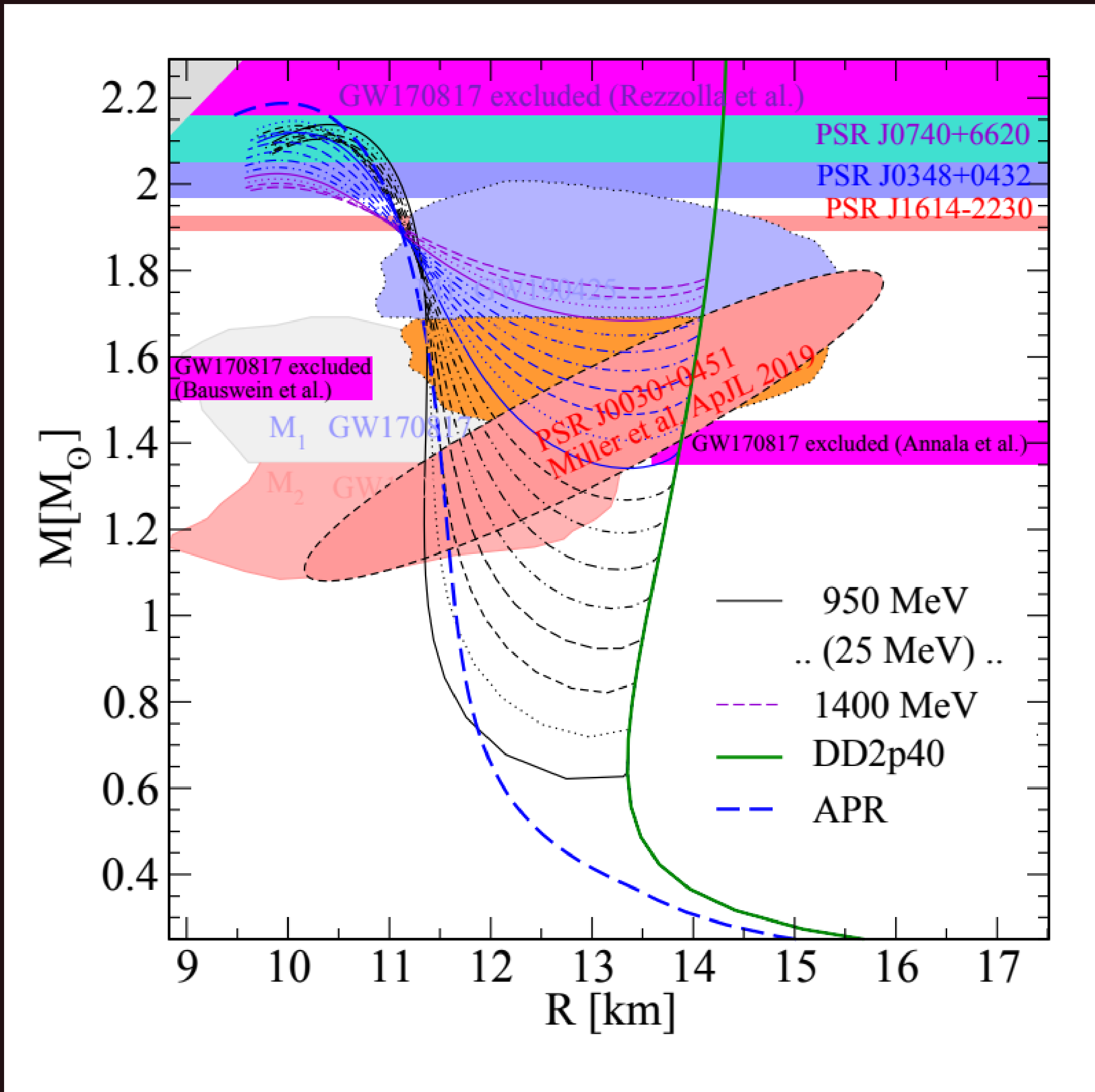

Blaschke, Ayriyan, Alvarez-Castillo et al., Universe 6 (2020) 81

Examples of hadronic EoS
all do fulfill the constraints
but **none of them is applicable** for
Massive stars (M > 1.5 M_sun),
Because of missing hyperons etc.

Which ways out?

→ stiff hypernuclear matter
→ early onset of deconfinement
(M_onset < 1.5 M_sun)

Old quark matter paradigm:

→ deconfinement softens EoS
→ hybrid stars compacter, lower M_{max}

LVC radius constraint
GW170817
(Abbott et al., PRL (2018))
GW190425
(Abbott et al., arxiv:2001.01761)
NICER mass -radius constraint
PSR J0030+0451
(Miller et al., ApJLett. (2019))

Constraints on NS mass and radii !

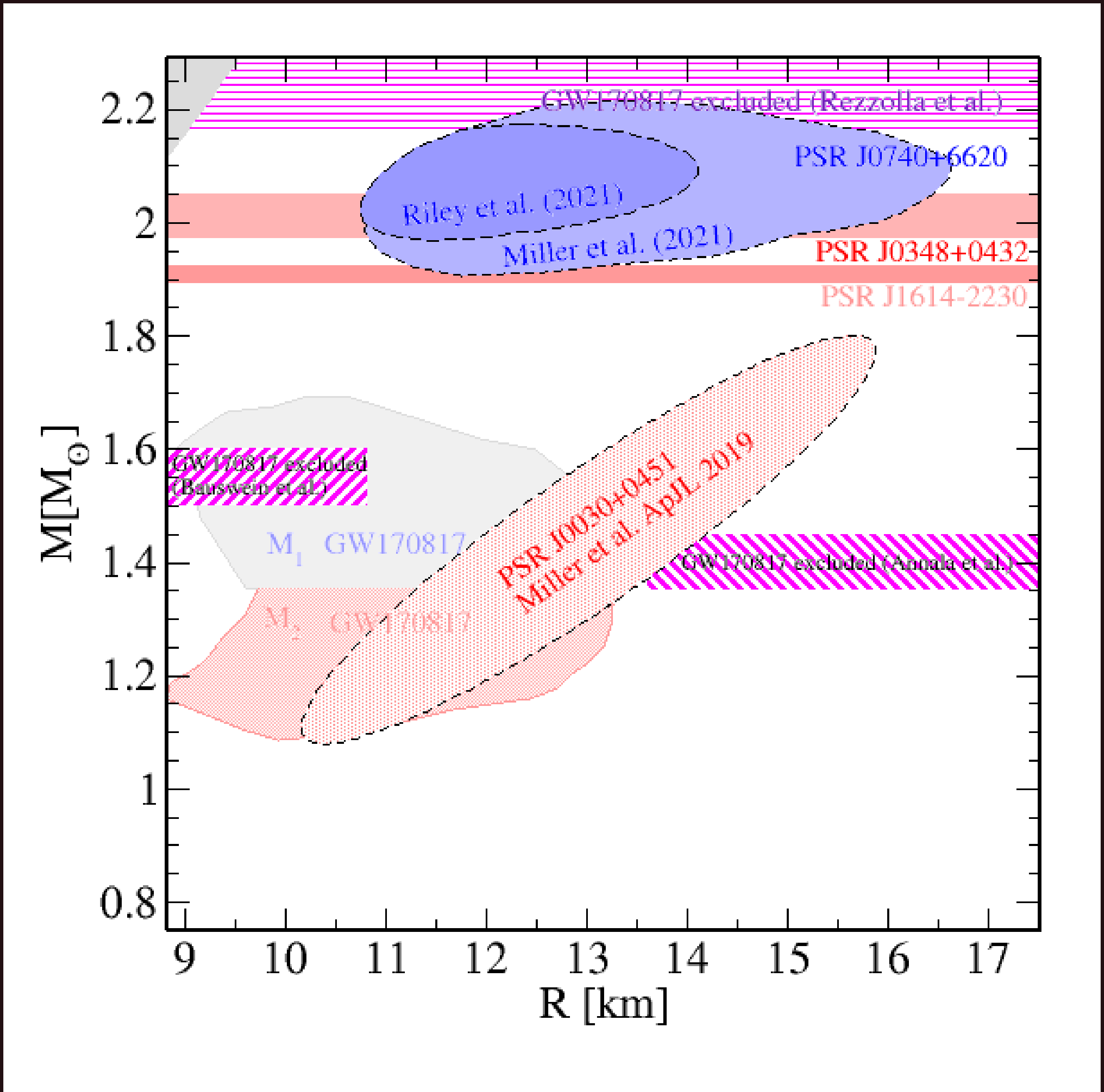

New NICER mass-radius data
PSR J0740+6620
(Riley et al., arxiv:2105.06980
Miller et al., arxiv:2105.06979)

Hypernuclear EoS out ?!
→ stiff hypernuclear matter
→ early onset of deconfinement
(M_onset < 1.5 M_sun)

New quark matter paradigm:
→ deconfinement to stiff QM EoS
→ hybrid stars larger, higher M_{max}

LVC radius constraint
GW170817
(Abbott et al., PRL (2018))
NICER mass -radius constraint
PSR J0030+0451
(Miller et al., ApJLett. (2019))
PSR J0740+6620
(Miller et al., arxiv:2105.06979)

Constraints on NS mass and radii !

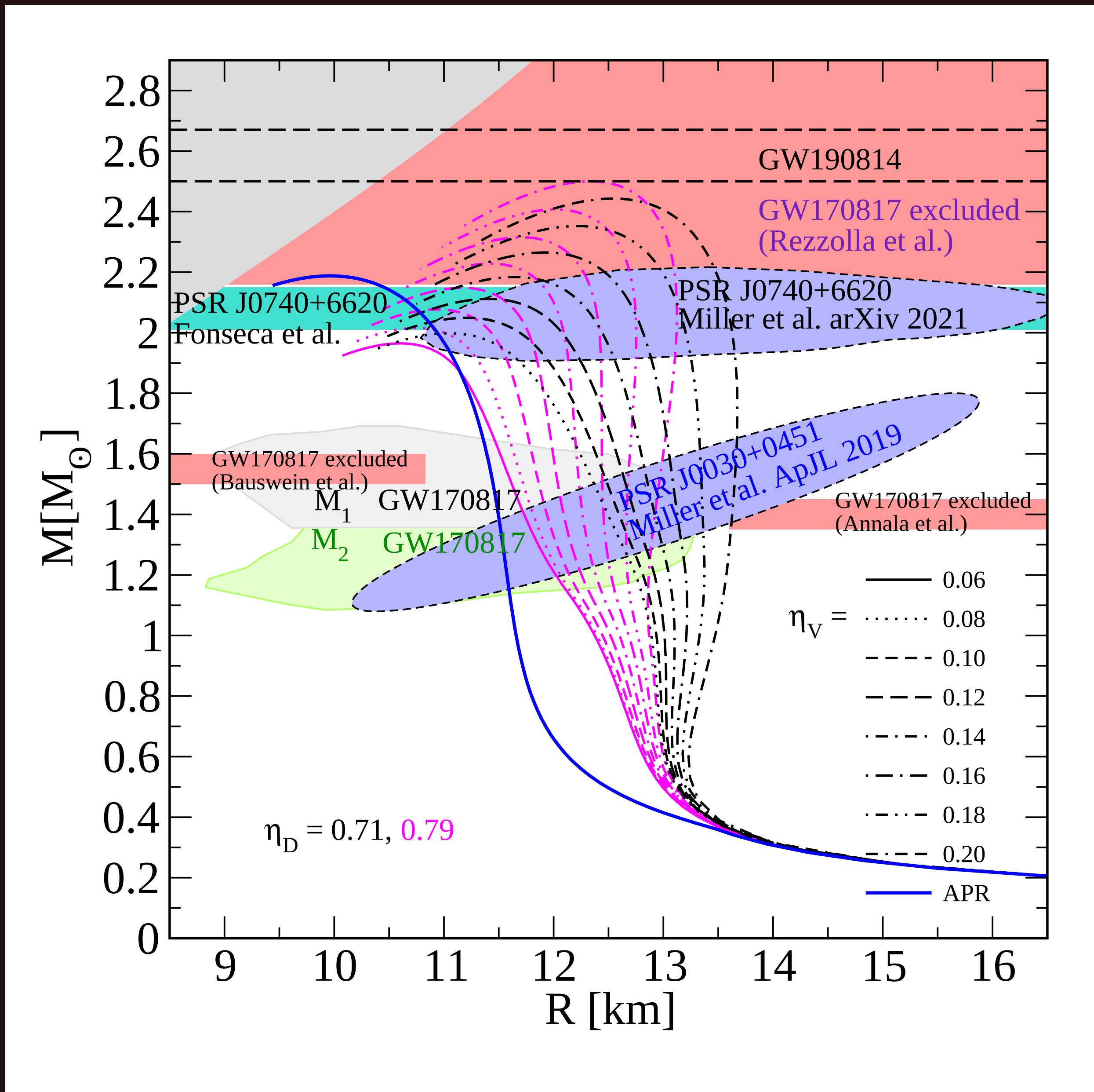

Ayriyan, Blaschke, Alvarez-Castillo et al., arXiv:2102.13485v2

GW190814 - Enigma

Heaviest NS or Lightest BH ??

M_1 = 22.2 – 24.3 M_o

M_2 = 2.50 – 2.67 M_o

(Abbott et al., ApJL 896:L44 (2020))

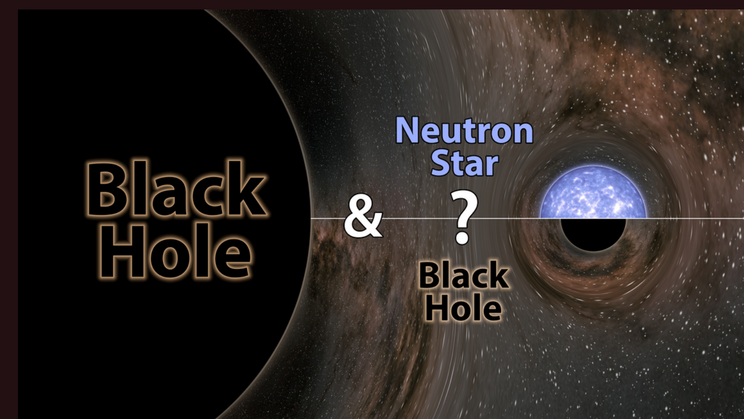

LVC radius constraint
GW170817
(Abbott et al., PRL (2018))
NICER mass -radius constraint
PSR J0030+0451
(Miller et al., ApJLett. (2019))
PSR J0740+6620
(Miller et al., arxiv:2105.06979)

NICER radius measurement on PSR J0740+6620

New, large NICER radius for J0740: Riley et al., 2105.06980; Miller et al., 2105.06979

1-σ regions, 60% confidence

Attention:

Above ~1.5 M_sun hyperons
Appear in the center of neutron stars.

Non-hyperonic nuclear EoS (APR)
Are no longer applicable for
High-mass neutron stars ~2M_sun !

Microscopic EoS need high-density
Stiffening of the hypernuclear EoS,
e.g., by multi-pomeron interactions.

Yamamoto et al., PRC 96 (2017)

Relativistic mean-field EoS have a
Maximal NS radius R_2.0 ~ 13 km

Way out:
early deconfinement to color
superconducting, stiff quark matter !

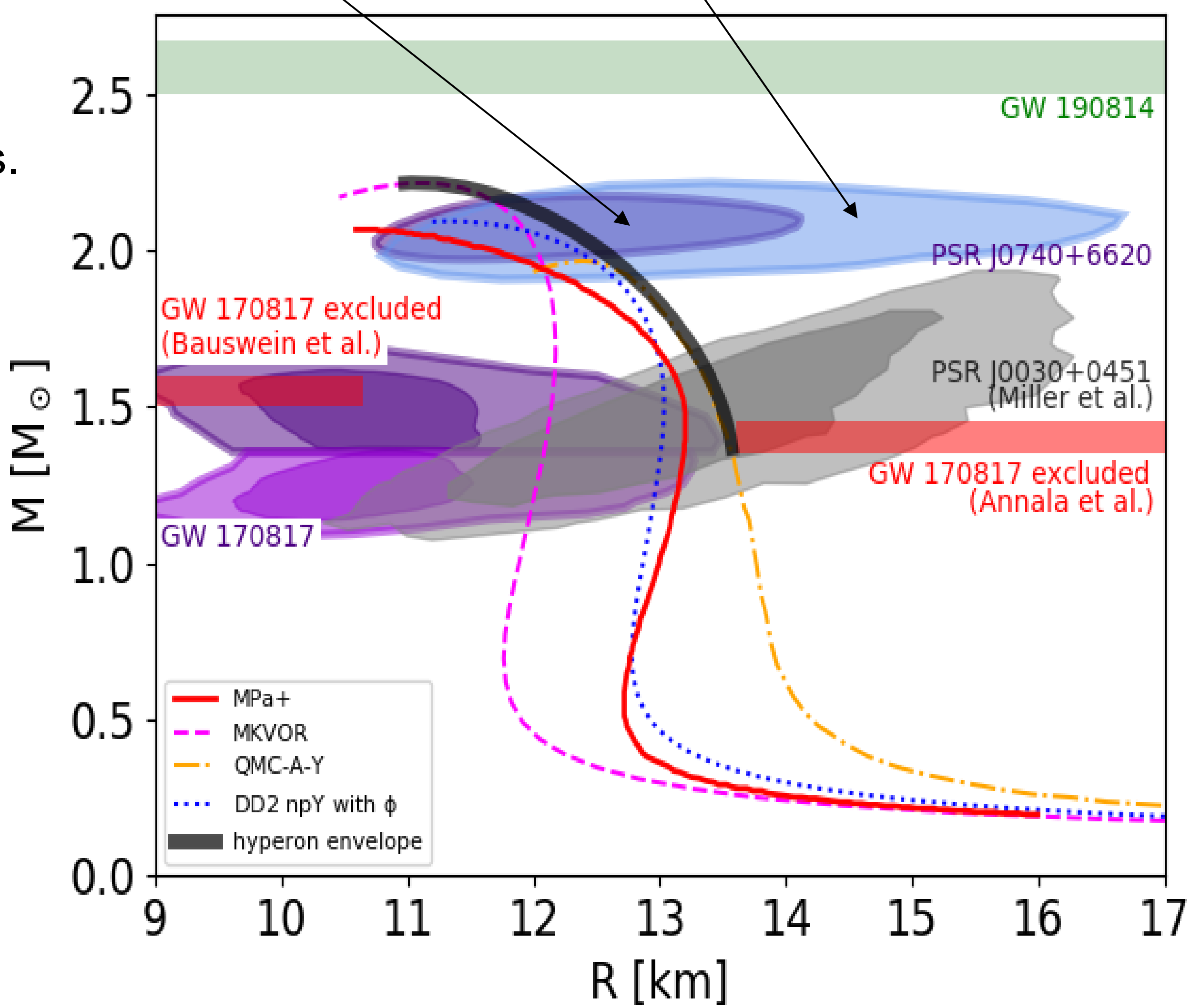

Shall the APR EoS be abandoned?

Y. Yamamoto, H. Togashi, T. Tamagawa, T. Furumoto, N. Yasutake, T. Rijken, PRC 96 (2017)

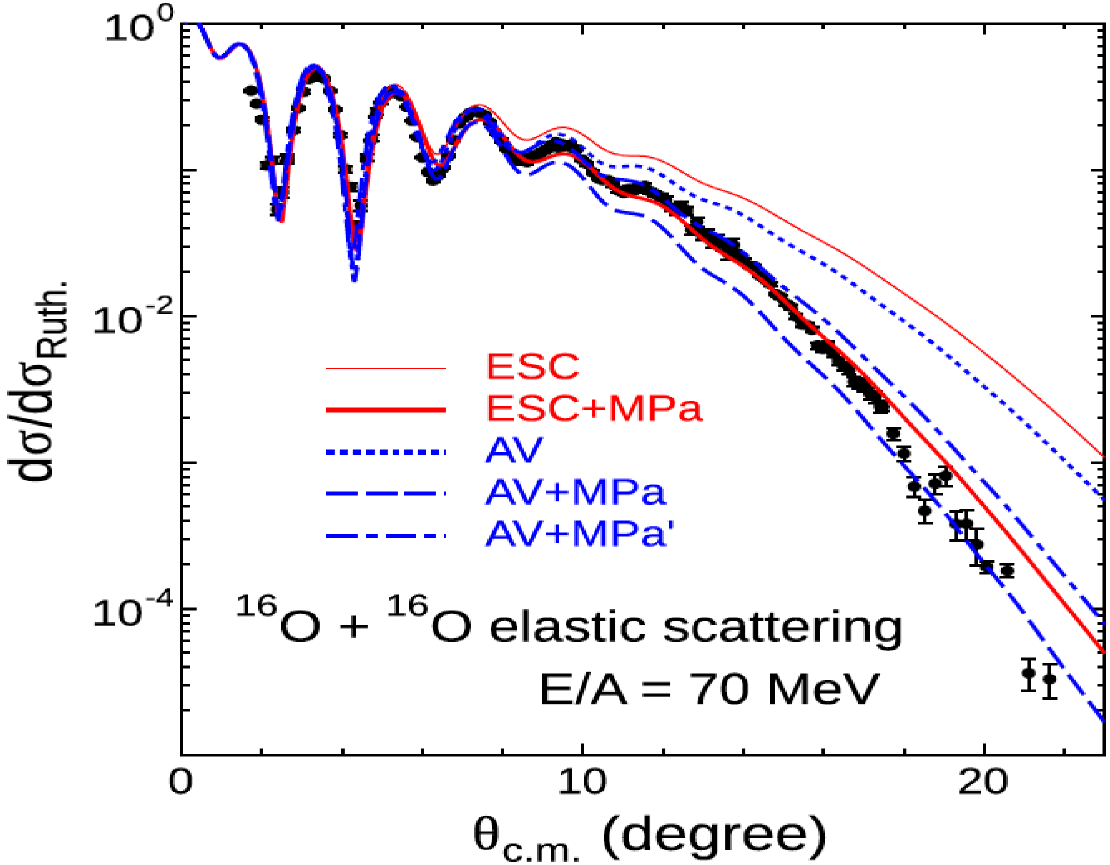

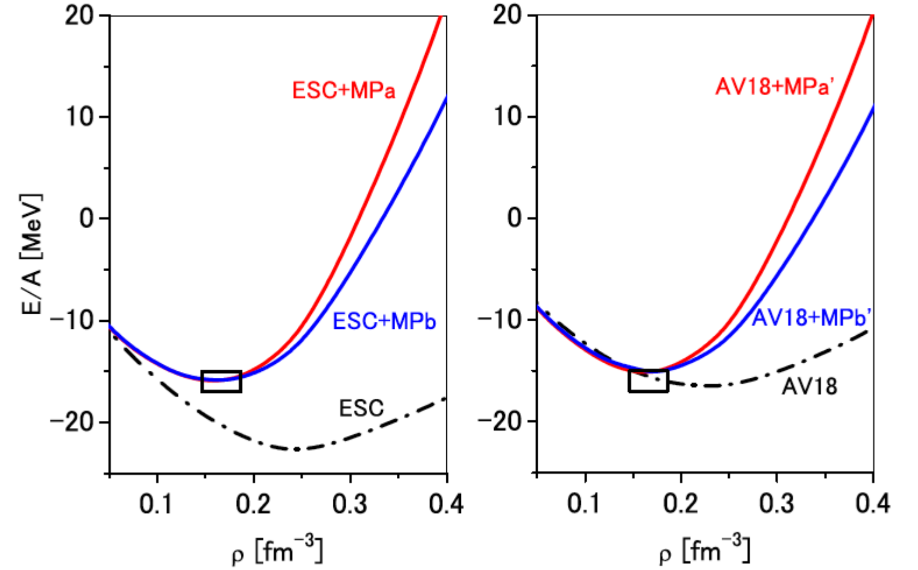

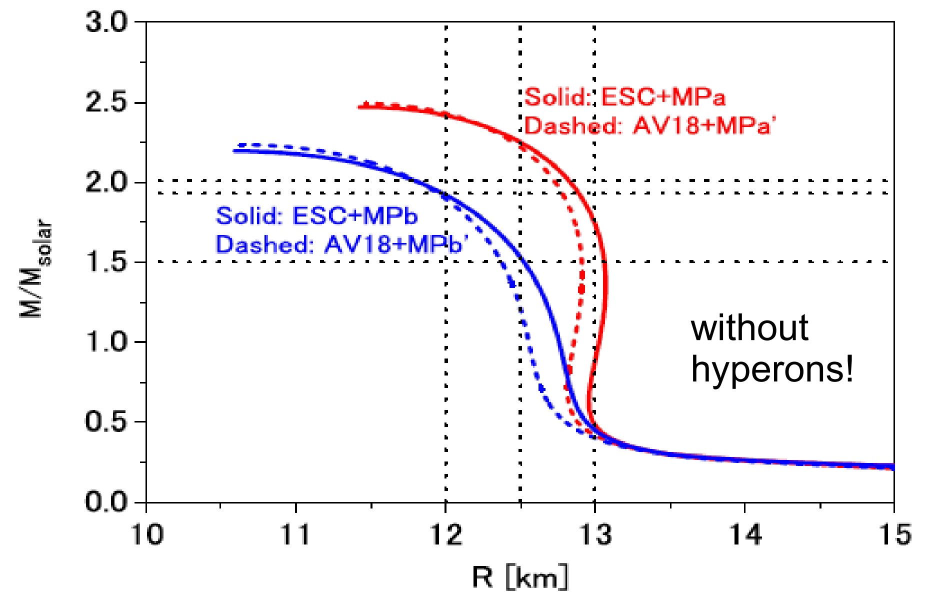

Short-range multipomeron exchange potential (MPP) added to AV18 potential gives significant improvement of large-angle scattering cross section (s.a.) and the Nuclear saturation properties, when compared to APR.
→ Neutron star radii R(M< 2 M_sun) > 12 km !!

What is the special point? What are its properties?

The TOV equation

$$\frac{\partial P(r)}{\partial r} = -\frac{\epsilon(r) M(r)\left(1+\frac{P(r)}{\epsilon(r)}\right)\left(1+\frac{4\pi r^3 P(r)}{M(r)}\right)}{r^2\left(1-\frac{2M(r)}{r}\right)}, \qquad \frac{\partial M(r)}{\partial r} = 4\pi r^2 \epsilon(r).$$

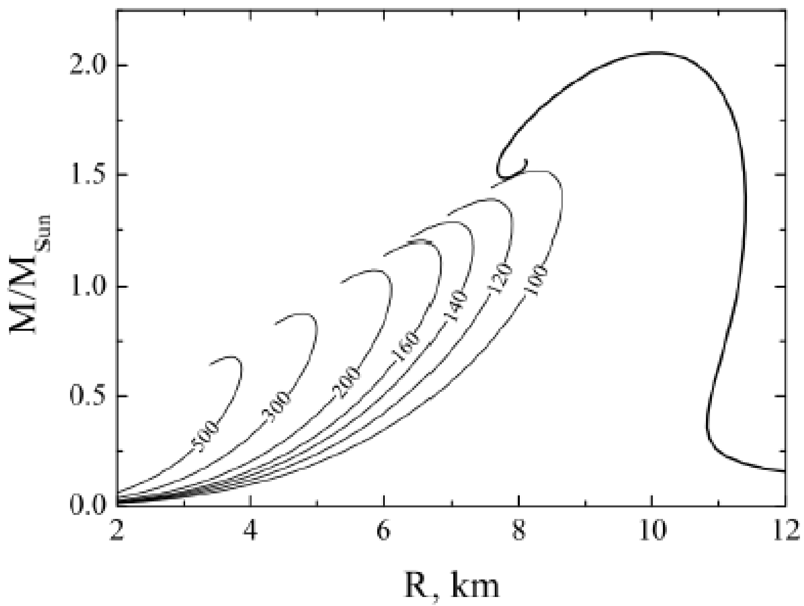

Fig. 1. Mass–radius diagram for a star made of ordinary matter (thick line) and purely quark stars (thin lines). The numbers at the lines indicate the parameter B.

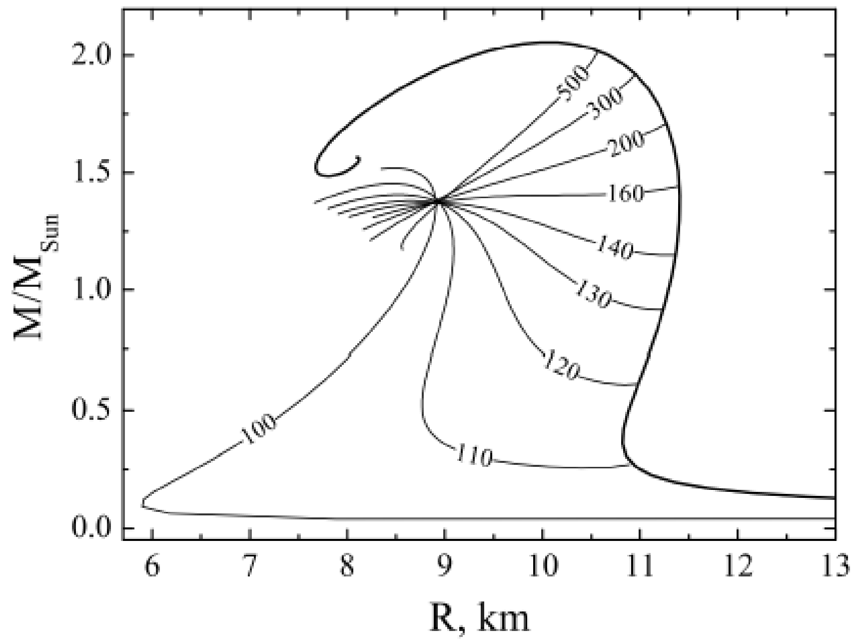

Fig. 2. Mass–radius diagram of hybrid stars for various values of the parameter B

[1]Yudin et al., Astron. Lett. **40** (2014), 201

What is the special point? What are its properties?

The constant–speed–of–sound (CSS) model:

– dimensionless baryochemical potential

$$\hat{\mu}_B = \frac{\mu_B}{\mu_{scale}} = \left(\frac{p+B}{A}\right)^{1/(1+\beta)},$$

– pressure

$$p(\mu_B) = A\hat{\mu}_B^{1+\beta} - B,$$

– baryon density

$$n_B(\mu_B) = (1+\beta)\frac{A}{\mu_{scale}}\hat{\mu}_B^{\beta},$$

– energy density

$$\epsilon = B + \beta A\hat{\mu}_B^{1+\beta},$$

– $p(\epsilon)$ relation: $\epsilon = \beta p + (1+\beta)B$.

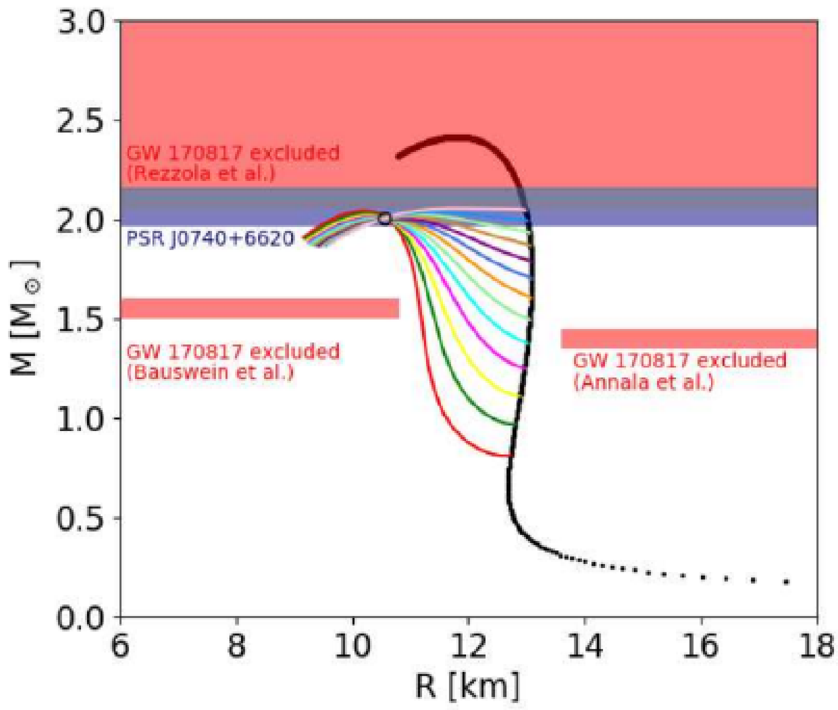

[3] Cierniak, Blaschke, Eur.Phys.J.ST **229** (2020) no.22-23, 3663-3673

What is the special point? What are its properties?

The constant–speed–of–sound (CSS) model:

– dimensionless baryochemical potential

$$\hat{\mu}_B = \frac{\mu_B}{\mu_{scale}} = \left(\frac{p+B}{A}\right)^{1/(1+\beta)},$$

– pressure

$$p(\mu_B) = A\hat{\mu}_B^{1+\beta} - B,$$

– baryon density

$$n_B(\mu_B) = (1+\beta)\frac{A}{\mu_{scale}}\hat{\mu}_B^{\beta},$$

– energy density

$$\epsilon = B + \beta A\hat{\mu}_B^{1+\beta},$$

– $p(\epsilon)$ relation: $\epsilon = \beta p + (1+\beta)B.$

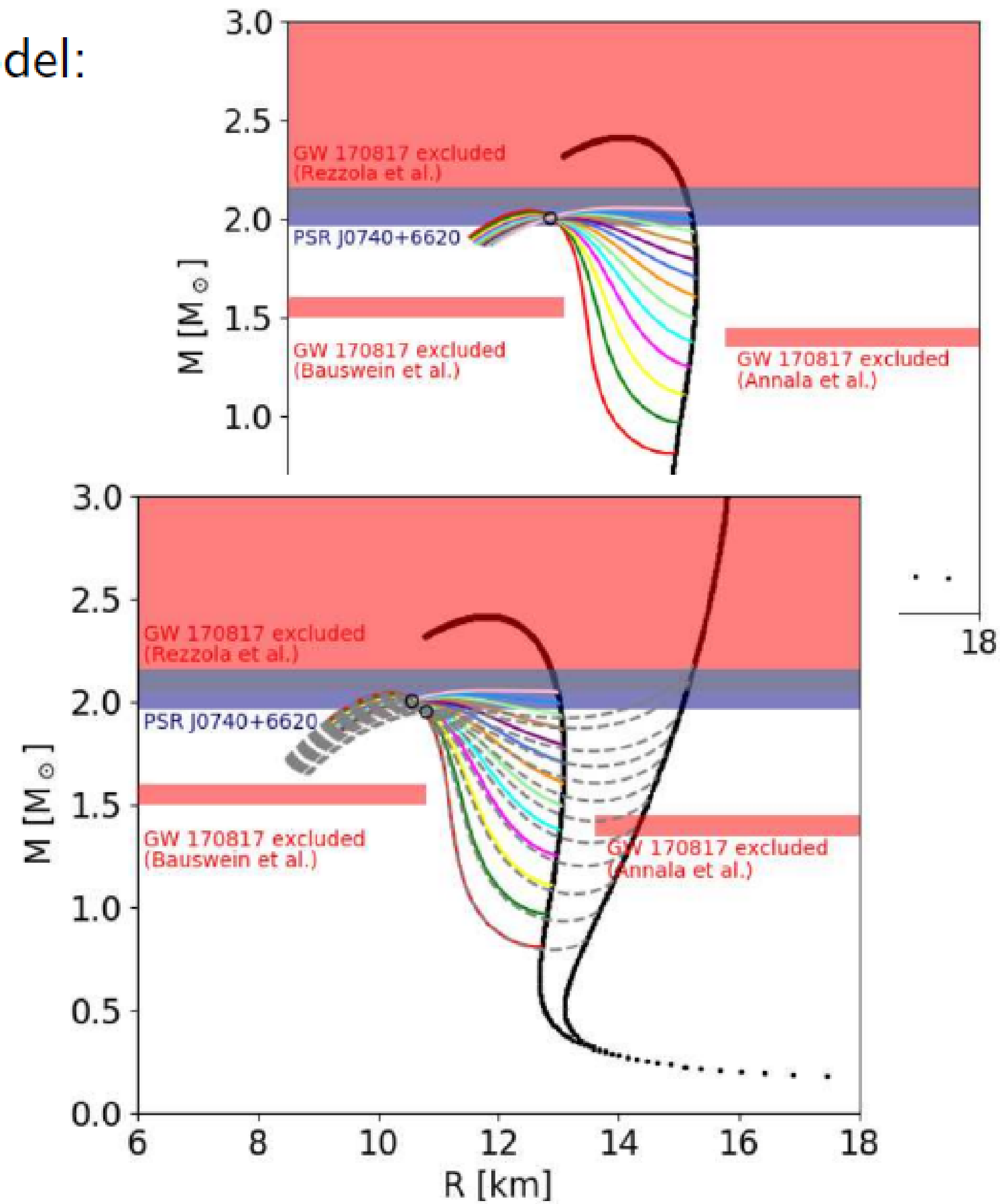

[3] Cierniak, Blaschke, Eur.Phys.J.ST **229** (2020) no.22-23, 3663-3673

What is the special point? What are its properties?

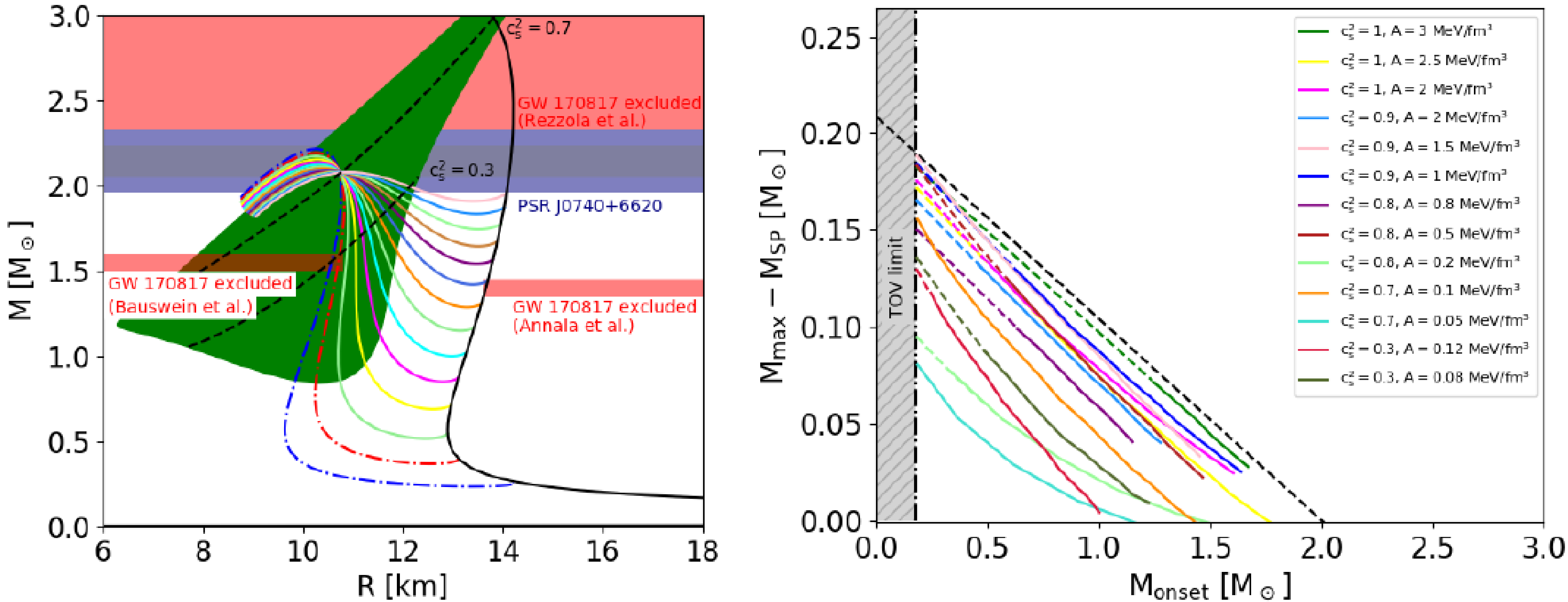

$$M_{max} = M_{SP} + 0.208 M_{\odot} - 0.104 M_{onset}$$

[3] Cierniak, Blaschke, Eur.Phys.J.ST **229** (2020) no.22-23, 3663-3673

What is the special point? What are its properties?

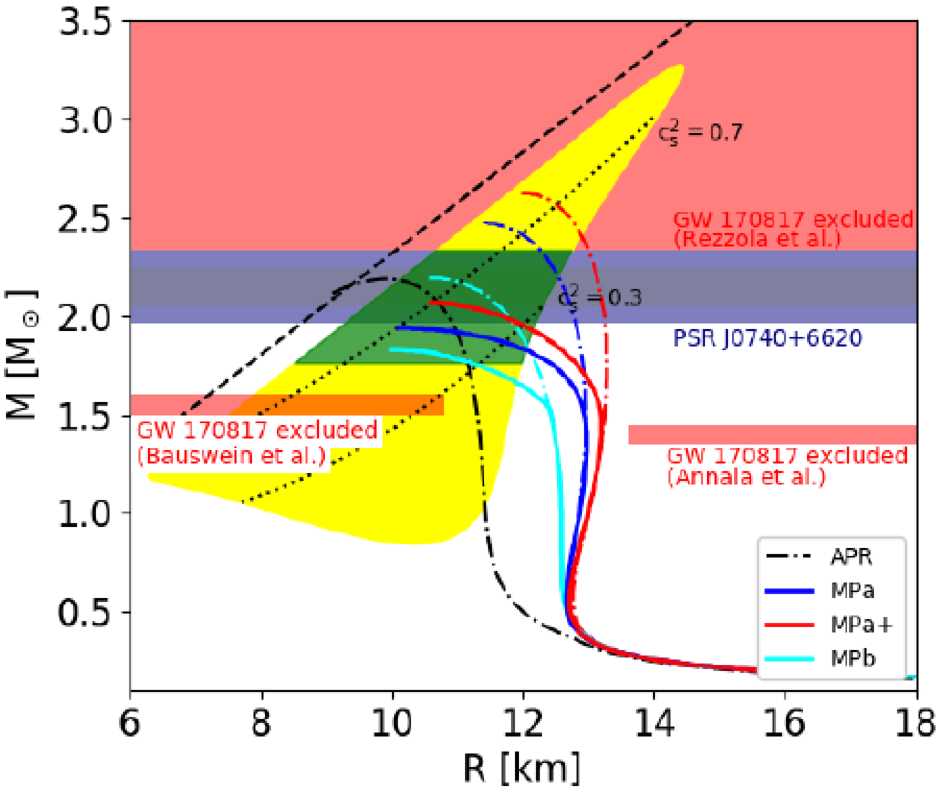

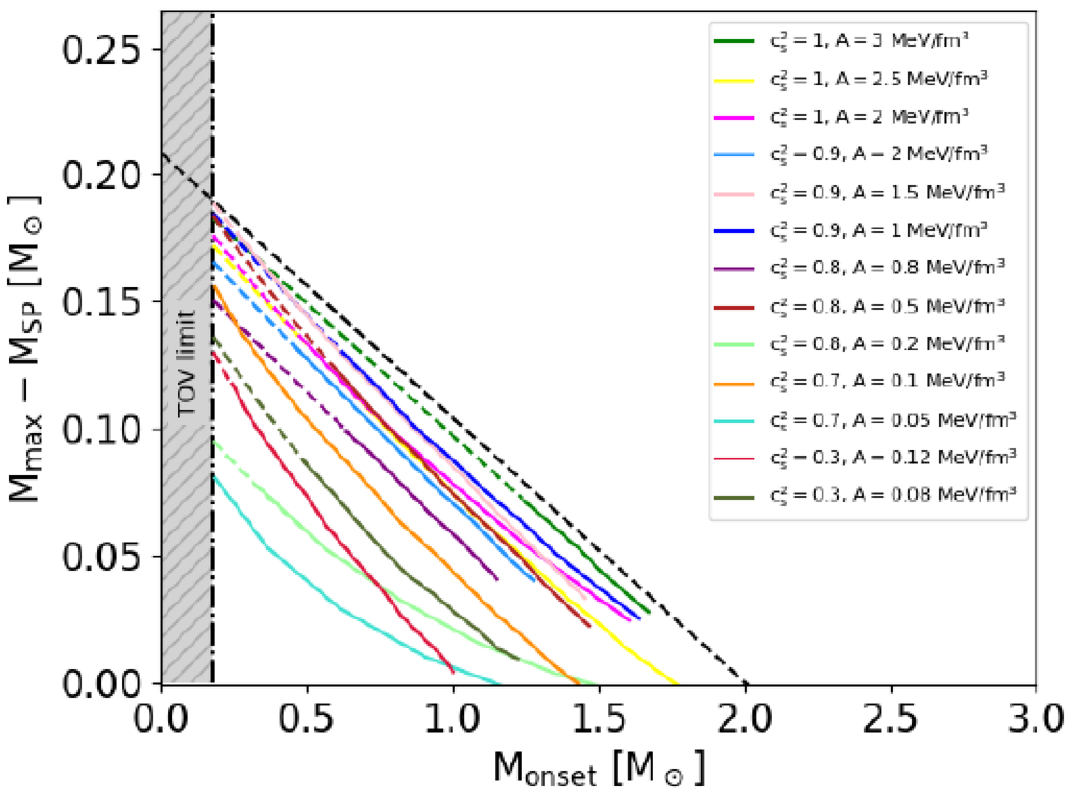

$$M_{max} = M_{SP} + 0.208 M_\odot - 0.104 M_{onset}$$

[3] Cierniak, Blaschke, Eur.Phys.J.ST **229** (2020) no.22-23, 3663-3673

Dependence on the phase transition construction?

The mixed phase parabolic ansatz:

$$P_M(\mu) \;=\; \alpha_2(\mu-\mu_c)^2 \;+\; \alpha_1(\mu-\mu_c) \;+\; (1+\Delta_P)P_c,$$

Gibbs condition for phase equilibrium:

$$P_H(\mu_H) = P_M(\mu_H)\ ,$$
$$P_Q(\mu_Q) = P_M(\mu_Q)\ ,$$
$$\frac{\partial^k}{\partial\mu^k}P_H(\mu_H) = \frac{\partial^k}{\partial\mu^k}P_M(\mu_H)\ ,$$
$$\frac{\partial^k}{\partial\mu^k}P_Q(\mu_Q) = \frac{\partial^k}{\partial\mu^k}P_M(\mu_Q)\ .$$

Derived parameters (k = 1):

$$\alpha_1 = \frac{-2\kappa_1+\kappa_2(\mu_c-\mu_H)}{2(\mu_c-\mu_Q)(\mu_H-\mu_Q)},$$

$$\alpha_2 = \frac{-2\kappa_1+\kappa_2(\mu_c-\mu_Q)}{2(\mu_c-\mu_H)(\mu_H-\mu_Q)},$$

$$\kappa_1 = n_Q(\mu_c-\mu_Q) - n_H(\mu_c-\mu_H) + P_Q - P_H,$$

$$\kappa_2 = n_Q - n_H.$$

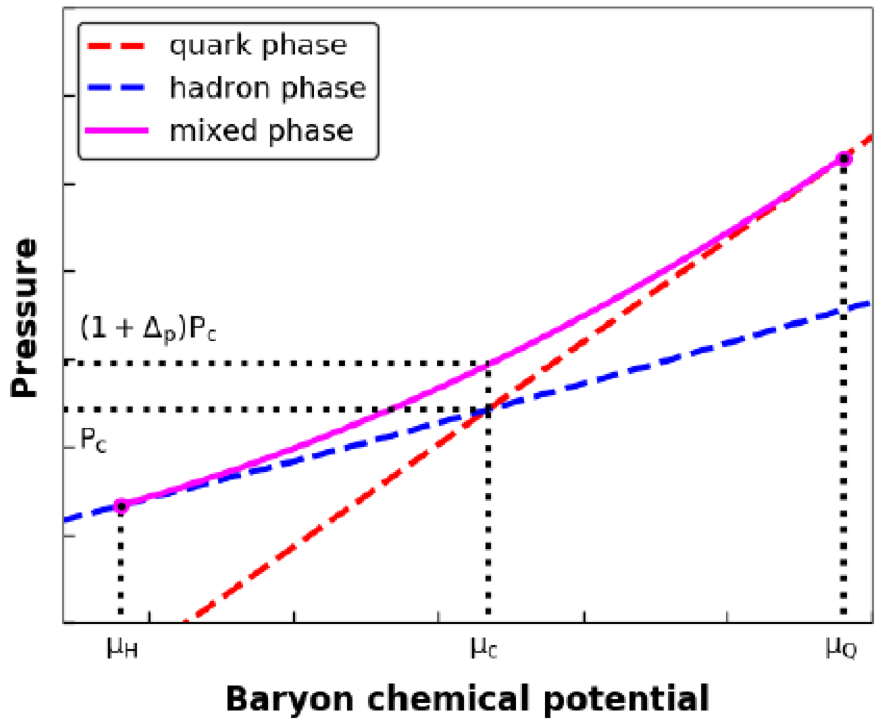

[4] Abgaryan, et al., Universe **4** (2018), 94

Dependence on the phase transition construction?

The mixed phase parabolic ansatz:

$$P_M(\mu) \ = \ \alpha_2(\mu - \mu_c)^2 \ + \ \alpha_1(\mu - \mu_c) \ + \ (1 + \Delta_P)P_c,$$

Gibbs condition for phase equilibrium:

$$P_H(\mu_H) = P_M(\mu_H) \ ,$$
$$P_Q(\mu_Q) = P_M(\mu_Q) \ ,$$
$$\frac{\partial^k}{\partial \mu^k} P_H(\mu_H) = \frac{\partial^k}{\partial \mu^k} P_M(\mu_H) \ ,$$
$$\frac{\partial^k}{\partial \mu^k} P_Q(\mu_Q) = \frac{\partial^k}{\partial \mu^k} P_M(\mu_Q) \ .$$

Derived parameters (k = 1):

$$\alpha_1 = \frac{-2\kappa_1 + \kappa_2(\mu_c - \mu_H)}{2(\mu_c - \mu_Q)(\mu_H - \mu_Q)},$$

$$\alpha_2 = \frac{-2\kappa_1 + \kappa_2(\mu_c - \mu_Q)}{2(\mu_c - \mu_H)(\mu_H - \mu_Q)},$$

$$\kappa_1 = n_Q(\mu_c - \mu_Q) - n_H(\mu_c - \mu_H) + P_Q - P_H,$$

$$\kappa_2 = n_Q - n_H.$$

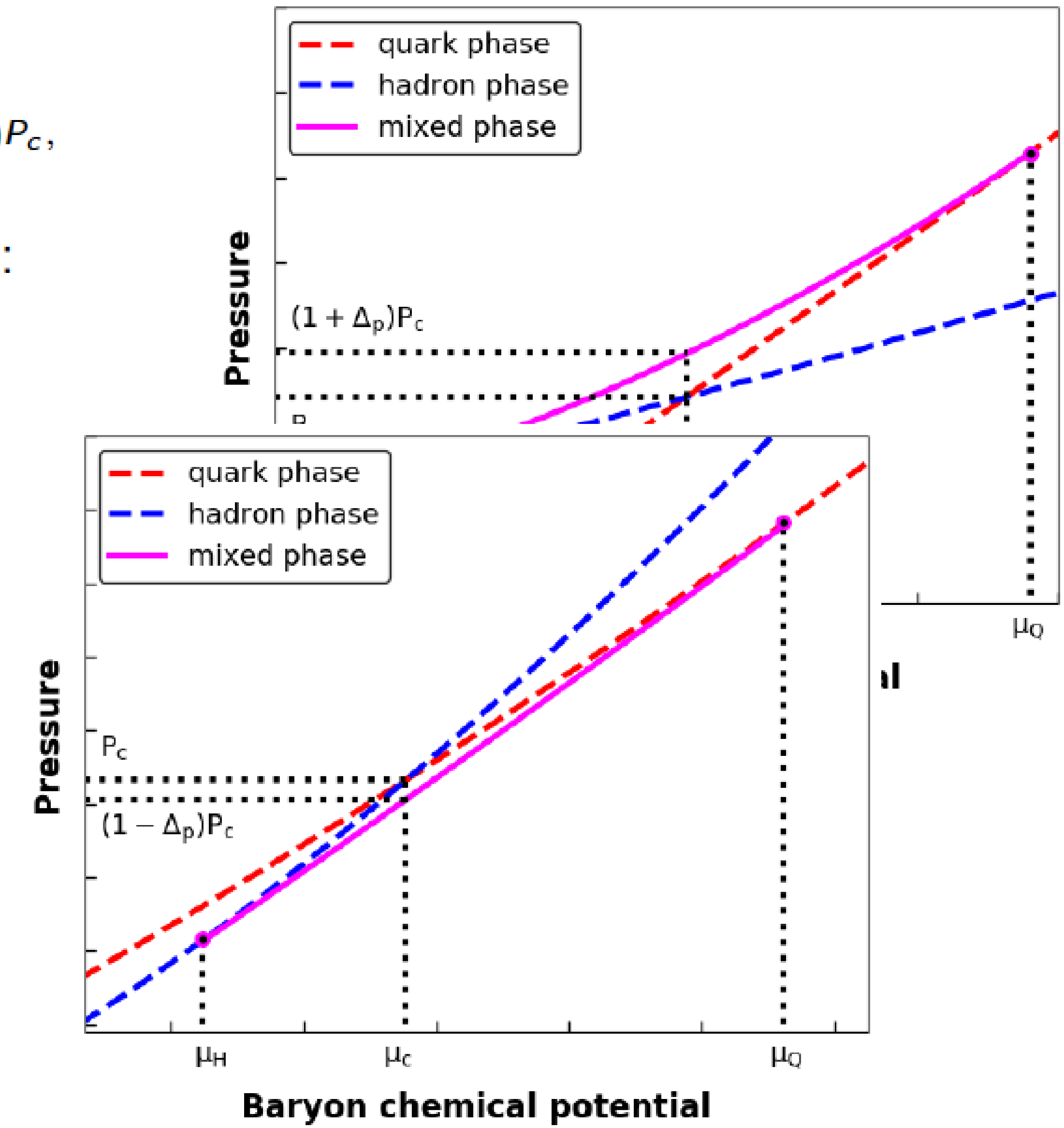

[4] Abgaryan, et al., Universe **4** (2018), 94

Dependence on the phase transition construction?

Invariance w.r.t. Maxwell −> mixed phase construction (pasta phases)

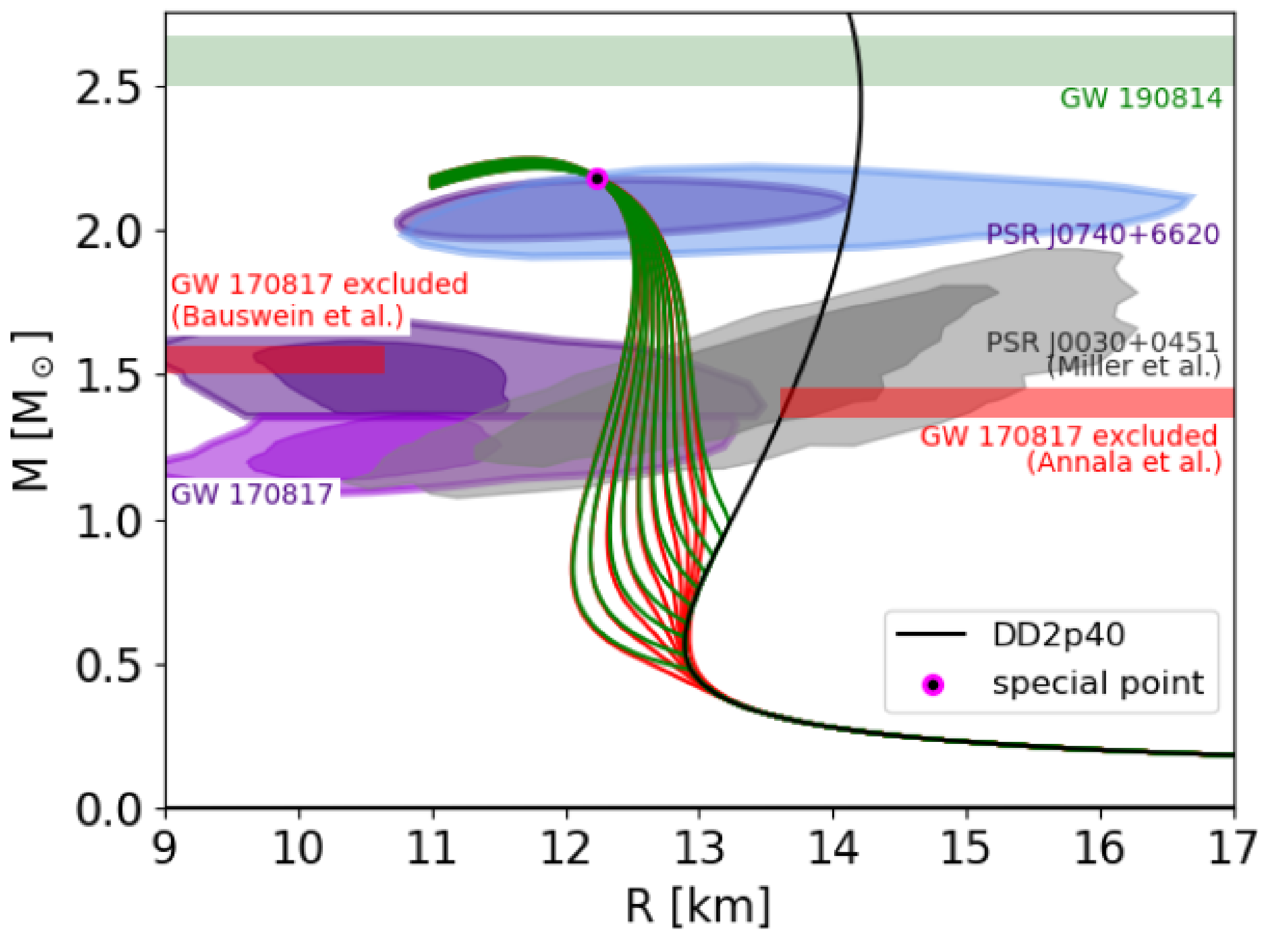

[5] Cierniak, Blaschke, Astron. Nachr. (2021), arXiV: 2106.06986

Dependence on the phase transition construction?

Invariance w.r.t. Maxwell $->$ interpolation construction (soft - stiff transition)

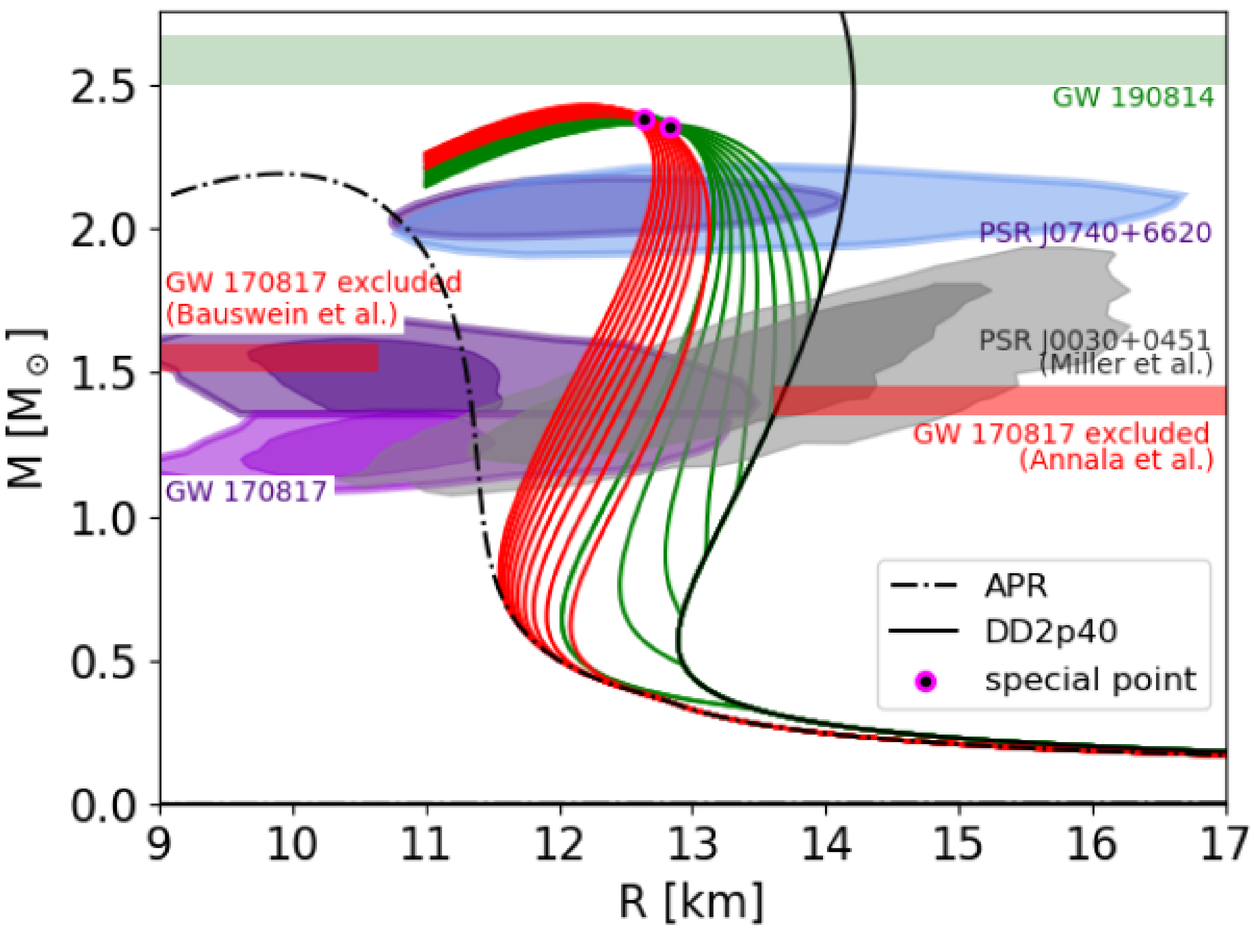

[5] Cierniak, Blaschke, Astron. Nachr. (2021), arXiV: 2106.06986

Mapping the special point locations ...

Special point locations for constant sound speed c_s

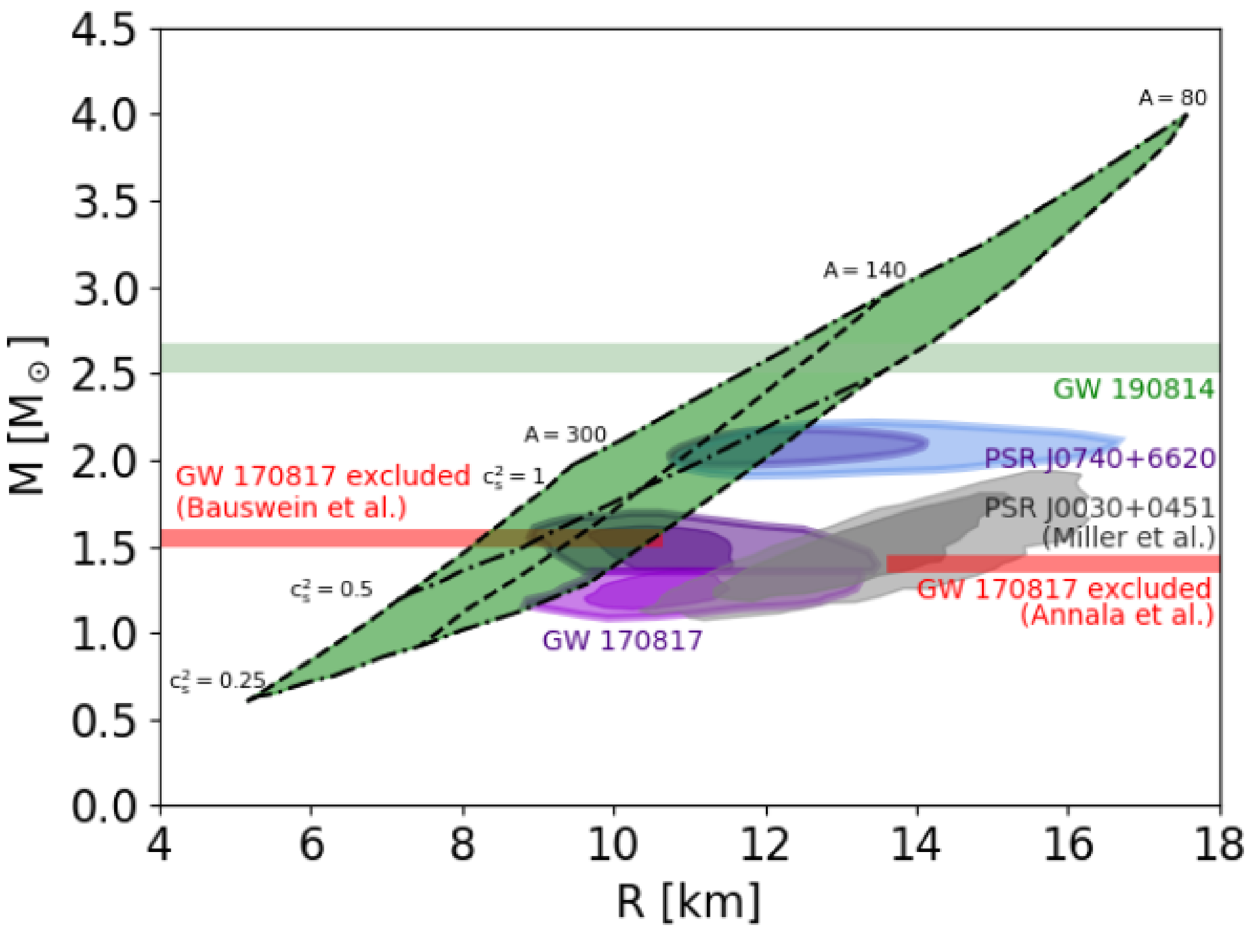

[5] Cierniak, Blaschke, Astron. Nachr. (2021), arXiV: 2106.06986

Mapping the special point locations ...

Special point locations for constant sound speed c_s

... and constant prefactor A

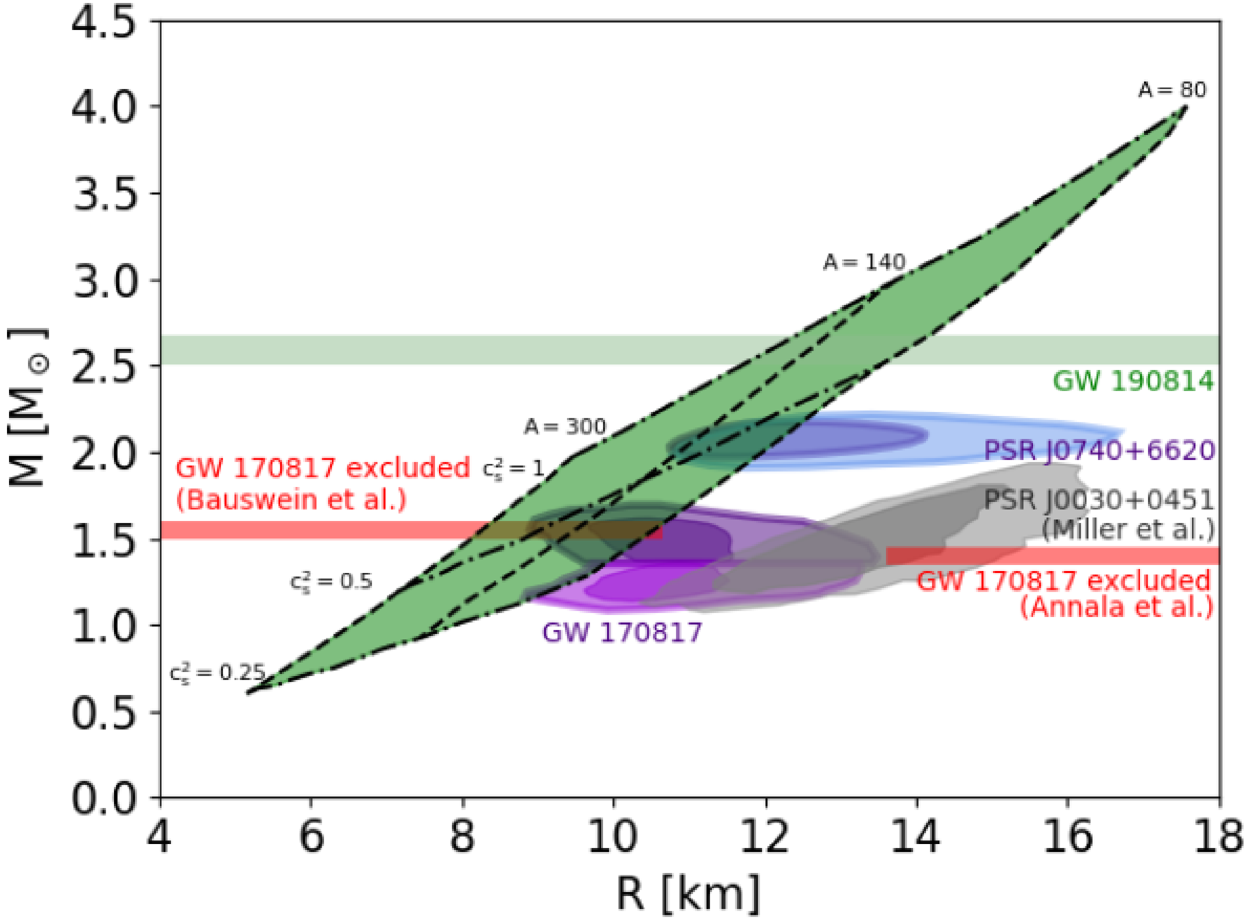

[5] Cierniak, Blaschke, Astron. Nachr. (2021), arXiV: 2106.06986

Mapping the special point locations ...

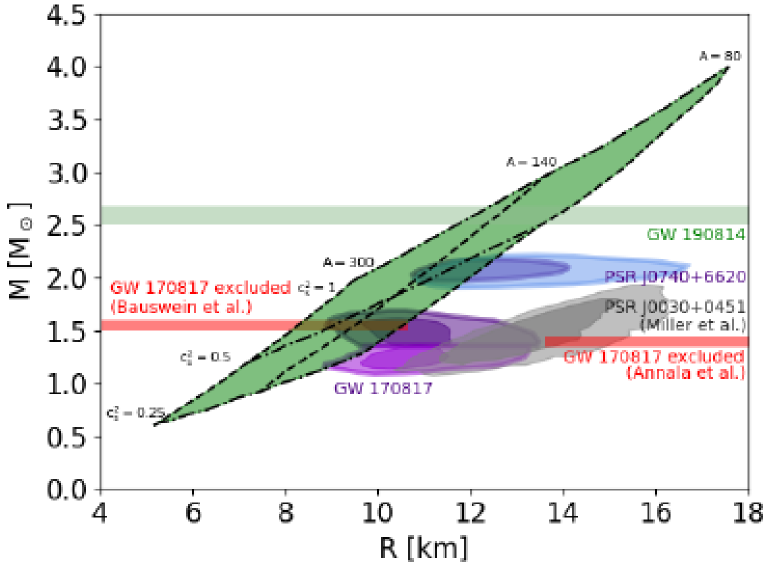

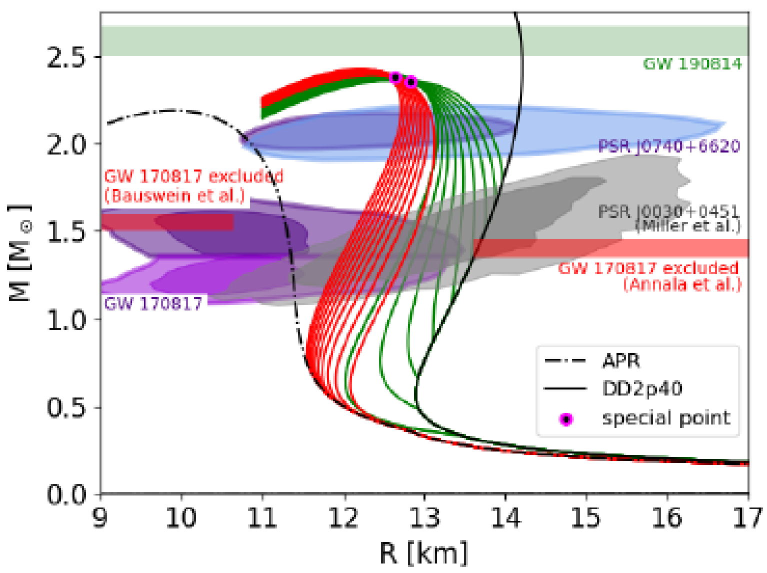

c_s^2	M_{SP} $[M_\odot]$	R_{min} [km]	R_{max} [km]
0.35	1.82	-	-
0.40	2.07	12.18	12.29
0.45	2.30	11.84	13.41
0.50	2.50	11.56	13.91
0.55	2.68	11.30	14.20
0.60	2.86	11.05	14.45
0.70	3.22	10.67	14.67
1.00	4.00	9.95	14.84

The values of c_s^2, largest possible M_{SP} and the radii range ($R_{min} - R_{max}$) of a 2 $M_\odot$ hybrid star.

---

[5] Cierniak, Blaschke, Astron. Nachr. (2021), arXiV: 2106.06986

Mapping the special point locations ...

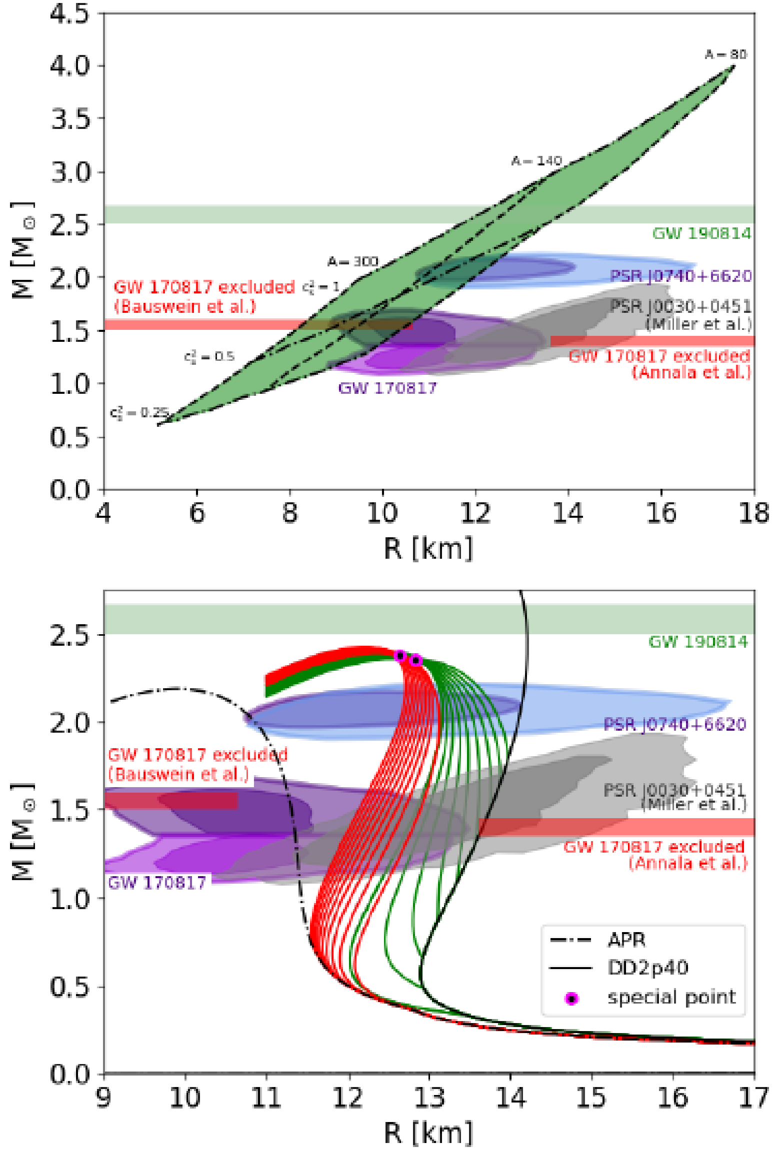

c_s^2	$M_{\rm SP}$ $[M_\odot]$	$R_{\rm min}$ [km]	$R_{\rm max}$ [km]
0.35	1.82	-	-
0.40	2.07	12.18	12.29
0.45	**2.30**	**11.84**	**13.41**
0.50	**2.50**	**11.56**	**13.91**
0.55	**2.68**	**11.30**	**14.20**
0.60	2.86	11.05	14.45
0.70	3.22	10.67	14.67
1.00	4.00	9.95	14.84

The values of c_s^2, largest possible M_{SP} and the radii range ($R_{min} - R_{max}$) of a 2 $M_\odot$ hybrid star. **Bold red rows correspond to the nlNJL fit from [6].**

[6] Antić, Shahrbaf, Blaschke, Grunfeld, arXiV: 2105.00029

Constant sound speed (CSS) vs. nonlocal NJL model

$$\mathcal{L} = \bar\psi\left(-i\partial\!\!\!/ + m_c\right)\psi - \frac{G_S}{2} j_S^f j_S^f - \frac{G_D}{2}[j_D^a]^\dagger j_D^a + \frac{G_V}{2} j_V^\mu j_V^\mu\,, \qquad \eta_D = G_D/G_S \text{ and } \eta_V = G_V/G_S$$

Nonlocal currents, formfactor g(z)

$$j_S^f(x) = \int d^4z g(z)\bar\psi(x+\frac{z}{2})\Gamma^f\psi(x-\frac{z}{2})\,,$$
$$j_D^a(x) = \int d^4z g(z)\bar\psi_C(x+\frac{z}{2})i\gamma_5\tau_2\lambda^a\psi(x-\frac{z}{2})\,,$$
$$j_V^\mu(x) = \int d^4z g(z)\bar\psi(x+\frac{z}{2})i\gamma_\mu\psi(x-\frac{z}{2})\,,$$

CSS equation of state

$$P(\mu) = A\left(\frac{\mu}{\mu_x}\right)^{1+\beta} - B,$$

Fitted relationship, see figure →

$$A = a_1\eta_D + b_1\eta_V^2 + c_1$$
$$c_s^2 = a_2\eta_D + b_2\eta_V^2 + c_2$$
$$B = a_3\eta_D + b_3\eta_V^2 + c_3,$$

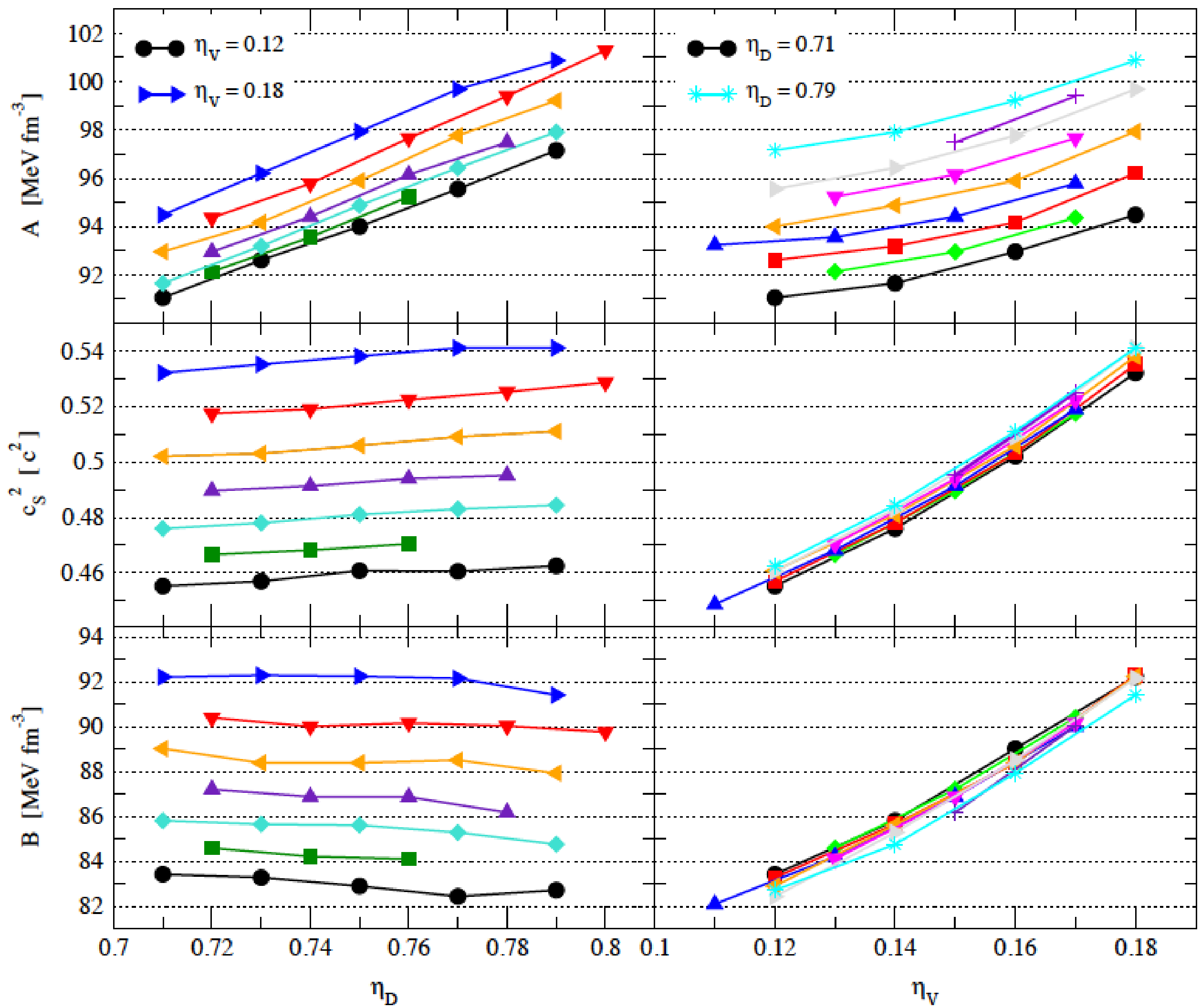

Perfect mapping nlNJL → CSS, Antic et al., arxiv:2105.00029

Constant sound speed (CSS) vs. nonlocal NJL model

"Trains" of special points, when η_D and η_V are varied systematically (grid)

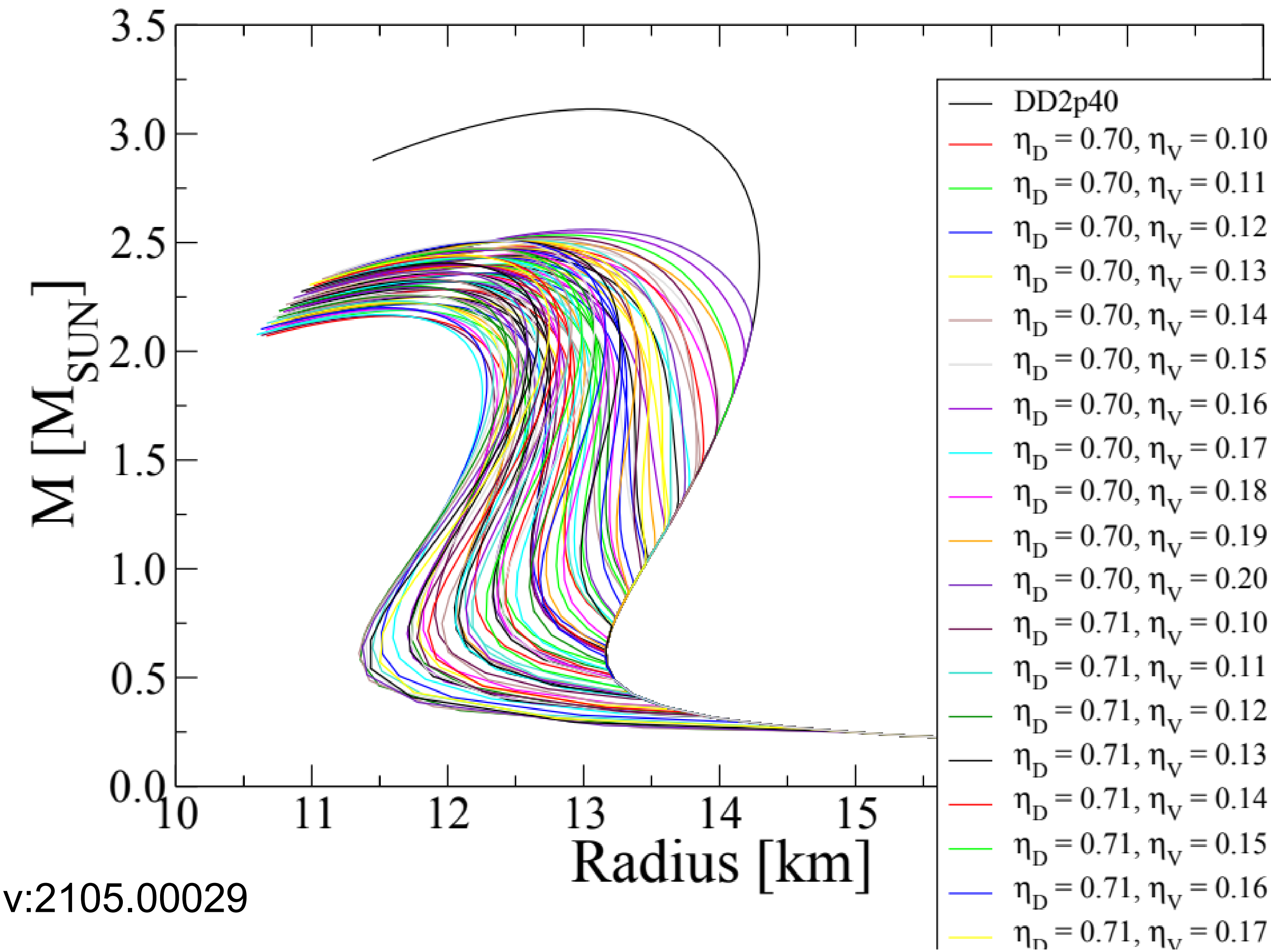

Antic et al., arxiv:2105.00029

Constant sound speed (CSS) vs. nonlocal NJL model

“Trains” of special points, when η_D and η_V are varied systematically (grid)

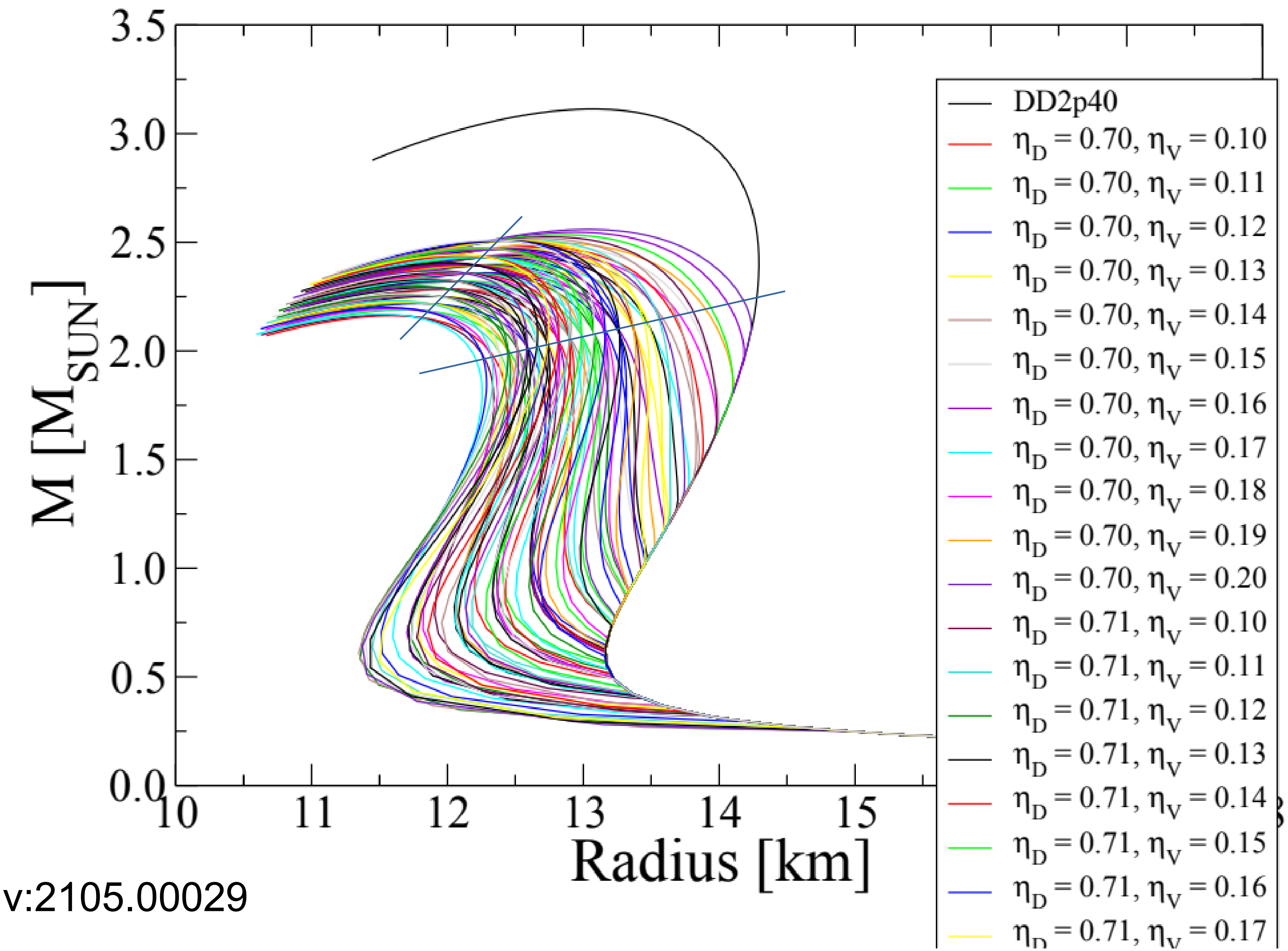

Antic et al., arxiv:2105.00029

Old paradigm: hybrid stars smaller and lighter

Works on **Special Point** with M. Cierniak: 2012.15785 & 2009.12353; EPJ ST 229, 3663 (2020)

Dense quark plasma in color superconducting phase: nlNJL mode

Constant-speed-of-sound (CSS) Equation of state (EoS)

$$p(\mu) = A(\mu/\mu_0)^{1+c_s^{-2}} - B,$$

$$p = c_s^2 \varepsilon - (1 + c_s^2) B$$

Perfect mapping nlNJL → CSS , Antic et al., arxiv:2105.00029

Maxwell construction with (1st order phase transition)
Relativistic Density Functional EoS "DD2pxy" by S. Typel
With density-dependent coupling
And excluded volume v=x.y fm^3

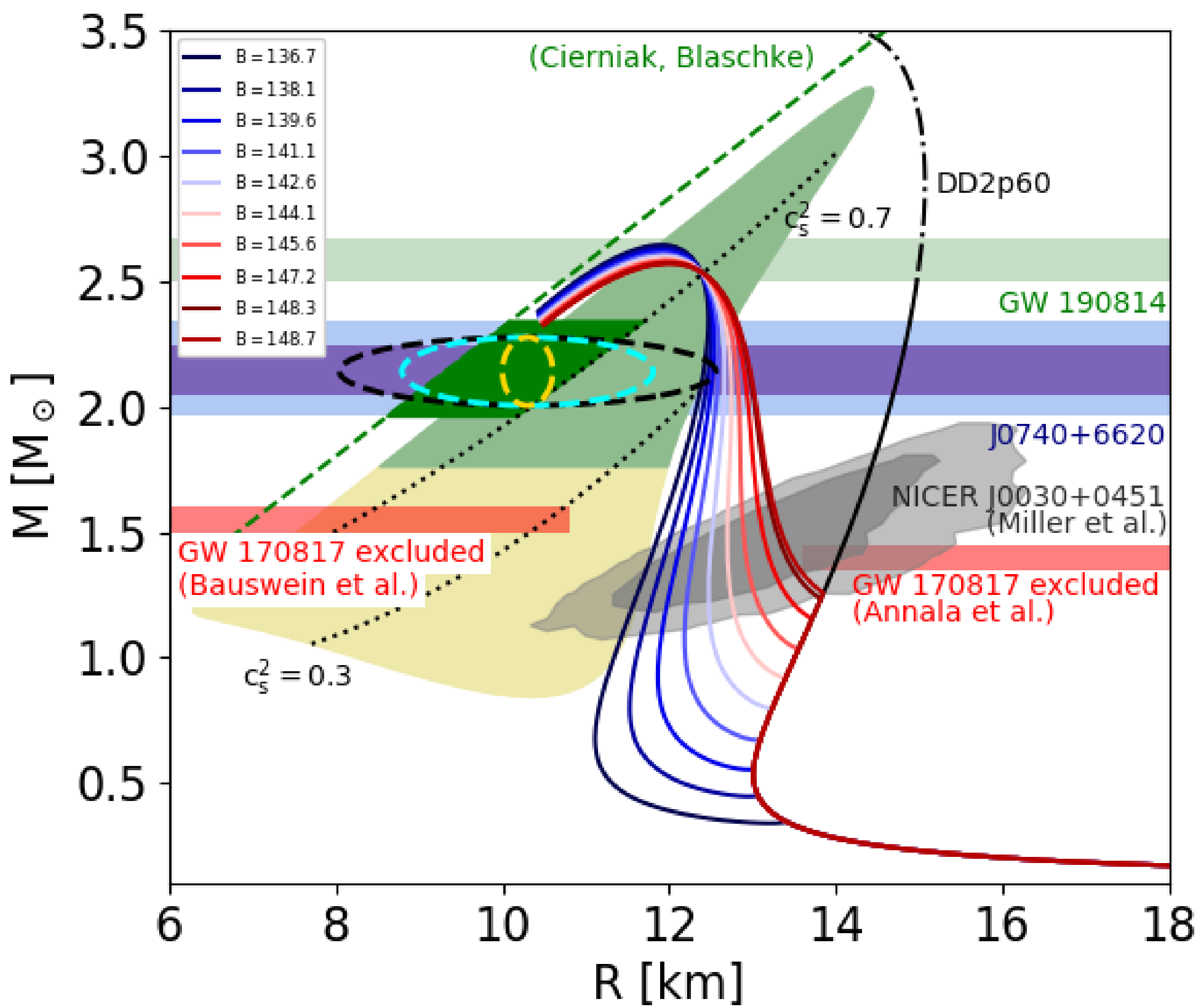

2.6 M_sun object can by a hybrid neutron star! With early onset of deconfinement and twins!
NICER radius measurement on PSR J0740+6620 will put constraints on this too!

New paradigm: hybrid stars larger and heavier

Work based on **Special Point location** with M. Cierniak, in preparation

Dense quark plasma in color superconducting phase: nlNJL model

Constant-speed-of-sound (CSS) Equation of state (EoS)

$$p(\mu) = A(\mu/\mu_0)^{1+c_s^{-2}} - B,$$

$$p = c_s^2\varepsilon - (1 + c_s^2)B$$

Perfect mapping nlNJL → CSS , Antic et al., arxiv:2105.00029

Maxwell construction with (1st order phase transition)
Relativistic Density Functional EoS “DD2-Y-T” by S. Typel
With density-dependent coupling

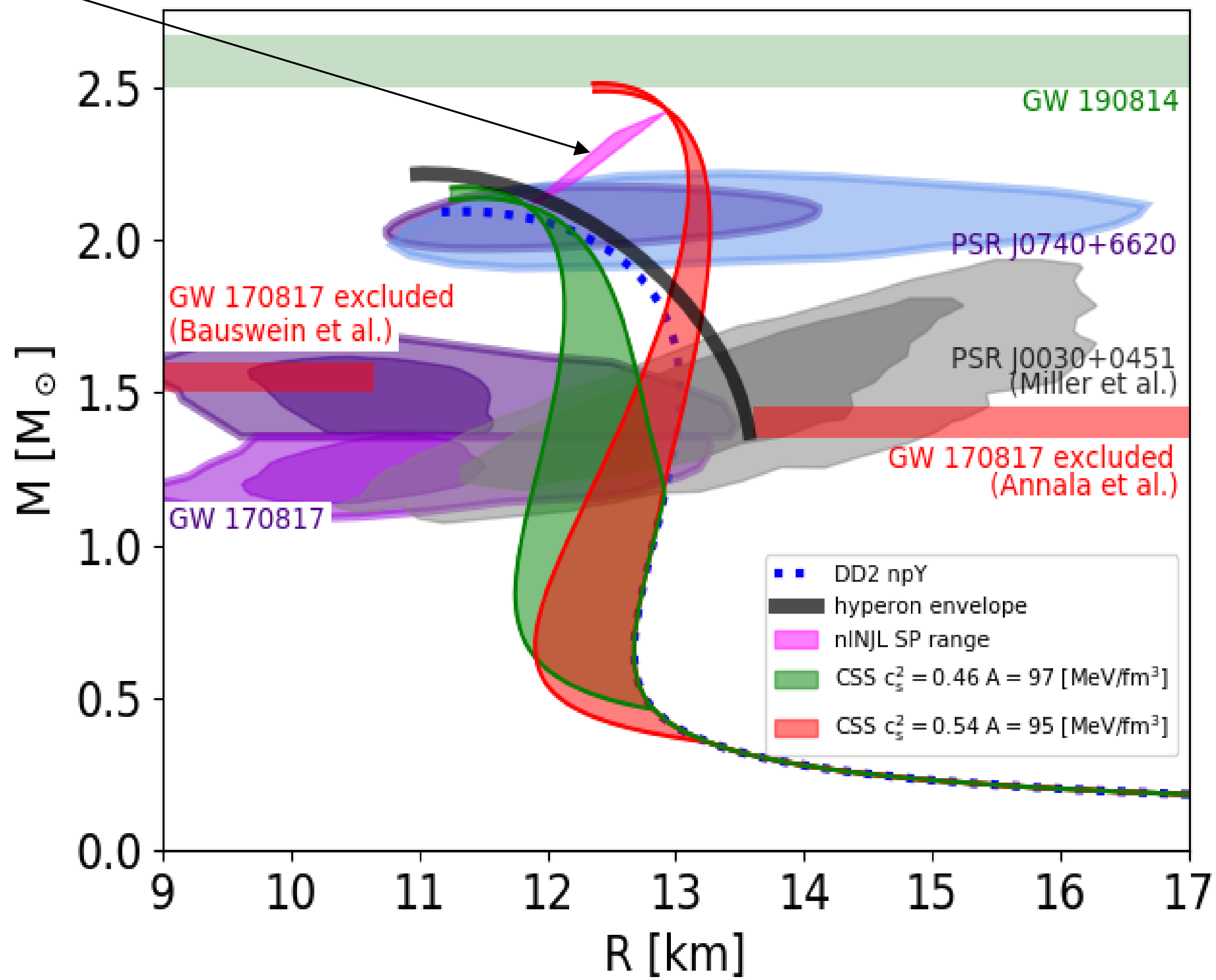

2.5 M_sun object can by a hybrid neutron star! With early onset of deconfinement!
NICER radius measurement on PSR J0740+6620 best described by hybrid stars!

CEP in the QCD phase diagram: HIC vs. Astrophysics

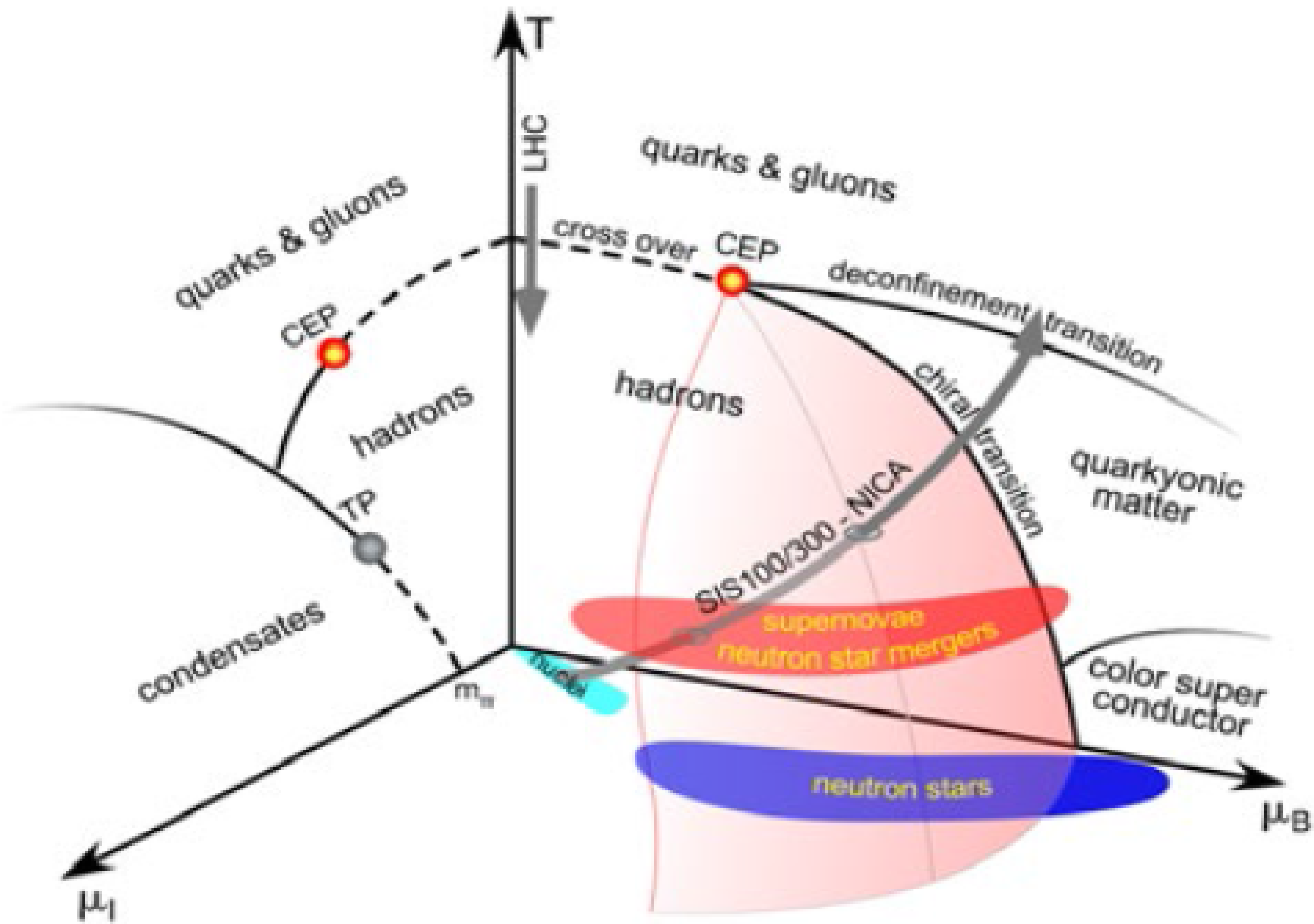

NuPECC Long Range Plan 2017; http://www.nupecc.org

A. Andronic, D. Blaschke, et al., "Hadron production ...", Nucl. Phys. A 837 (2010) 65 - 86

Binary neutron star merger simulation

S. Blacker & A. Bauswein (GSI Darmstadt), 1.35 M_sun + 1.35 M_sun

https://www.gsi.de/fileadmin/theorie/simulation-neutron-star-merger.mp4

Population of the QCD phase diagram with mixed phase, 6… 25 ms

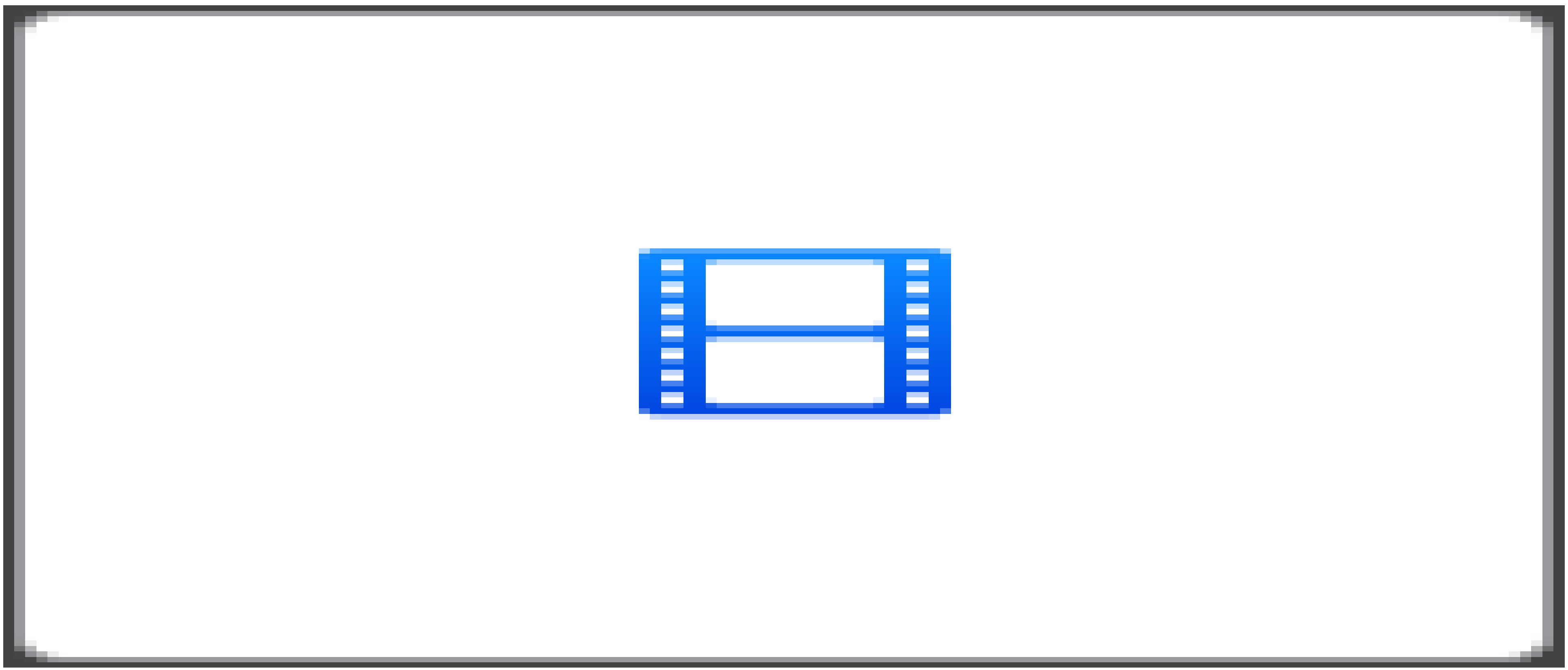

S. Blacker, A. Bauswein, et al., Phys. Rev. D 102 (2020) 123023

Binary neutron star merger simulation

S. Blacker & A. Bauswein (GSI Darmstadt), 1.35 M_sun + 1.35 M_sun

https://www.gsi.de/fileadmin/theorie/simulation-neutron-star-merger.mp4

Population of the QCD phase diagram with mixed phase, 6… 25 ms

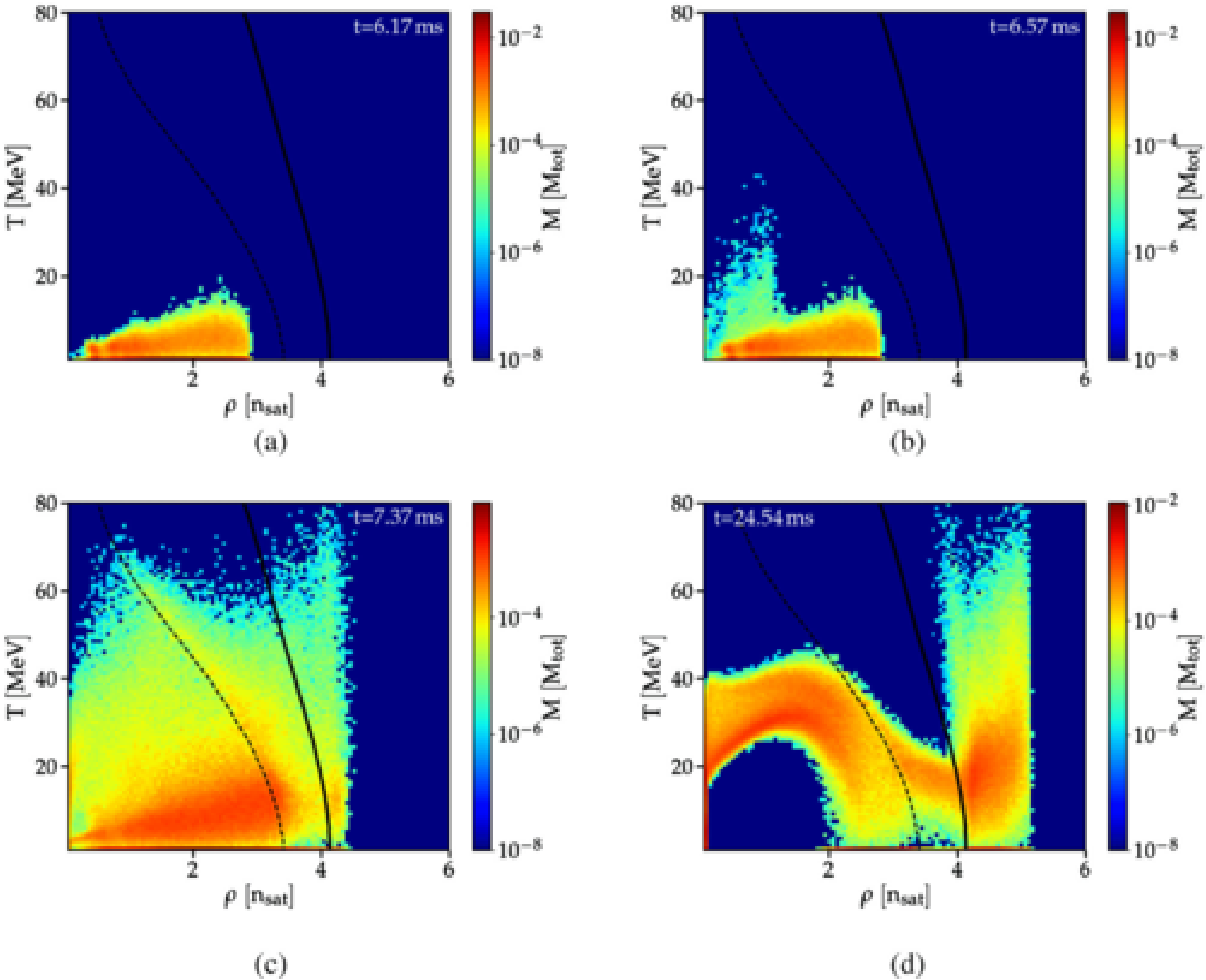

EoS for applications to supernova and merger Simulation:

CompOSE

With deconfinement:

https://compose.obspm.fr/eos/166

S. Blacker, A. Bauswein, et al., Phys. Rev. D 102 (2020) 123023

Hybrid star formation in postmerger phase

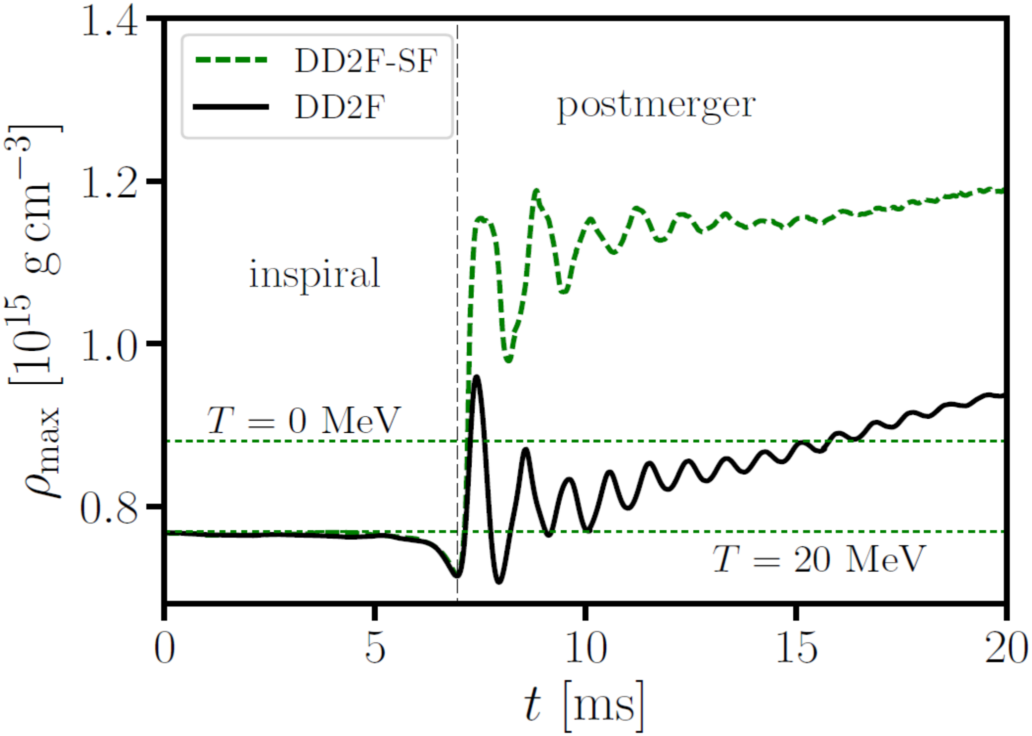

Strong phase transition in postmerger GW,
A. Bauswein et al. arxiv:1809.01116

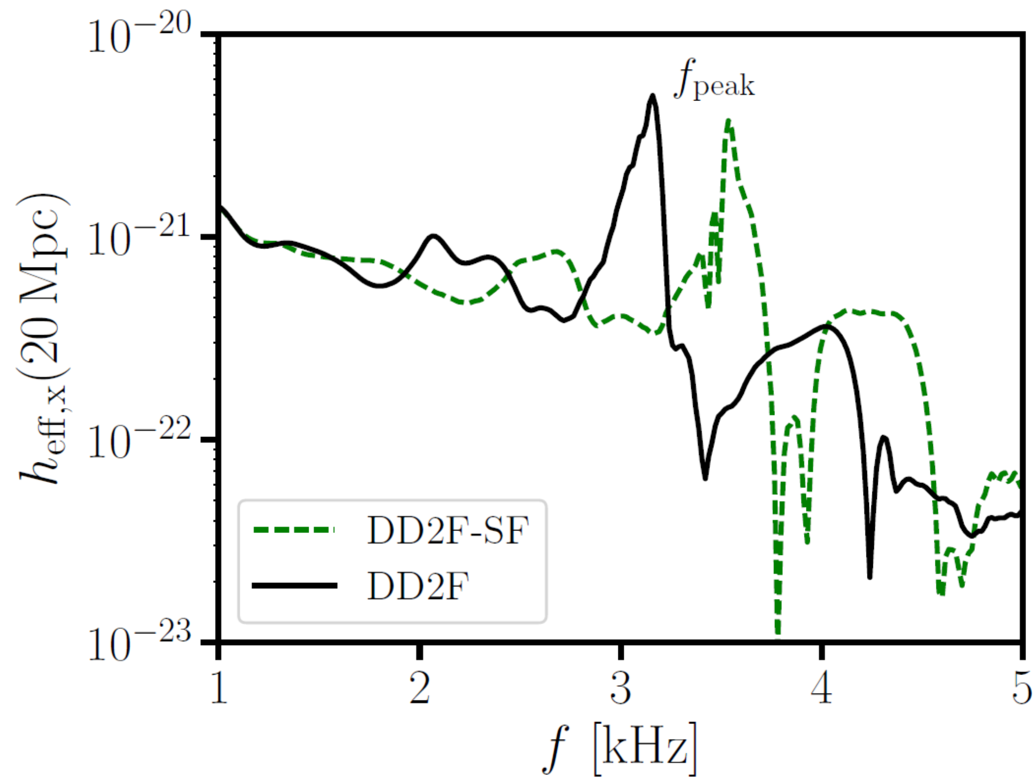

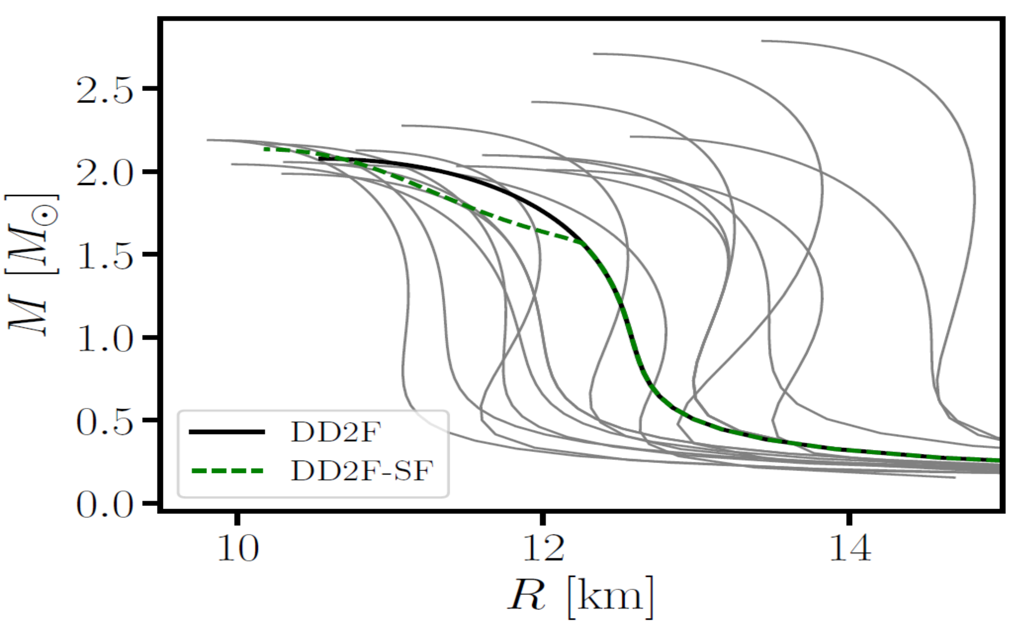

Hybrid star formation during NS merger
→ higher densities and compacter star
→ higher peak frequency of the GW

A. Bauswein et al., PRL 122 (2019) 061102

Hybrid star formation in postmerger phase

Strong phase transition in postmerger GW signal,
A. Bauswein et al., PRL 122 (2019) 061102; [arxiv:1809.01116]

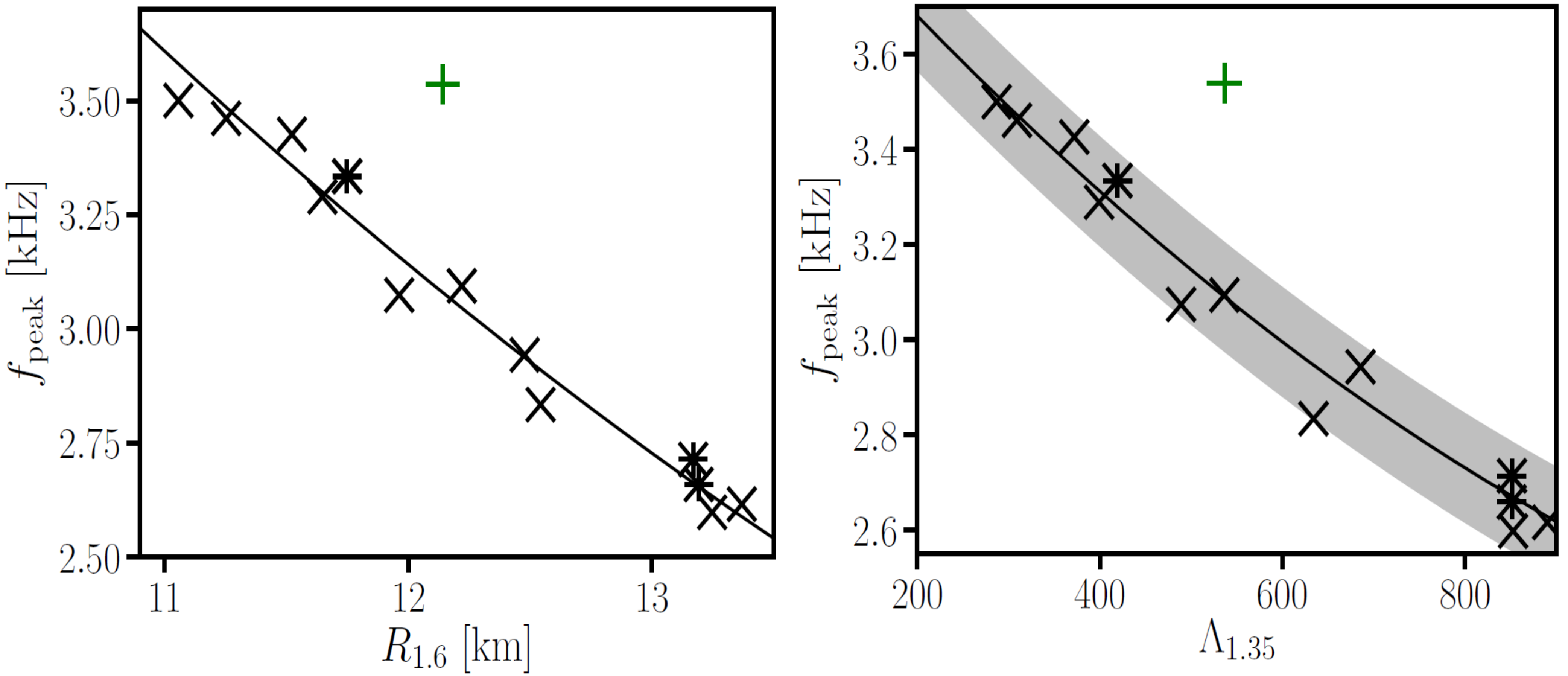

Strong deviation from **f_{peak} – $R_{1.6}$** relation signals **strong phase transition in** NS merger**!**

Complementarity of **f_{peak}** from postmerger with tidal deformability **$\Lambda_{1.35}$** from inspiral phase.

Hybrid star formation in postmerger phase

Strong PT in postmerger GW signal, S. Blacker et al., arxiv:2006.03789, PRD102 (2020) 123023

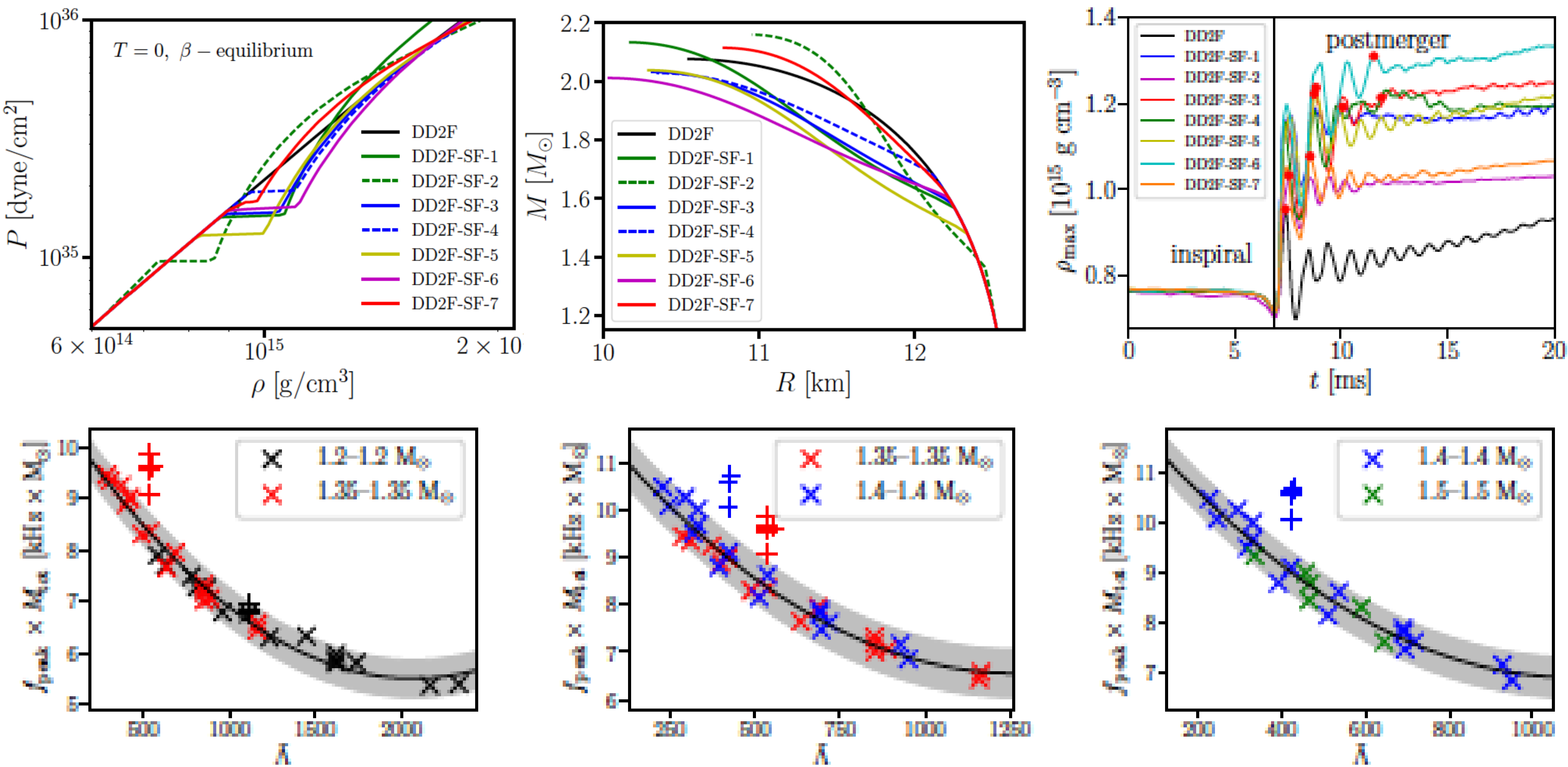

Dominant postmerger frequency f_{peak} vs. tidal deformability $\Lambda_{1.35}$ from inspiral phase:
Results from hybrid models appear as **outliers** of the grey band (maximal deviation of purely hadronic models from a least squares fit) = signalling a **strong phase transition in** NS **!**

GW signal of deconfinement in merger of hybrid stars

Merger of hybrid stars with early phase transition: Bauswein & Blacker, EPJ ST 229 (2020)

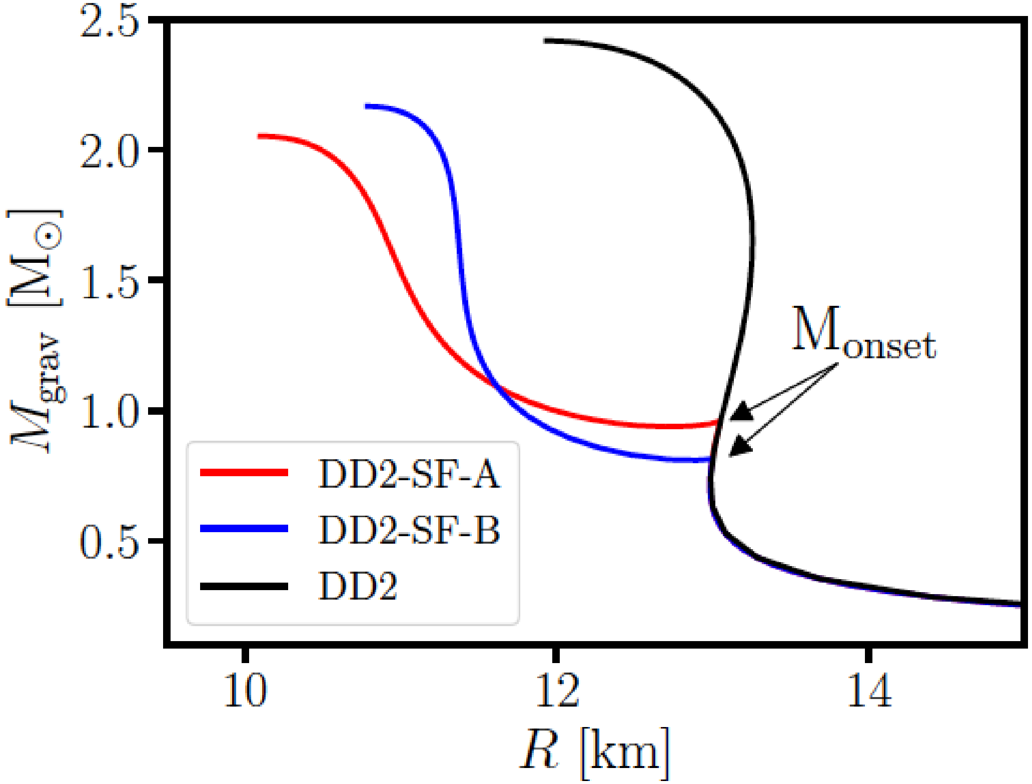

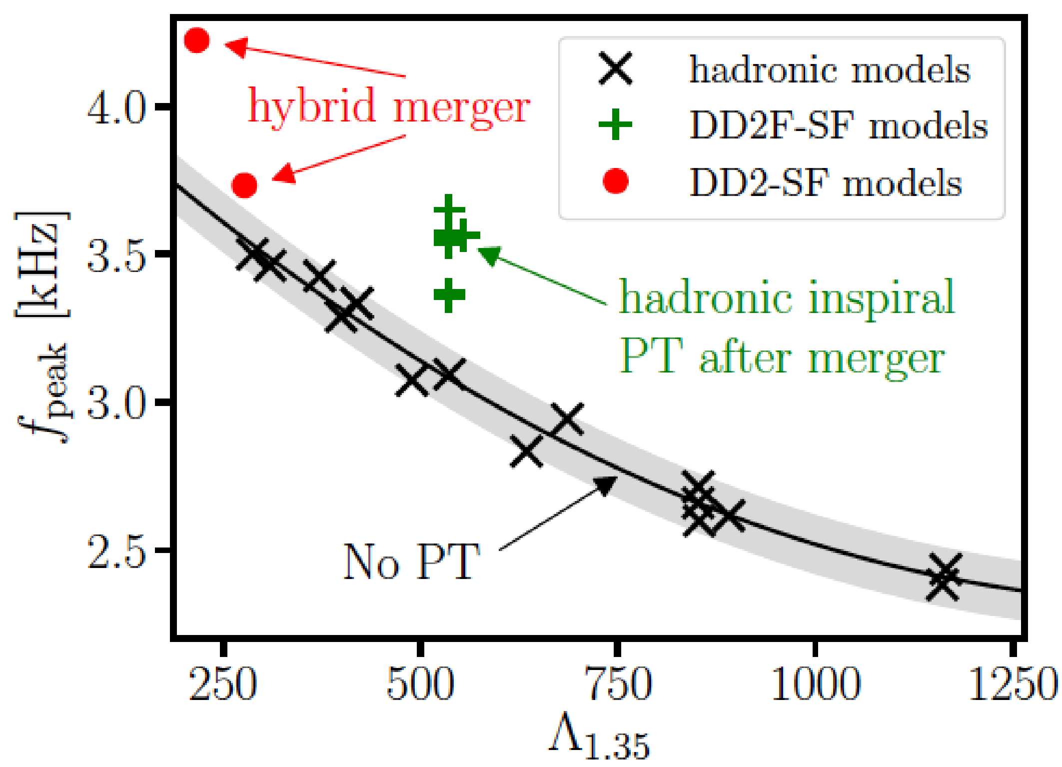

The combination of stiff hadronic EoS (DD2) and string-flip (SF) model allows for early onset of deconfinement in low-mass neutron stars and even third-family solutions (mass twins).
For these cases, the event GW170817 could have been a **merger of two hybrid stars**!
Also in these cases (red dots in above figure) a **significant deviation** from the grey band of Purely hadronic star mergers without a phase transition is obtained!

Deconfinement transition as SN explosion mechanism

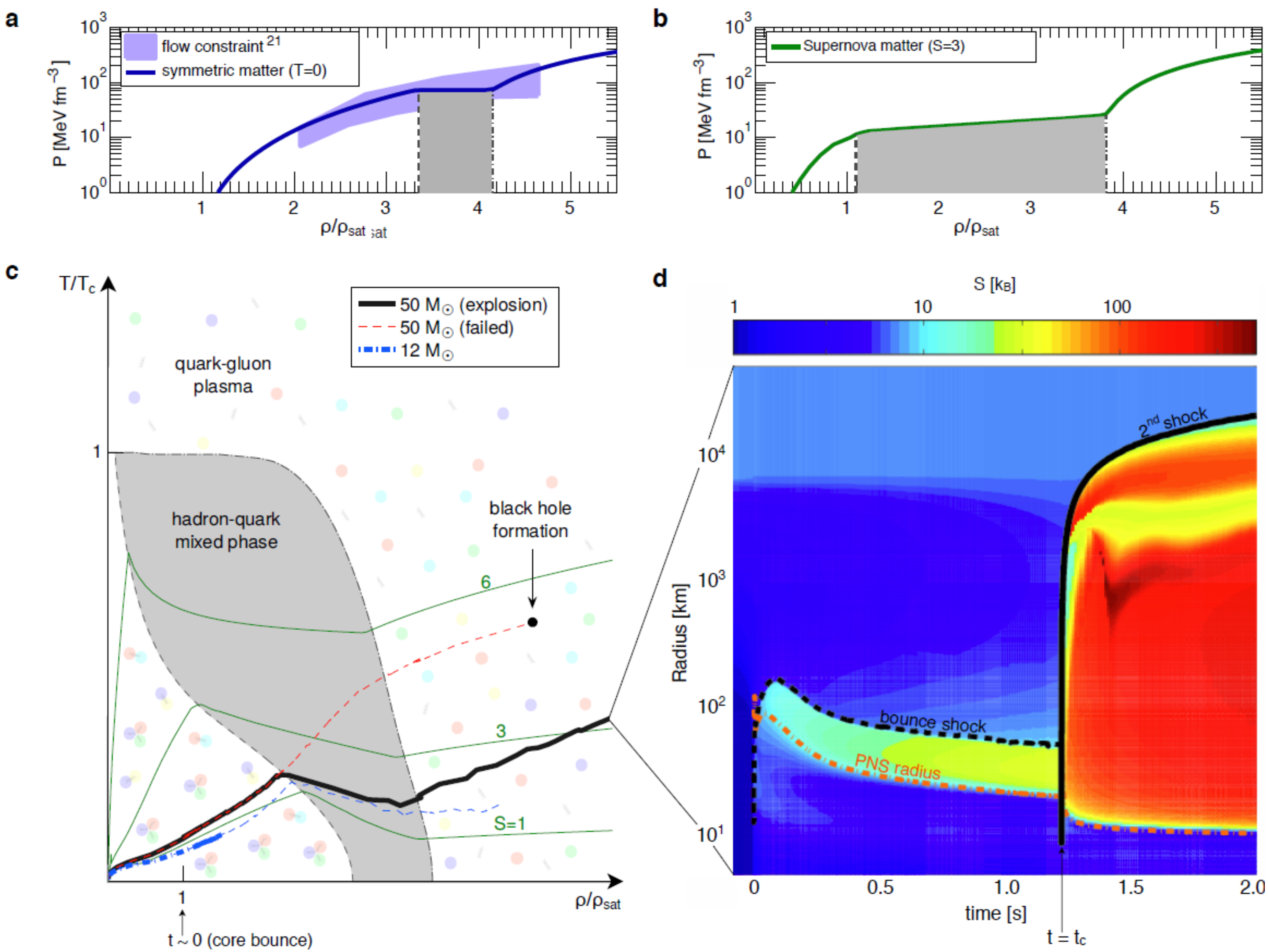

Progenitor:
$M = 50\ M_O$

T. Fischer, N.-U. Bastian et al., Quark deconfinement as supernova engine of massive blue Supergiant star explosions, Nature Astronomy 2 (2018) 980-986; arxiv:1712.08788

Population of the QCD Phase Diagram in Mergers & SNe

Binary NS merger, 1.35 M_sun + 1.35 M_sun

SN explosion, 50 M_sun

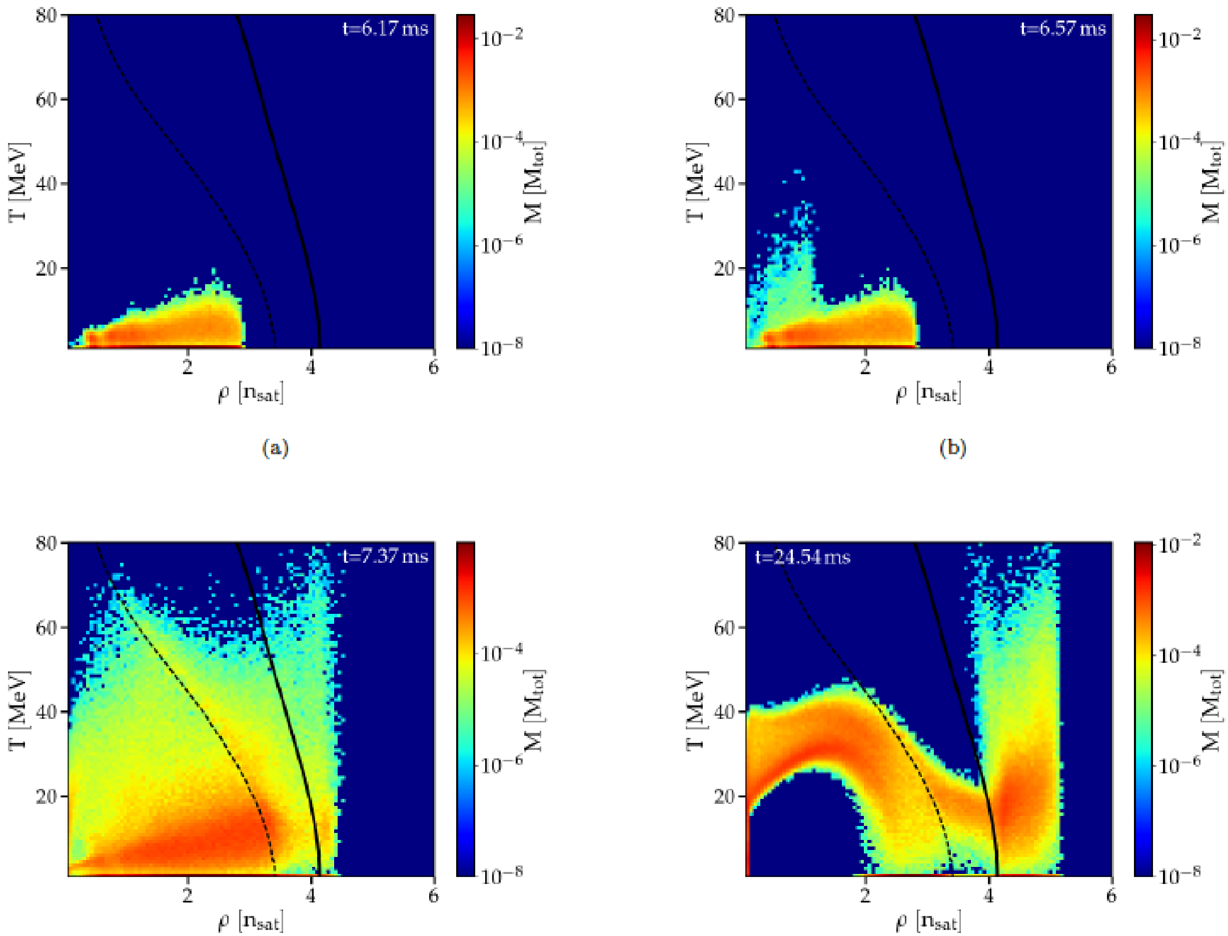

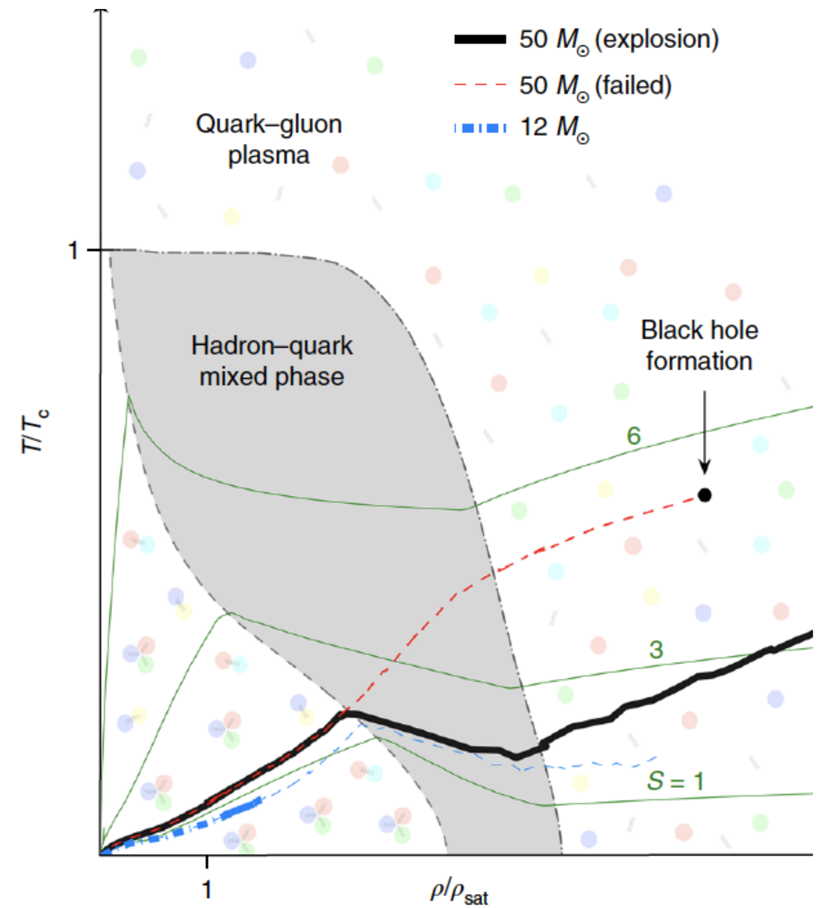

S. Blacker, A. Bauswein et al.,
Phys. Rev. D102 (2020) 123023; arxiv:2006.03789

T. Fischer et al.,
Nat. Astron. 2 (2018) 980;
arxiv:1712.08788

Population of the QCD Phase Diagram

Binary NS merger,
1.35+1.35 M_sun

SN explosion,
Progenitor 50 M_sun

Ultrarelativistic HIC,
√s [GeV]=16, 10, 7, 4

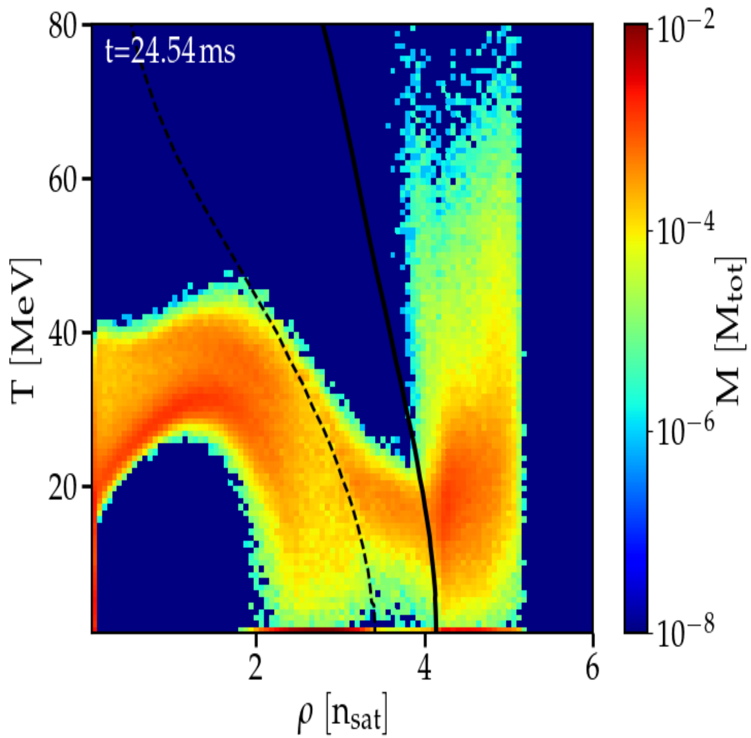

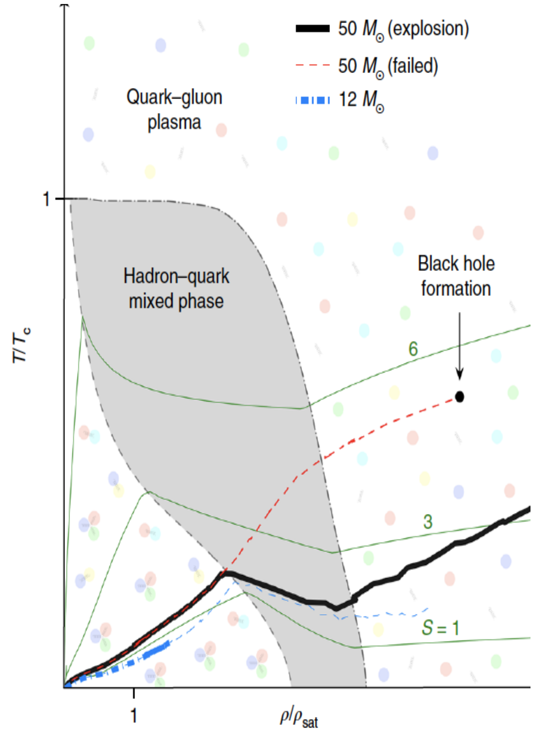

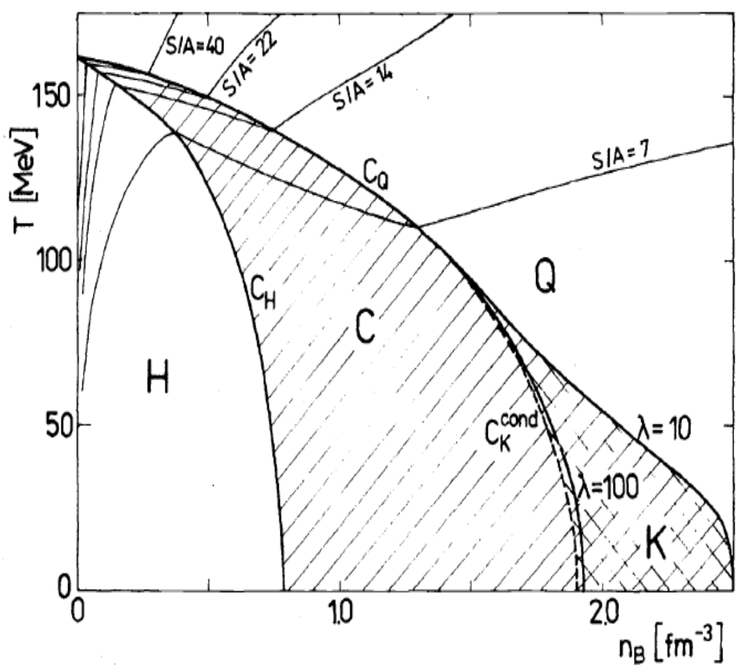

S. Blacker, A. Bauswein et al.,
PRD 102 (2020) 123023
arXiv:2006.03789

T. Fischer et al.,
Nat. Astron. 2 (2018) 980
arXiv:1712.08788

H.W. Barz, B. Friman et al.,
PRD 40 (1989) 157
GSI Preprint, GSI-89-13

CEP in the QCD phase diagram: HIC vs. Astrophysics

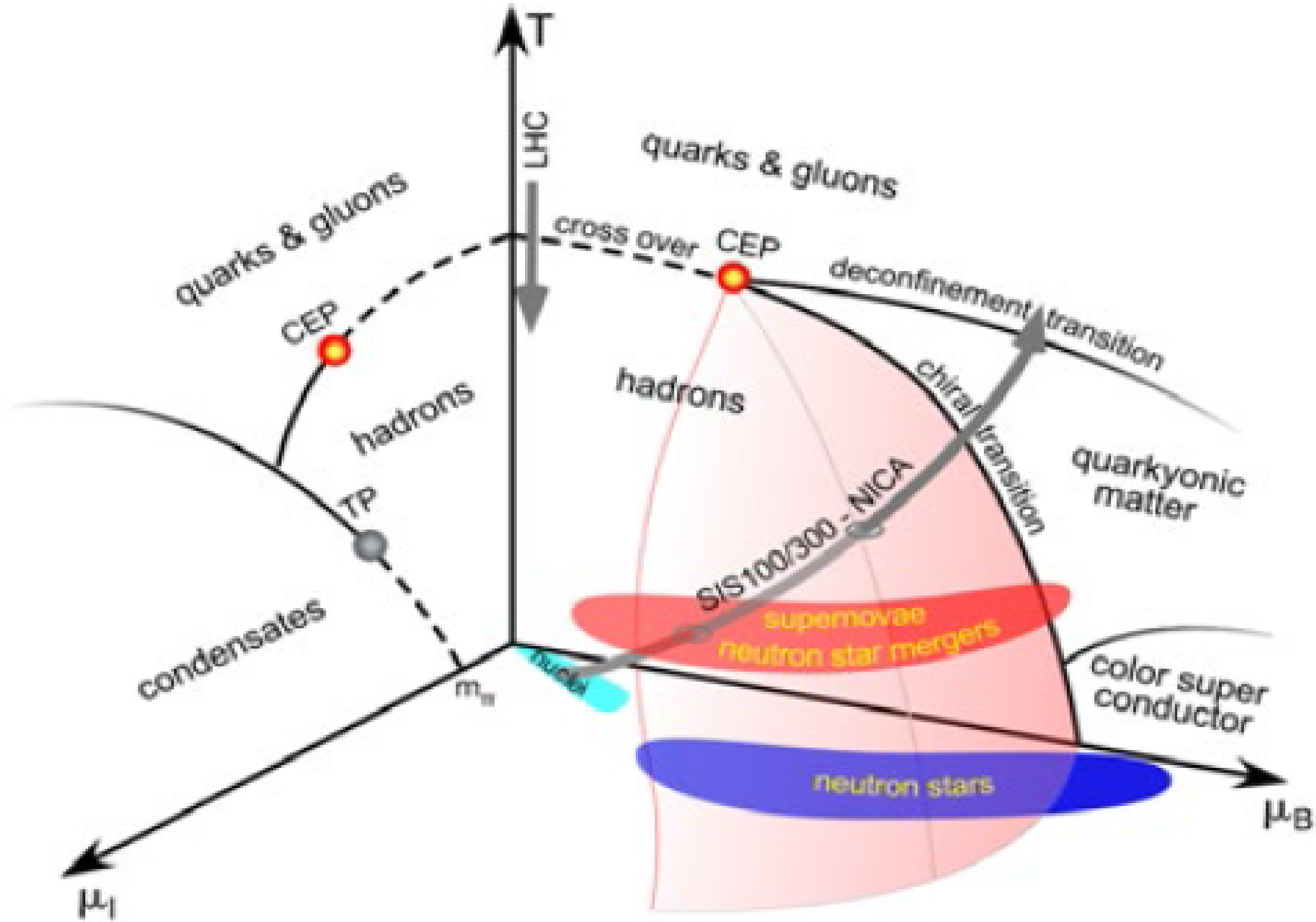

NuPECC Long Range Plan 2017; http://www.nupecc.org

A. Andronic, D. Blaschke, et al., “Hadron production ...”, Nucl. Phys. A 837 (2010) 65 - 86

CEP in the QCD phase diagram: HIC vs. Astrophysics

NICA experiments (BM @N, MPD)

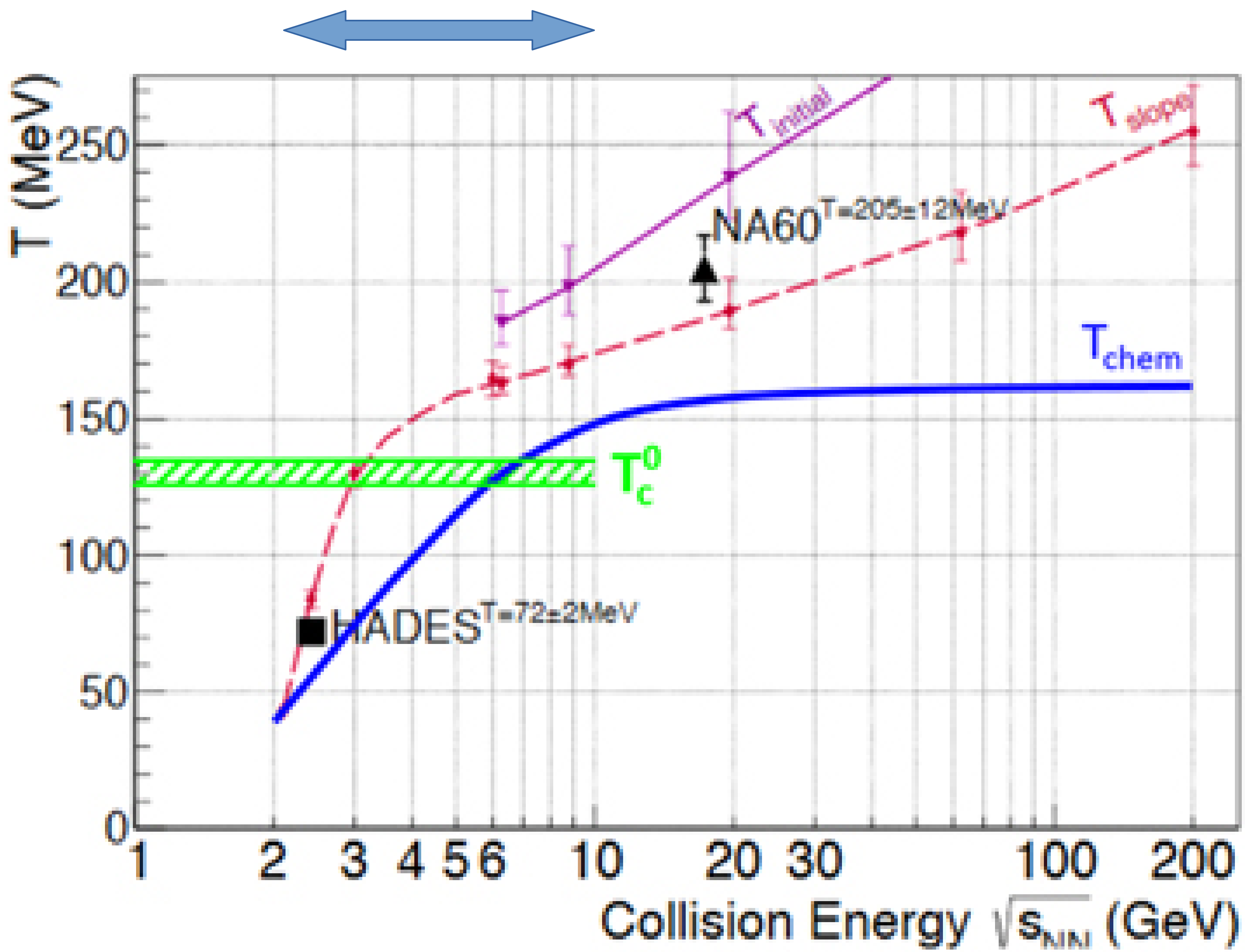

P. Senger, Phys. Scripta 96 (2021) 054002; and references therein !

The NICA Facility at JINR Dubna

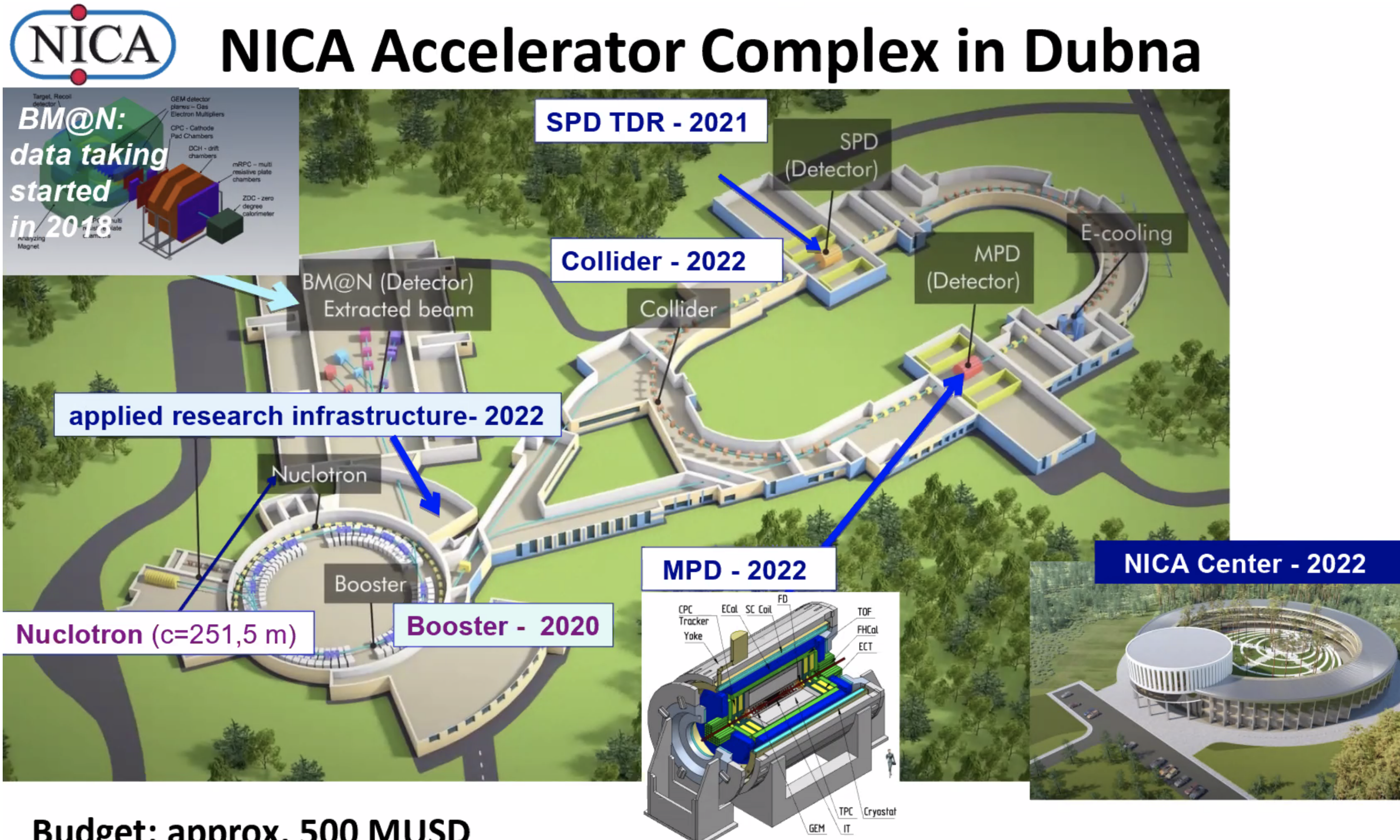

Budget: approx. 500 MUSD

The NICA Facility at JINR Dubna

NICA

NICA construction live

The NICA Facility at JINR Dubna

NICA: Unique and complementary

Collider advantage:
- *coverage of max. phase space*
- *minimally biased acceptance*
- *free of target parasitic effects*

In NICA Collider energy range maximum possible net-baryon density is reached

Fixed target advantage:
- *high rate of interactions*
- *easily upgradeable*

T. Galatyuk, Nucl.Phys. A982 (2019);

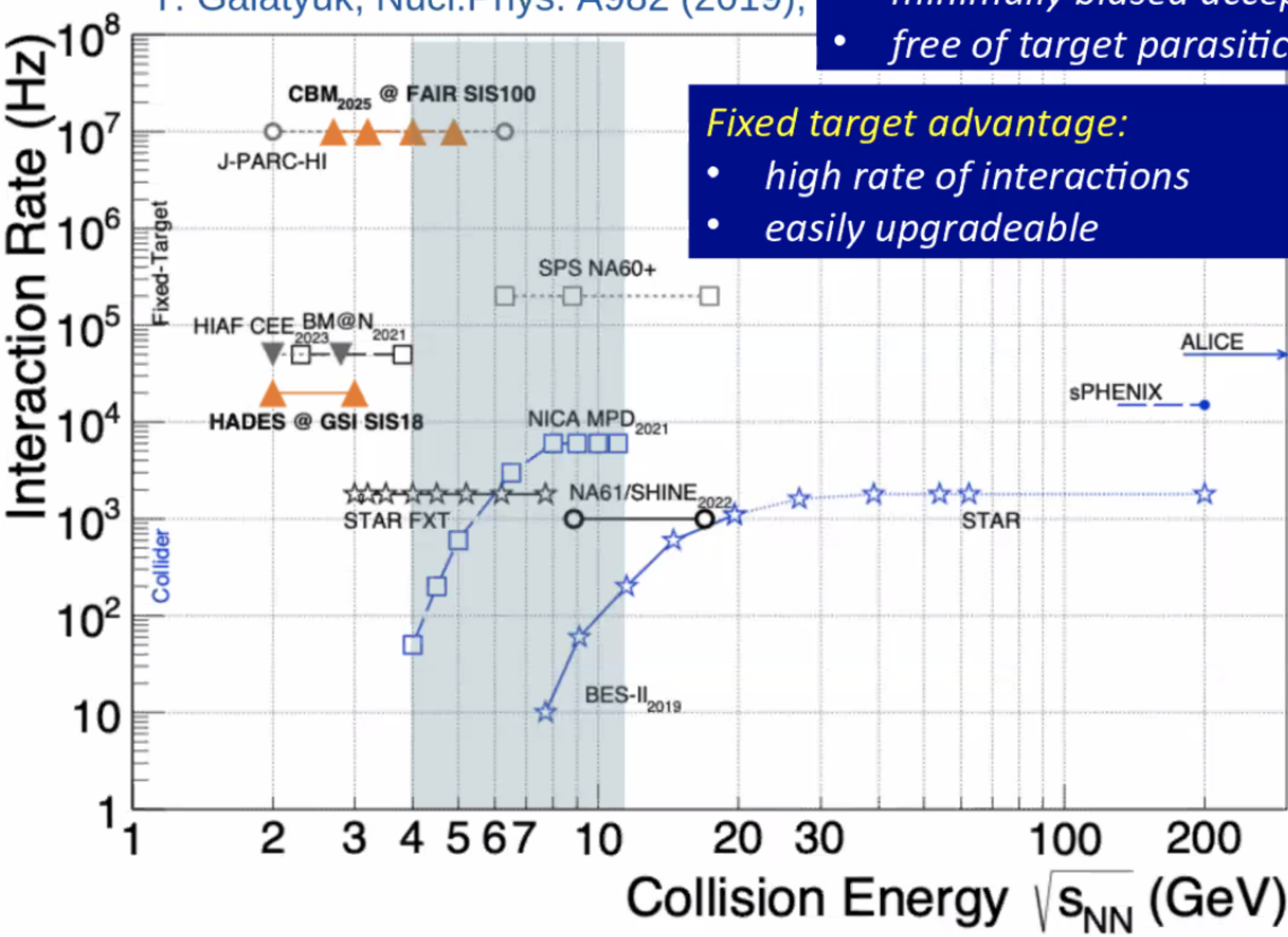

NUPECC Long Range Plan 2017

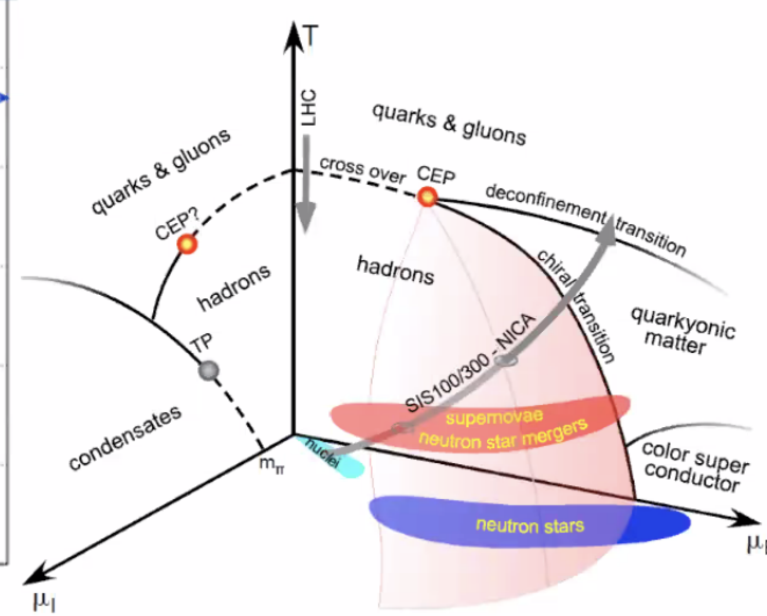

The NICA Facility at JINR Dubna

NICA Main parameters of accelerator complex

Nuclotron

Parameter	**SC synchrotron**
particles	↑p, ↑d, nuclei (Au, Bi, ...)
max. kinetic energy, GeV/u	10.71 (↑p); 5.35 (↑d) **3.8** (Au)
max. mag. rigidity, Tm	38.5
circumference, m	251.52
vacuum, Torr	10^{-9}
*intensity, **Au** /pulse*	1 10^{9}

Booster

	value
ion species	A/Z ≤ 3
max. energy, MeV/u	**600**
magnetic rigidity, T m	1.6 – 25.0
circumference, m	210.96
vacuum, Tor	10^{-11}
*intensity, **Au** /p*	1.5 10^{9}

The Collider

Design parameters, Stage II

45 T*m, 11 GeV/u for Au^{79+}

Ring circumference, m	**503,04**
Number of bunches	**22**
r.m.s. bunch length, m	**0,6**
β, m	**0,35**
Energy in c.m., Gev/u	**4-11**
r.m.s. $\Delta p/p$, 10^{-3}	**1,6**
IBS growth time, s	**1800**
Luminosity, cm^{-2} s^{-1}	**$1x10^{27}$**

Stage I:

- ***without ECS in Collider, with stochastic cooling***
- ***reduced number of RF***
- ***reduced luminosity***

Collision system limited by source. *Now Available: C(A=12), N(A=14), Ne(A=20), Ar(A=40), Fe(A=56), Kr(A=78-86), Xe(A=124-134), Bi(A=209)*

The NICA Facility at JINR Dubna

Booster commissioning

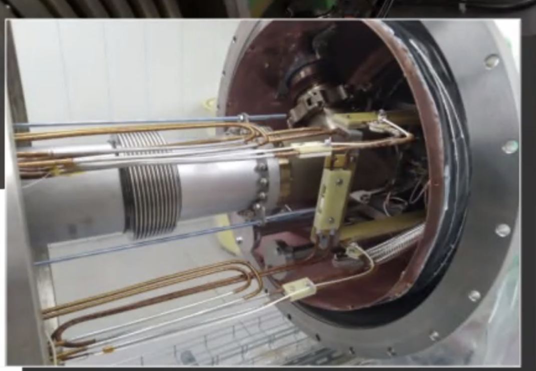

- ✓ ***Booster fully assembled in the tunnel***
- ✓ ***Commissioning and test ongoing for beam diagnostics, beam acceleration, electron cooling, power supply, magnets, cryogenics***

The NICA Facility at JINR Dubna

Experiment with BM@N: Short-Range Correlations (SRC)

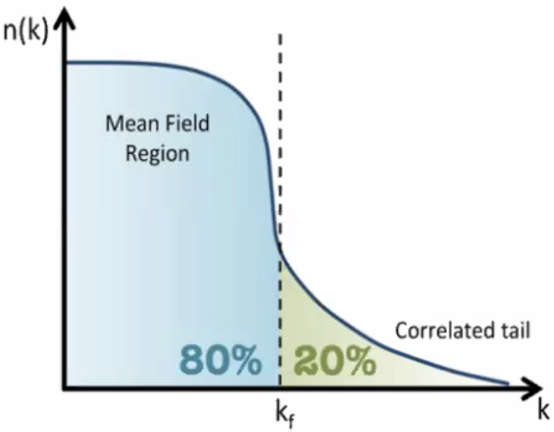

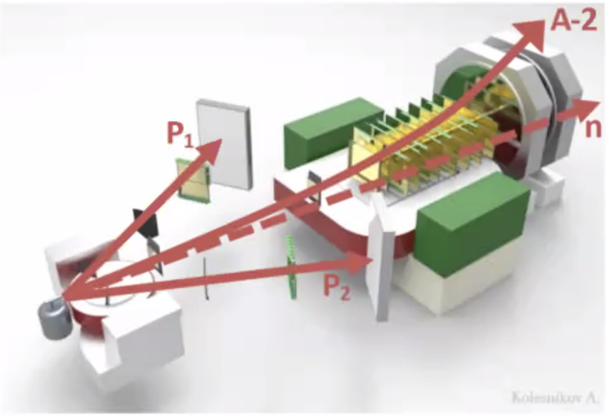

Experiment at BM@N with a 4A GeV C-beam:

$^{12}C + p \rightarrow 2p + {}^{10}{}_{4}Be + p$ (pp SRC)

First fully exclusive measurement in inverse kinematics probing the residual A-2 nuclear system!

M. Patsyuk et al., arXiv:2102.02626

Accepted for publication in **nature physics**

Experiment with BM@N: Λ's in C + C, Al, Cu at 4A GeV

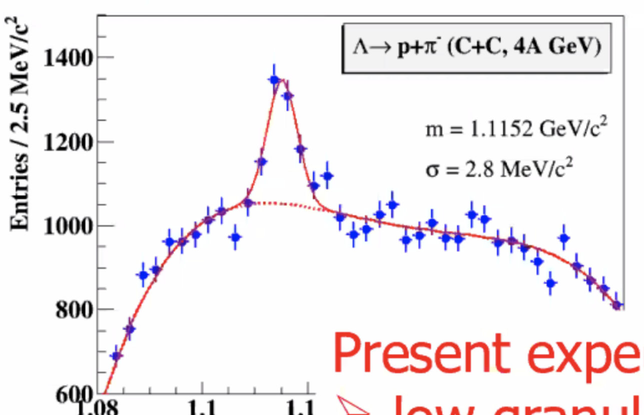

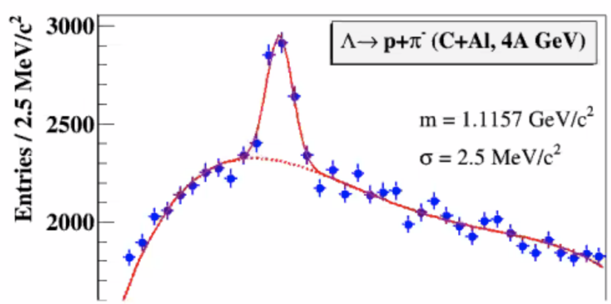

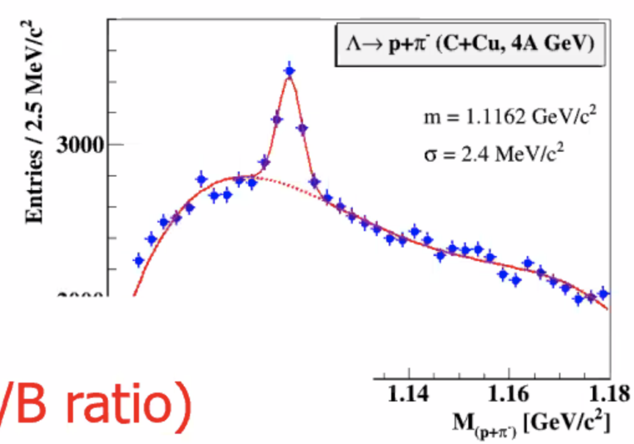

Present experimental limitations:

- low granularity tracking systems (small S/B ratio)
- air gaps in beam line from Nuclotron (low beam quality)
- no vacuum beam pipe in BM@N (large background)

The NICA Facility at JINR Dubna

NICA

Interior of MPD Hall

Opening of solenoid sarcophagus: Mar. 23rd

The NICA Facility at JINR Dubna

Electromagnetic Calorimeter (ECAL)

- Pb+Sc "Shashlyk" — read-out: WLS fibers + MAPD — L ~35 cm (~ 14 X_0)
- Segmentation (4x4 cm²) — $\sigma(E)$ better than 5% @ 1 GeV — time resolution ~500 ps

Barrel ECAL = 38400 ECAL towers (2x25 half-sectors x 6x8 modules/half-sector x 16 towers/module)

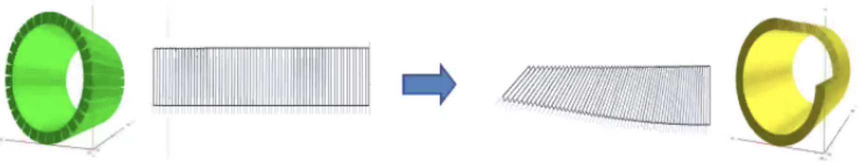

Projective geometry

So far ~300 modules (16 towers each) = 3 sectors are produced
Another 3 sectors are planned to be completed by May 2021
Chinese collaborators will produce 8 sectors by the end of 2021
25% of all modules are produced by JINR (production area in Protvino)
75% produced in China, currently funding is secured for approx. 25%

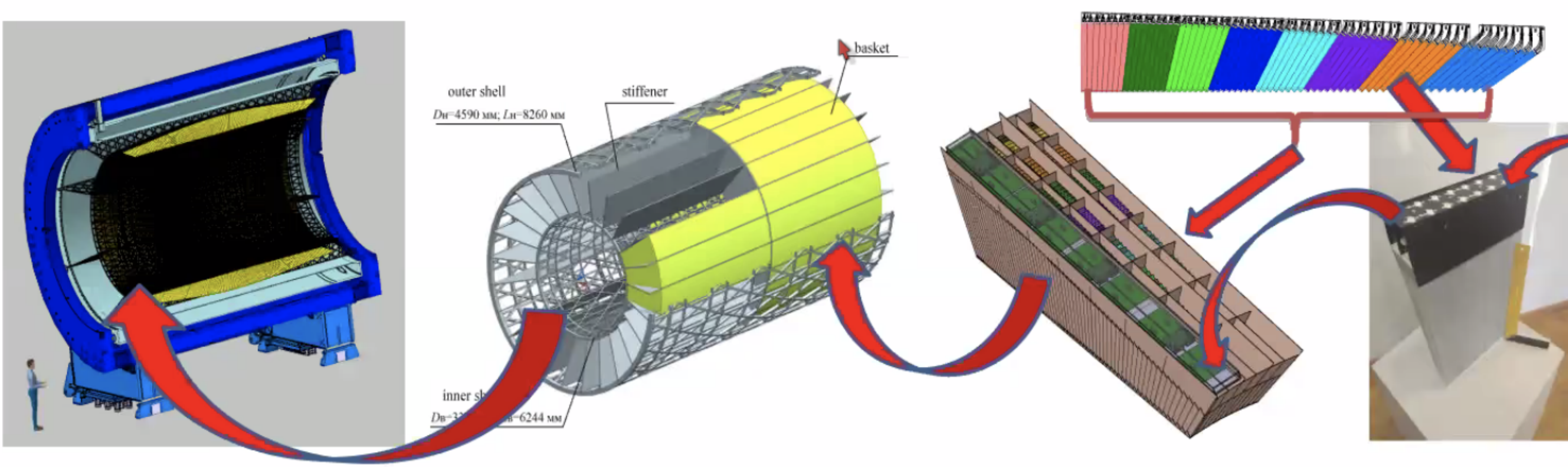

Sectors in dedicated Containers

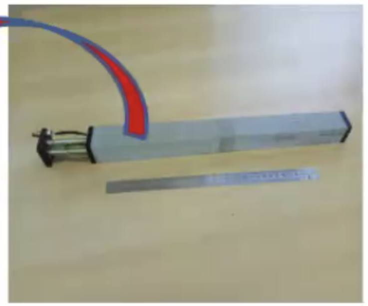

Photo of one element

The NICA Facility at JINR Dubna

NICA

Electromagnetic probes in ECAL

- Realistic ECAL reconstruction & analysis – large acceptance ECAL with good energy resolution: ideal tool for measurement of neutral mesons in a wide momentum range

Photon energy resolution

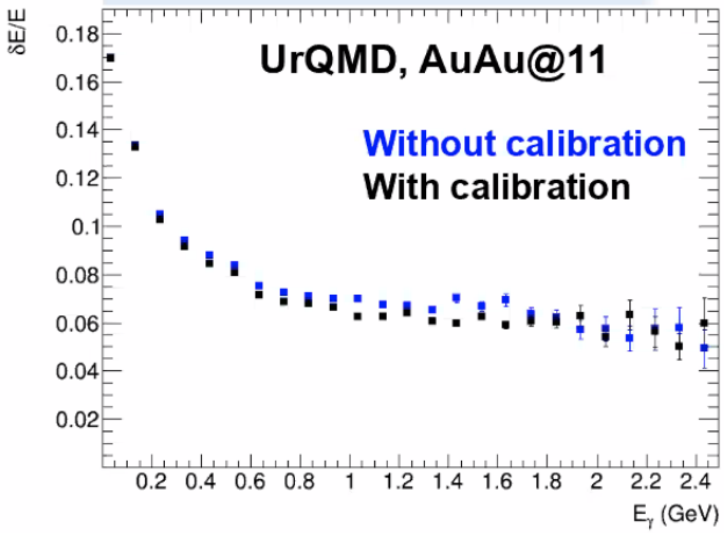

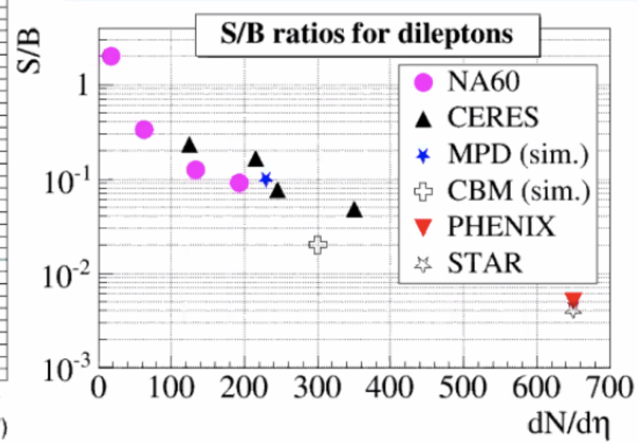

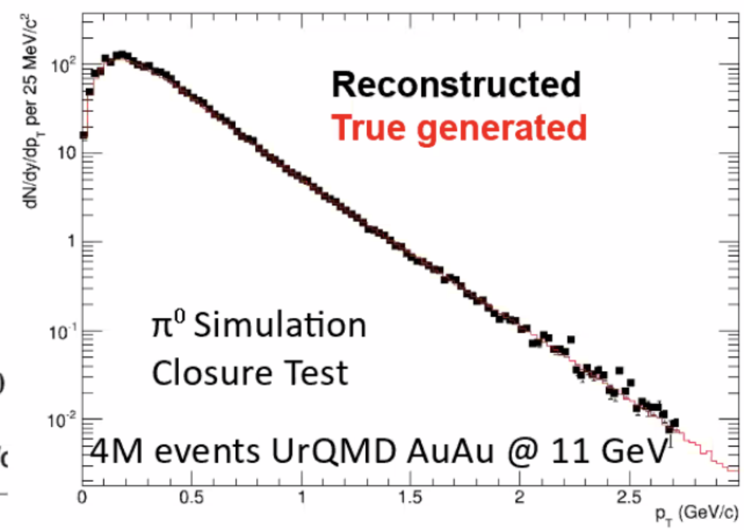

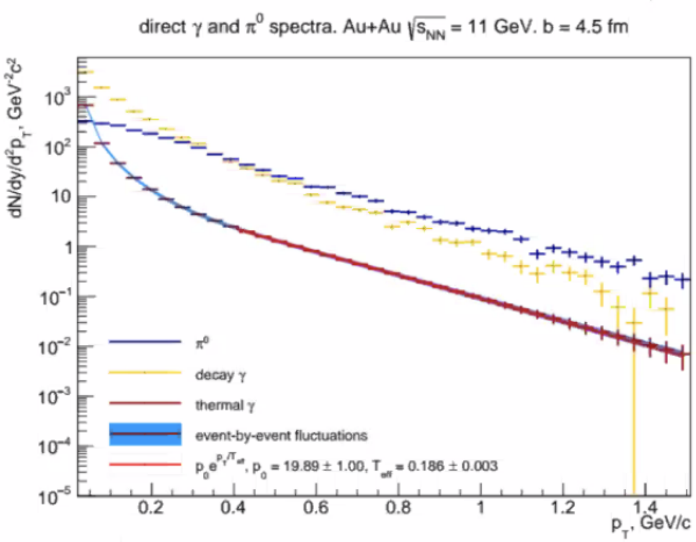

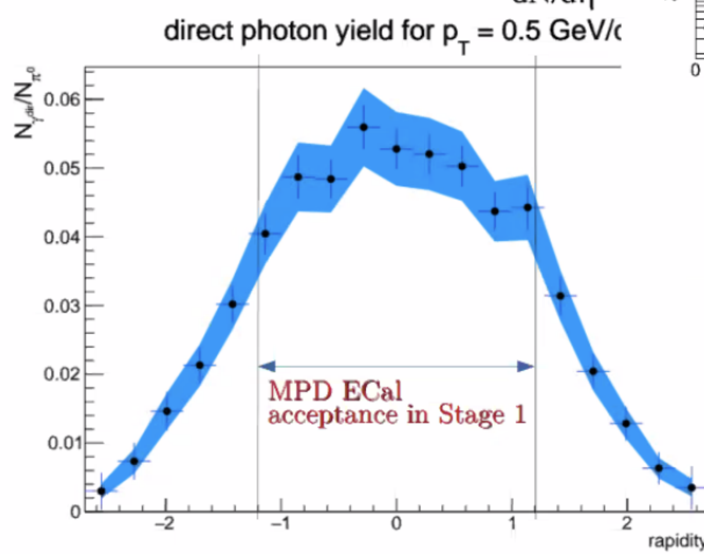

- Promising feasibility studies for prompt photon measurements in MPD

The NICA Facility at JINR Dubna

NICA

Hadroproduction with MPD

- **Particle spectra, yields & ratios are sensitive to bulk fireball properties and phase transformations in the medium**
- **Uniform acceptance and large phase coverage are crucial for precise mapping of the QCD phase diagram**

✓ *0-5% central Au+Au at 9 GeV from the PHSD event generator, which implements partonic phase and CSR effects*
✓ *Recent reconstruction chain, combined dE/dx+TOF particle ID, spectra analysis*

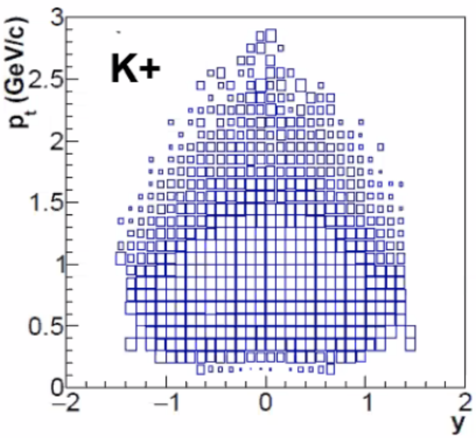

- MPD provides large phase-space coverage for identified pions and kaons (> 70% of the full phasespace at 9 GeV)
- Hadron spectra can be measured from p_T=0.2 to 2.5 GeV/c
- Extrapolation to full p_T-range and to the full phase space can be performed exploiting the spectra shapes (see BW fits for p_T-spectra and Gaussian for rapidity distributions)

Ability to cover full energy range of the „horn" with consistent acceptance

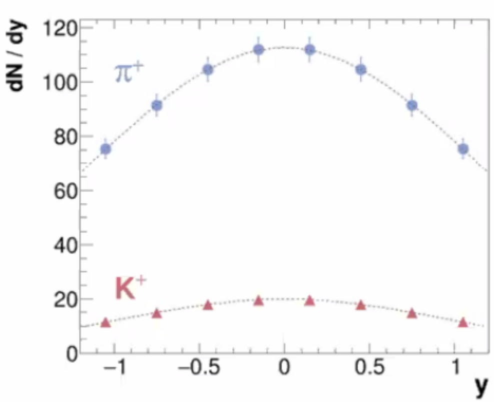

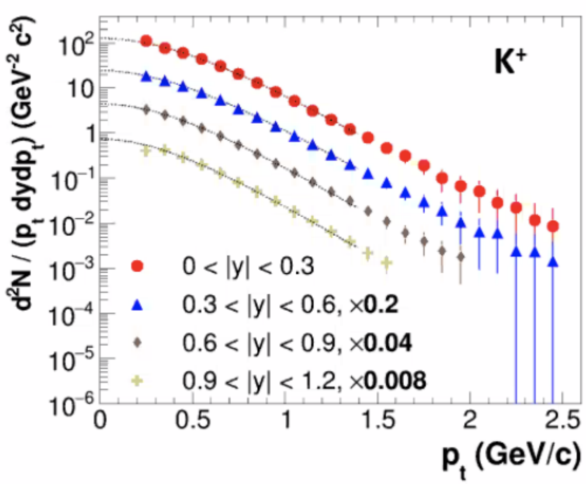

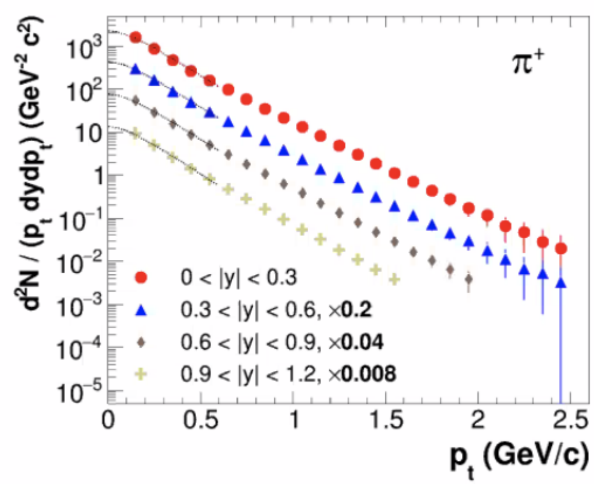

The NICA Facility at JINR Dubna

NICA

Strange and multi-strange baryons

Stage'1 (TPC+TOF): Au+Au @ 11 GeV, PHSD + MPDRoot reco.

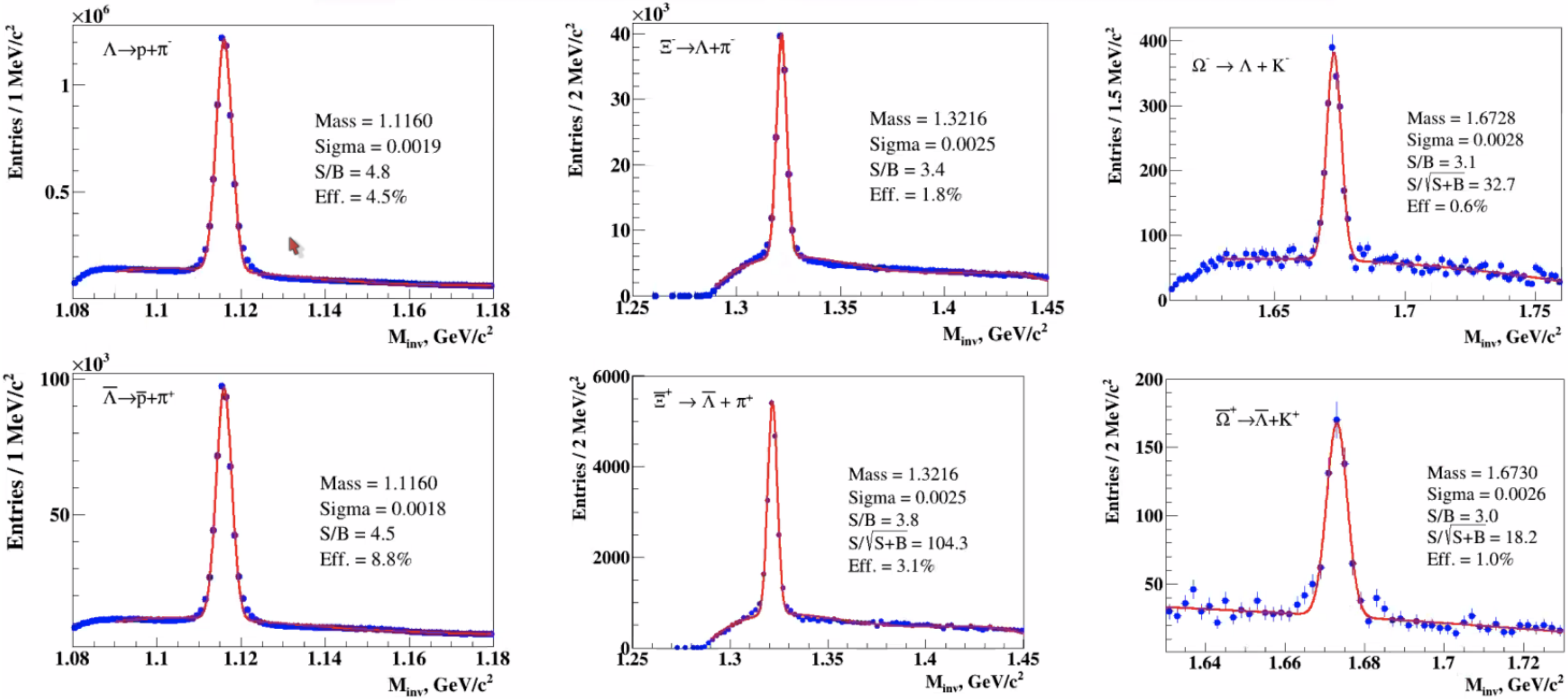

particle	Λ	anti-Λ	Ξ⁻	anti-Ξ⁺	Ω ⁻	anti–Ω⁺
yield in 10 weeks	$3 \cdot 10^8$	$3.5 \cdot 10^6$	$1.5 \cdot 10^6$	$8.0 \cdot 10^4$	$7 \cdot 10^4$	$1.5 \cdot 10^4$

The NICA Facility at JINR Dubna

NICA

NICA Facility running plan

- **Year 2021:**
  - Extensive commissioning of Booster accelerator
  - Heavy-ion (Fe/Kr/Xe) run of full Booster+Nuclotron setup
- **Year 2022:**
  - Completion of NICA Collider and transfer lines
- **Year 2023:**
  - Initial run of NICA with Bi+Bi @ 9.2 AGeV (other energies a second priority)
  - Goal to reach luminosity of 10^{25} $cm^{-2}s^{-1}$
- **Year 2024:**
  - Goal to have Au+Au collisions and acceleration in NICA (up to 11 AGeV)
- **Beyond 2024:**
  - Maximizing luminosity, possibility of collision energy and system size scan

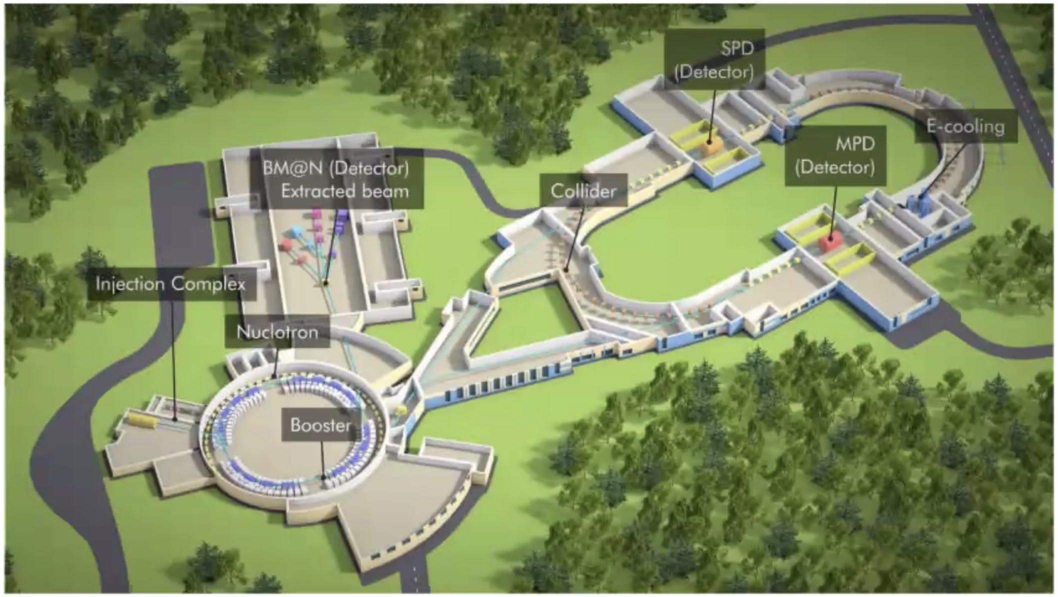

2nd CEP in QCD phase diagram: Quark-Hadron Continuity?

Gluons ↔ Vector mesons
Quarks ↔ Baryons
Goldstones ↔ Pseudoscalar mesons

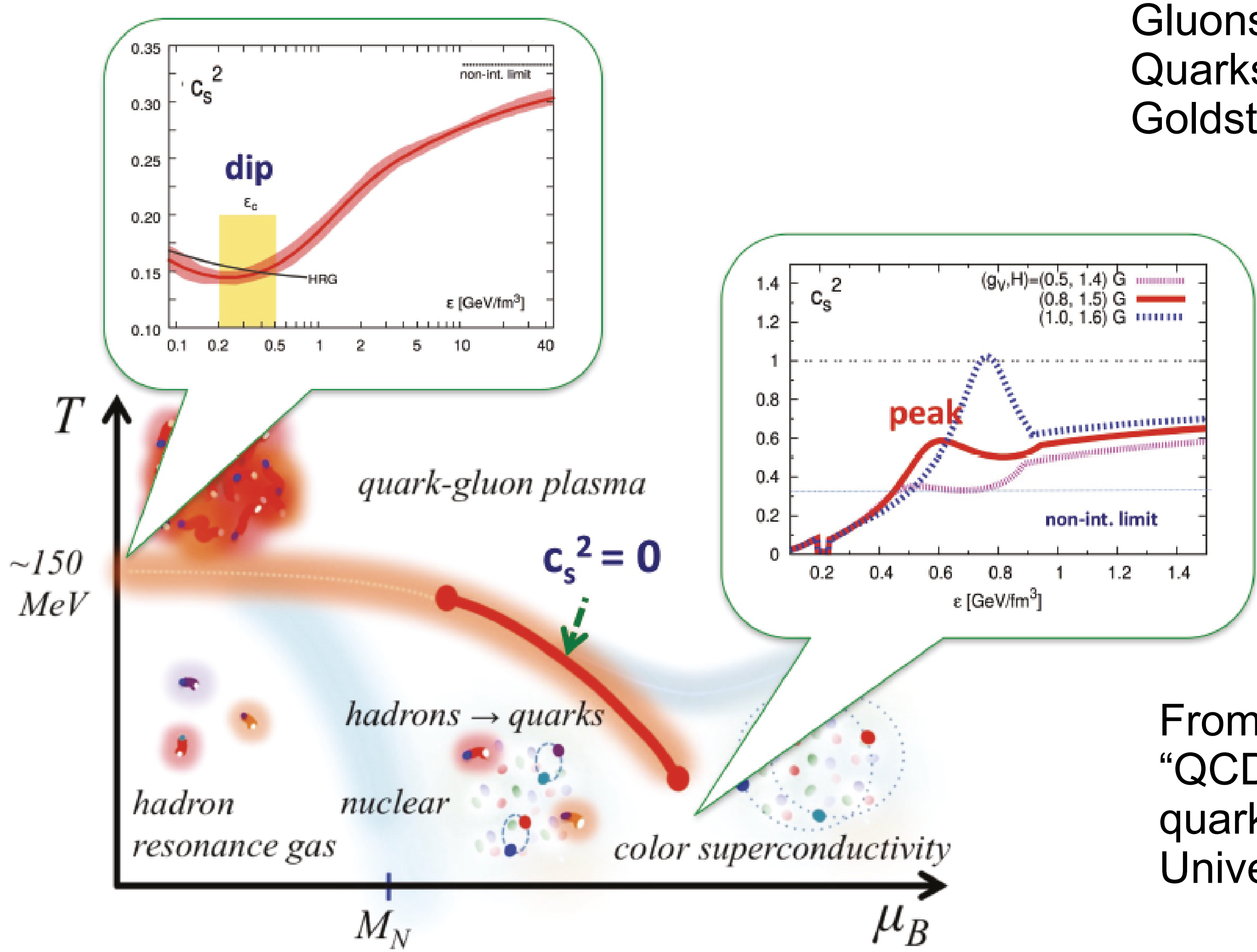

From: T. Kojo,
"QCD equations of state in quark-hadron continuity",
Universe 4 (2018) 42

T. Schaefer & F. Wilczek, Phys. Rev. Lett. 82 (1999) 3956
C. Wetterich, Phys. Lett. B 462 (1999) 164
T. Hatsuda, M. Tachibana, T. Yamamoto & G. Baym, Phys. Rev. Lett. 97 (2006) 122001

2^{nd} or no CEP in QCD phase diagram: Crossover all over ?

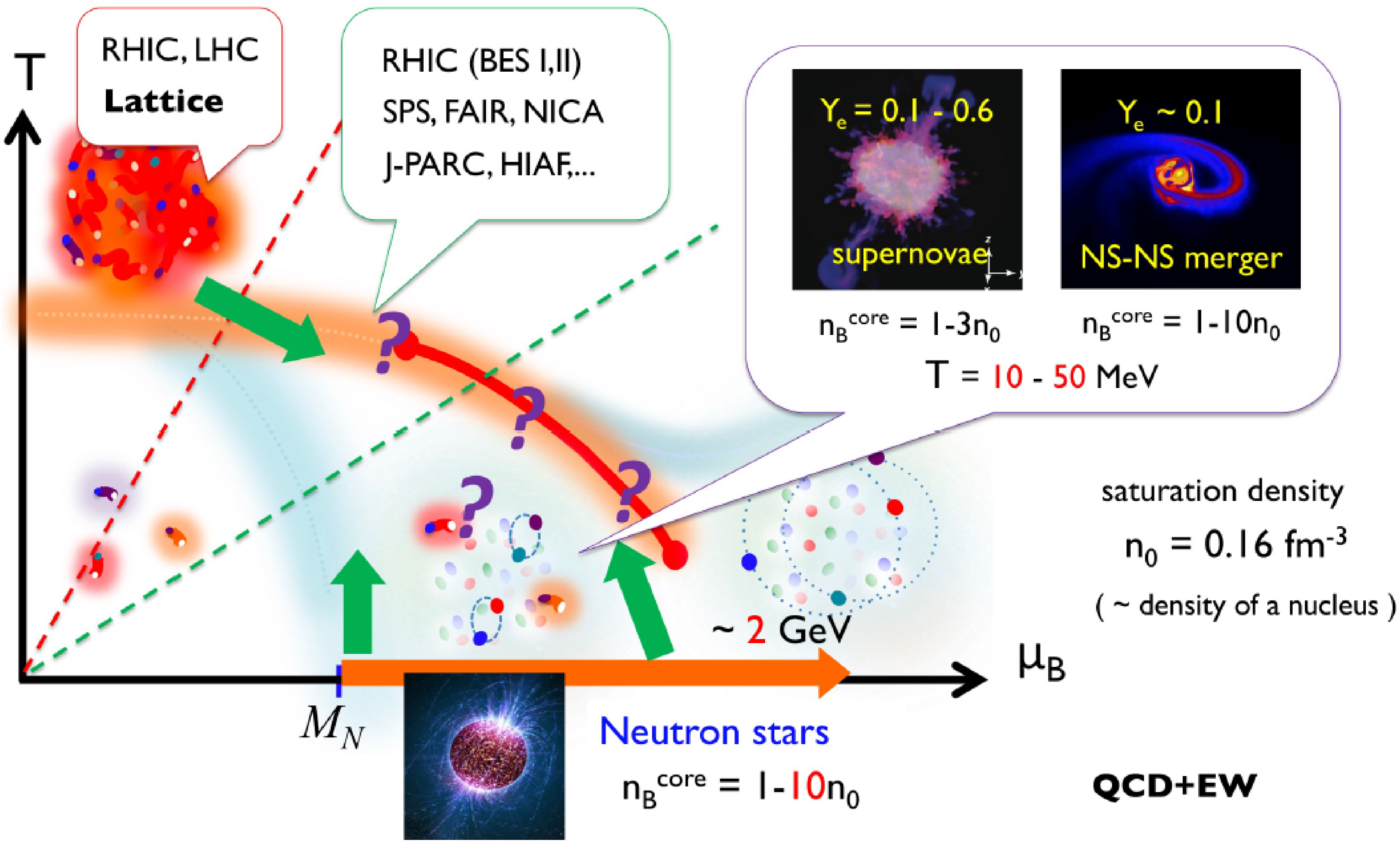

From: T. Kojo, "Delineating the properties of neutron star matter in cold, dense QCD", PoS Lattice2019, 244

Conclusions

- First observations of binary mergers open new possibilities to constrain properties of the Quark-gluon plasma at low temperatures and high baryon densities. Hybrid EoS are developed that allows to estimate quark plasma parameters in hypermassive (proto-) neutron stars

- GW170817: narrow window of small radii at 1.4 M_{sun} (Capano et al.: $10.4 < R_{1.4}[km] < 11.9$) strongly suggests an early onset of deconfinement with a critical density $n_c < 2\, n_0$ and an onset mass $M_{onset} < 1.0\, M_{sun}$ [Blaschke & Cierniak: 2012.15785]

- GW190814: the lighter object in the extemely asymmetric merger with its 2.6 M_{sun} can be either the heaviest neutron star or the lightest black hole. The central baryon density in such high-mass hybrid stars reaches 5.3 n_0. Our EoS allows it to be a hybrid star ...

- NICER radius measurement on PSR J0740+6620 triggers a new paradigm: NS with $M > 2M_{sun}$ should have a deconfined quark matter core when $R_{2.0} > 13$ km !

  Such a result is similar to the "two families" scenario of Drago & Pagliara, PRD 102 (2020) For the baryon density at the center of a star with 2.1 M_{sun} we find $n < 5\, n_0$, $n_0 = 0.15\, fm^{-3}$.

- Consequences for supernova simulations: A new lower limit for onset of deconfinement?

- Consequences for merger simulations: Check the GW signal for deconfinement !

- Good news for entering a color superconducting quark matter phase at NICA (BMaN, MPD)

Backup Slides:

Limits of Neutron Star Physics

GW190814

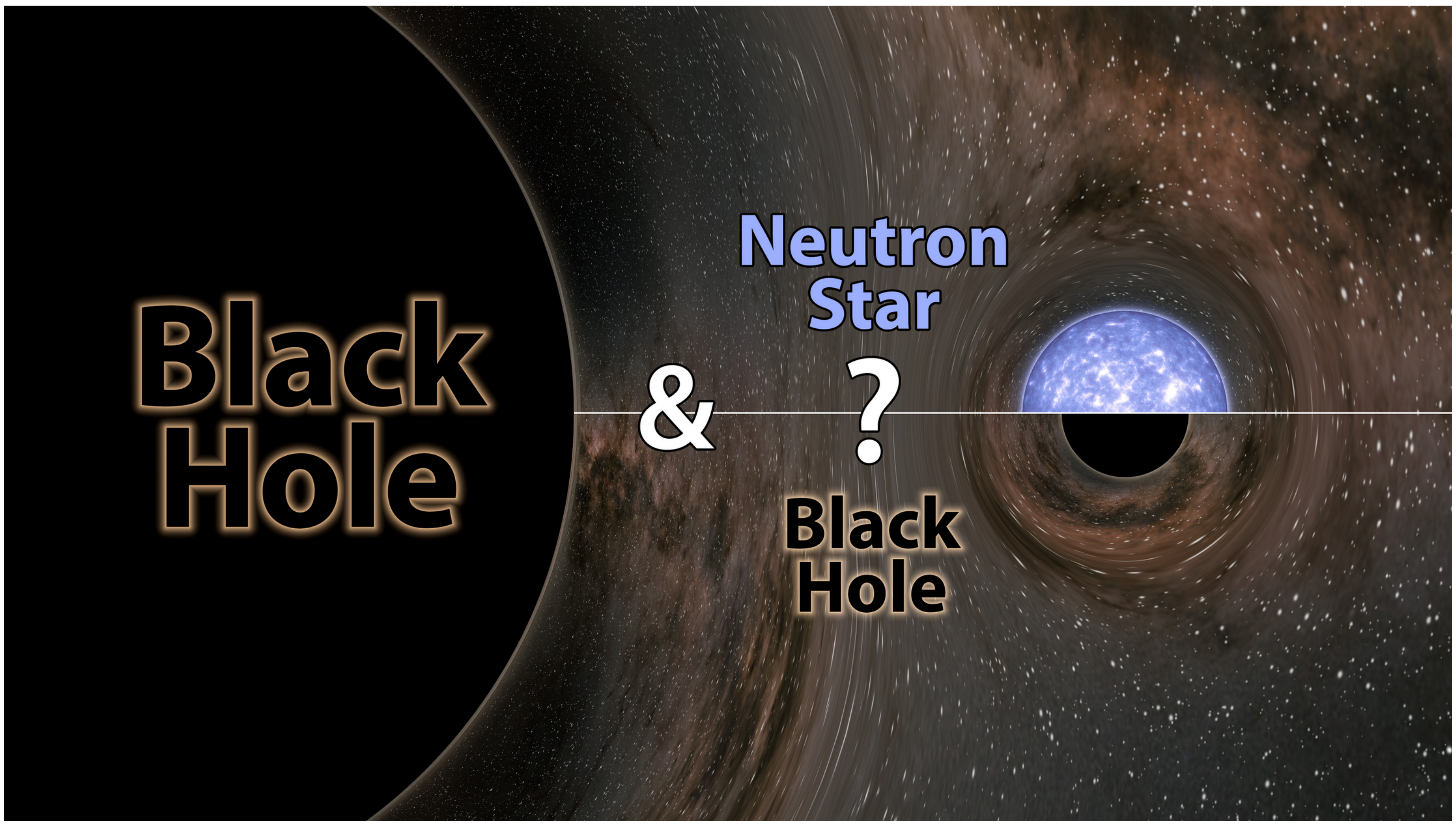

What is the limiting Mass of a neutron Star?

Was GW190814 a Merger of a 23-M_sun Black hole with the

Lightest Black hole

Or

Heaviest Neutron star

at 2.6 M_sun ??

GW170817 – a merger of two compact stars

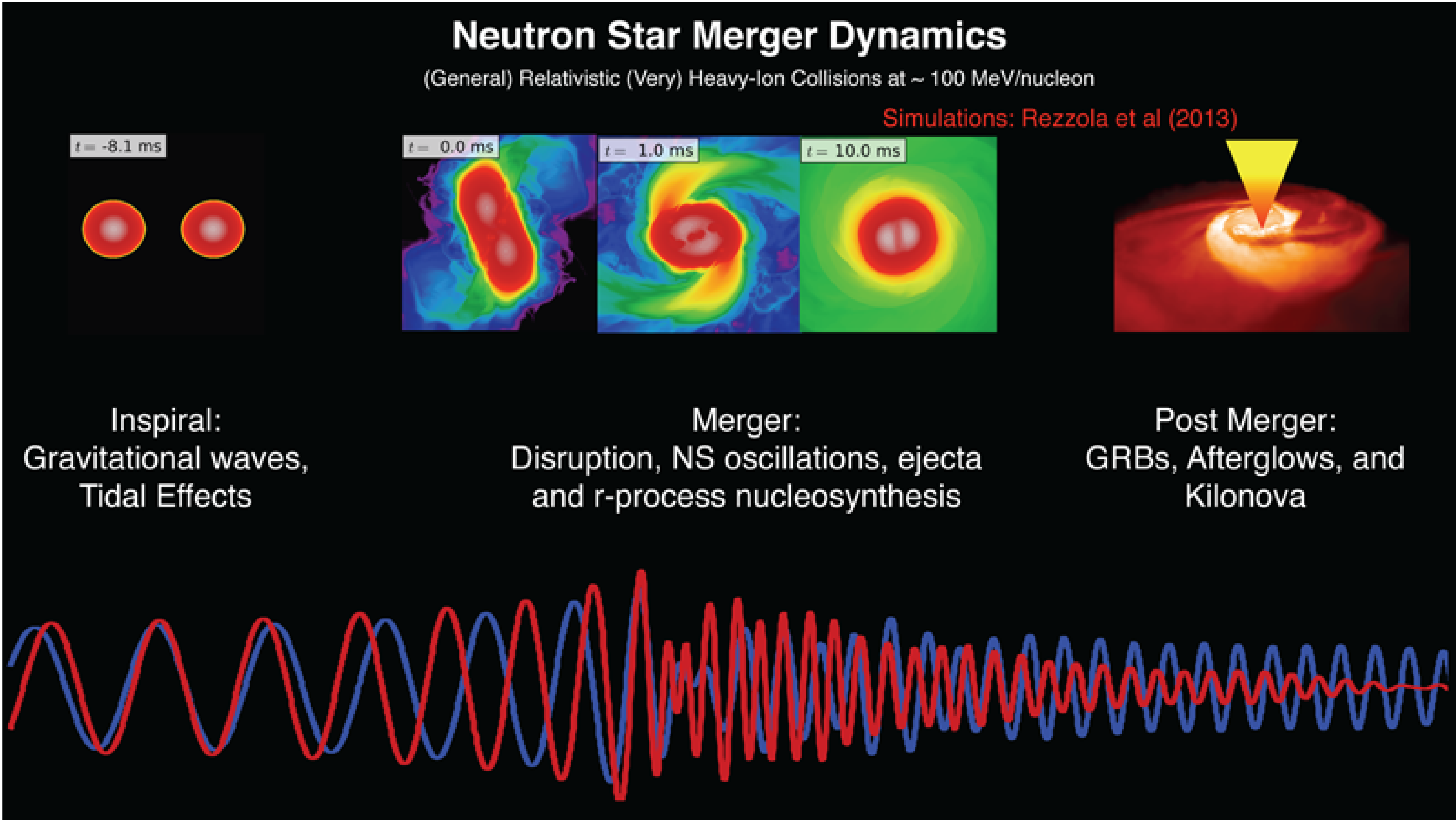

Symposium @ INT Seattle, March 2018

Can NICER prove J0740+6620 to be a hybrid star?

Work with Mateusz Cierniak, arxiv:2009.12353; EPJ ST 229 (2020) 3663
arxiv:2012.15785; AN (2021) accepted

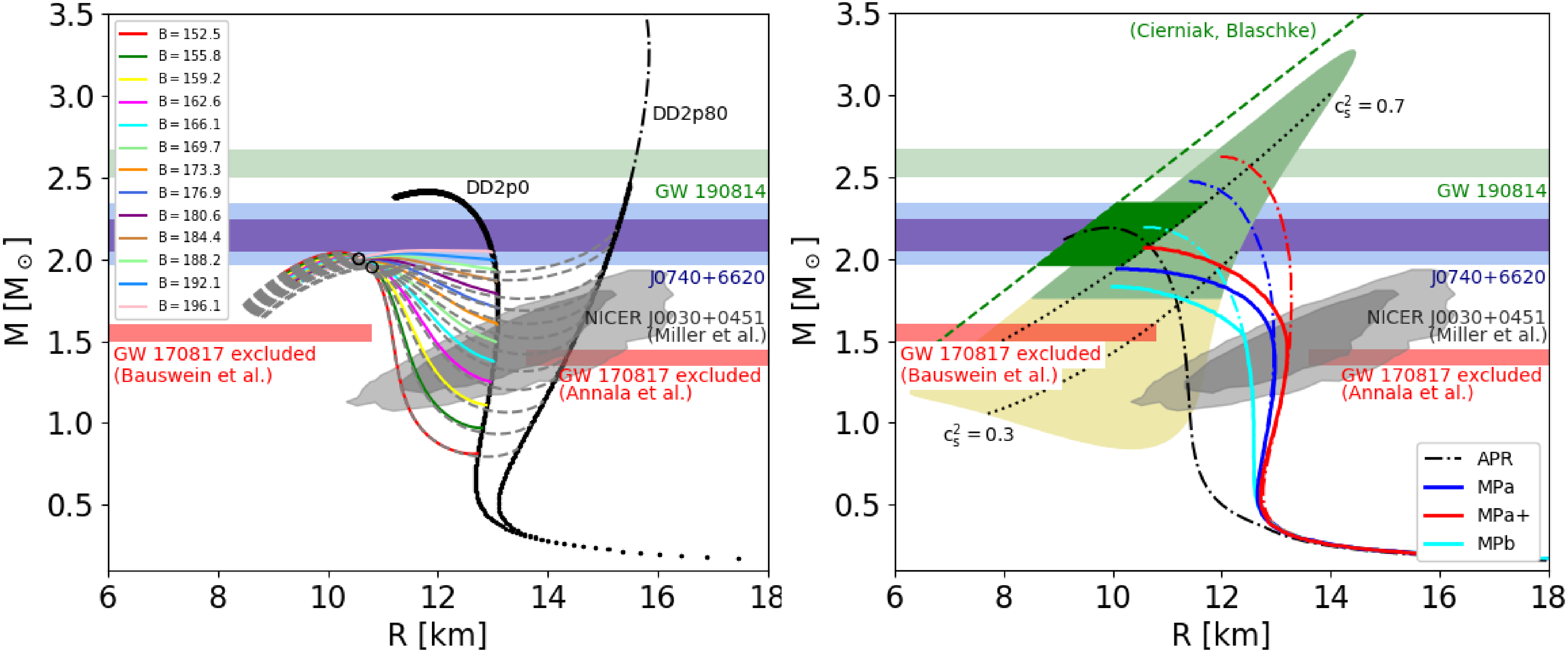

If radius of PSR J0740+6620 is measured in the dark-green region then it must harbor a core of superconducting quark matter!

Can NICER prove J0740+6620 to be a hybrid star?

Work with Mateusz Cierniak, arxiv:2009.12353; EPJ ST 229 (2020) 3663
arxiv:2012.15785; AN (2021) accepted

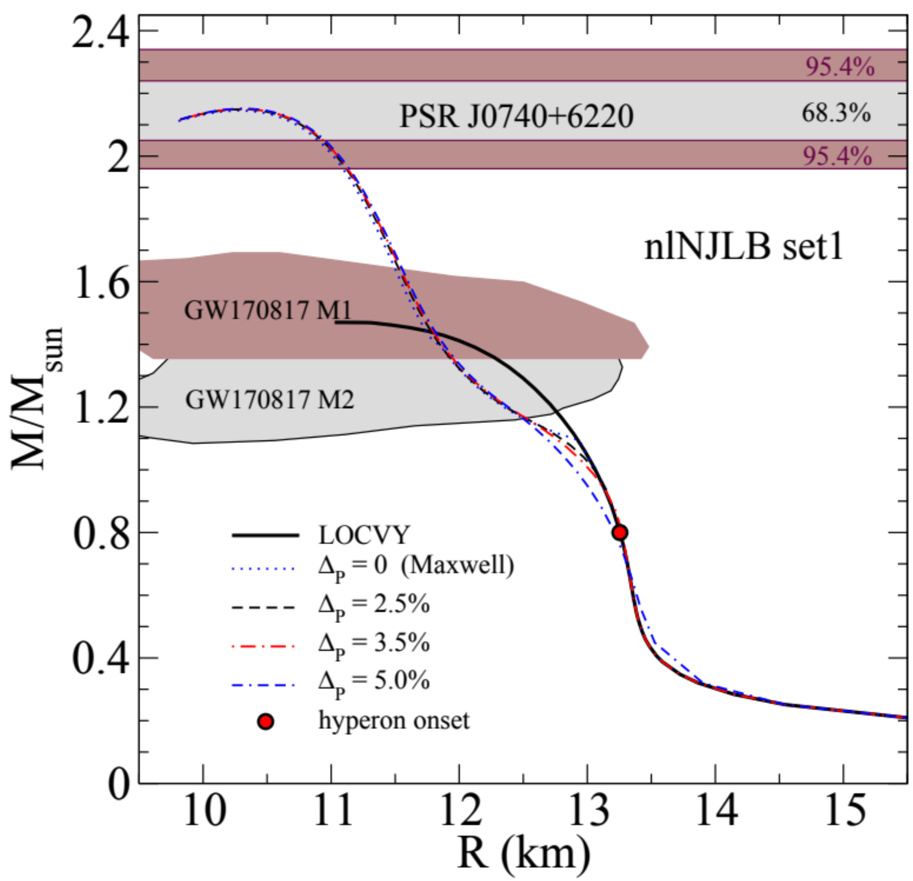

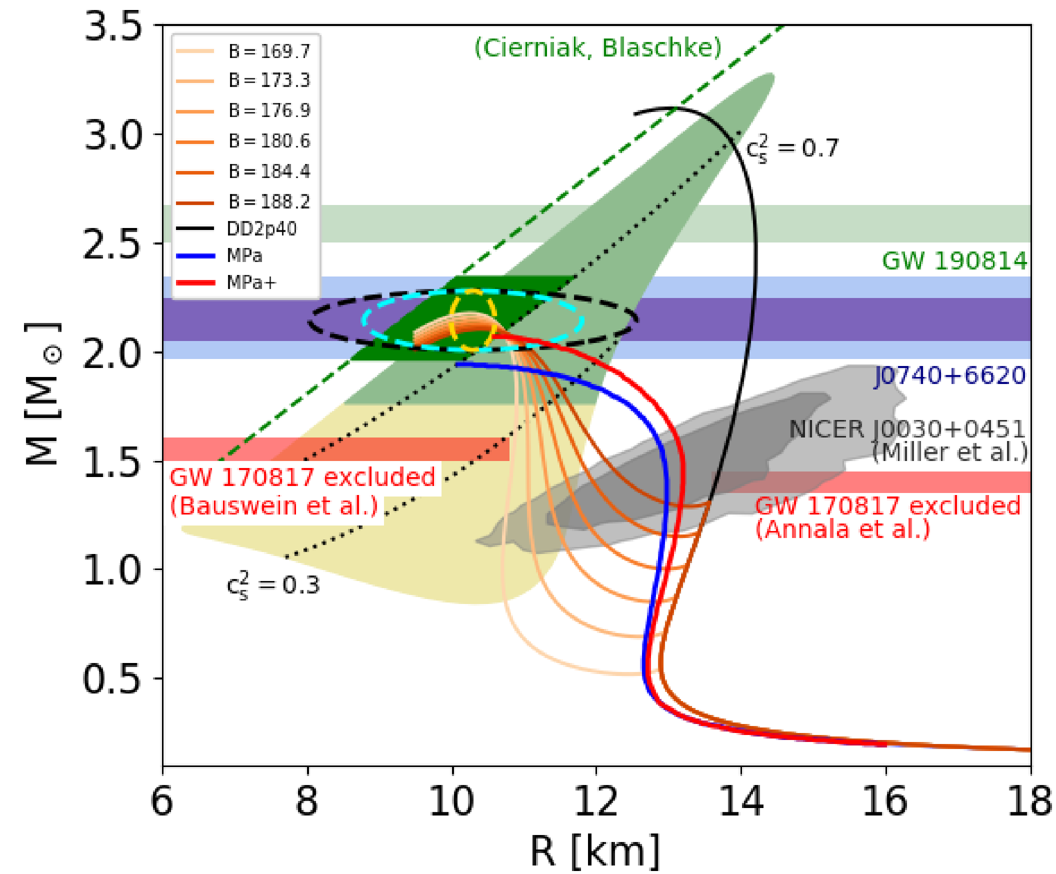

If radius of PSR J0740+6620 is measured at ~10.5 km, then it is also compatible with the hybrid star solution of the hyperon puzzle; M. Shahrbaf et al., J. Phys. G 47 (2020) 115201

If radius of PSR J0740+6620 is measured at 10.2 km with the accuracy of the yellow ellipse, then it must harbor a core of superconducting quark matter!